FYSS3315: Cyclotron operators' course
Fall 2022

Taneli Kalvas
taneli.kalvas@jyu.fi
FL114

University of Jyväskylä, Department of physics

https://tim.jyu.fi/view/kurssit/fysiikka/fyss3315-2022/main

Course

- Lectures 4×2 hours
- Practical training 4×4 hours
- Shift with a senior student operator 10–12 hours

Gives the qualification needed for acting as a paid student operator at the Accelerator Laboratory.

The radiation safety (FYSS3310, 4 credit) highly recommended!

Lecture contents

- Introduction to accelerator physics
- Ion sources
- Ion optics
- More about beams
- Beam diagnostics
- The cyclotron
- Vacuum physics and technology
- Radiation safety

Much of the content is shared with FYSS3410 (5 credits), but this course is more practical.

Symbols

$Q =$ charge state

$q = Q \cdot e =$ charge

$M =$ mass number

$m = M \cdot m_u$ mass

$E_K =$ kinetic energy

$E_U =$ potential energy

$\Delta V =$ potential difference

$\vec{E} =$ electric field

$\vec{B} =$ magnetic field

$\vec{x} = (x, y, z) =$ position (vector)

$\vec{v} = (v_x, v_y, v_z) =$ velocity (vector)

$\vec{a} = (a_x, a_y, a_z) =$ acceleration (vector)

$\beta =$ velocity relative to speed of light

$\gamma =$ relativistic gamma

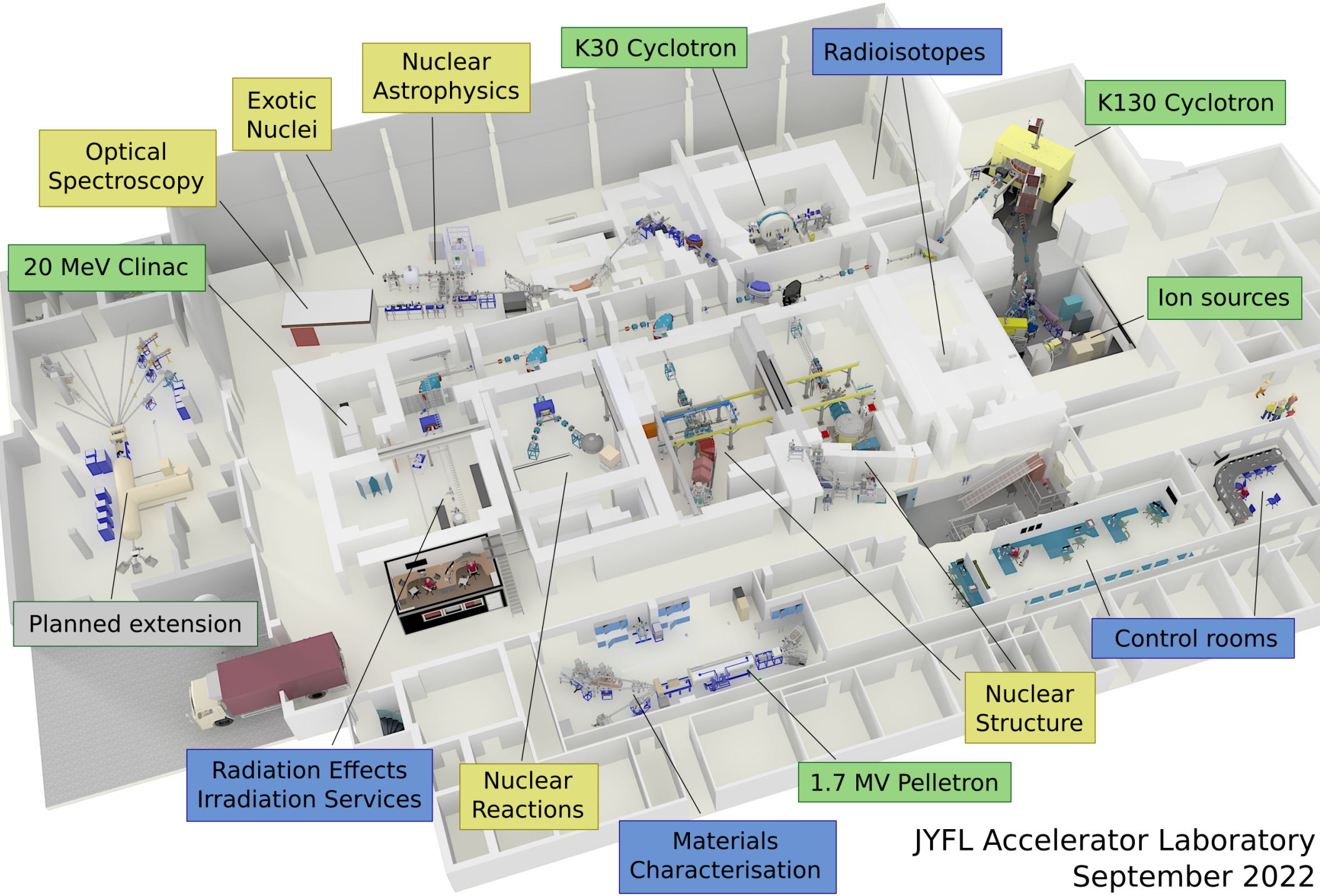
Optical Spectroscopy
Exotic Nuclei
Nuclear Astrophysics
K30 Cyclotron
Radioisotopes
K130 Cyclotron
20 MeV Clinac
Ion sources
Planned extension
Control rooms
Nuclear Structure
Radiation Effects Irradiation Services
Nuclear Reactions
1.7 MV Pelletron
Materials Characterisation
JYFL Accelerator Laboratory
September 2022

Introduction to accelerator physics

Accelerating particles

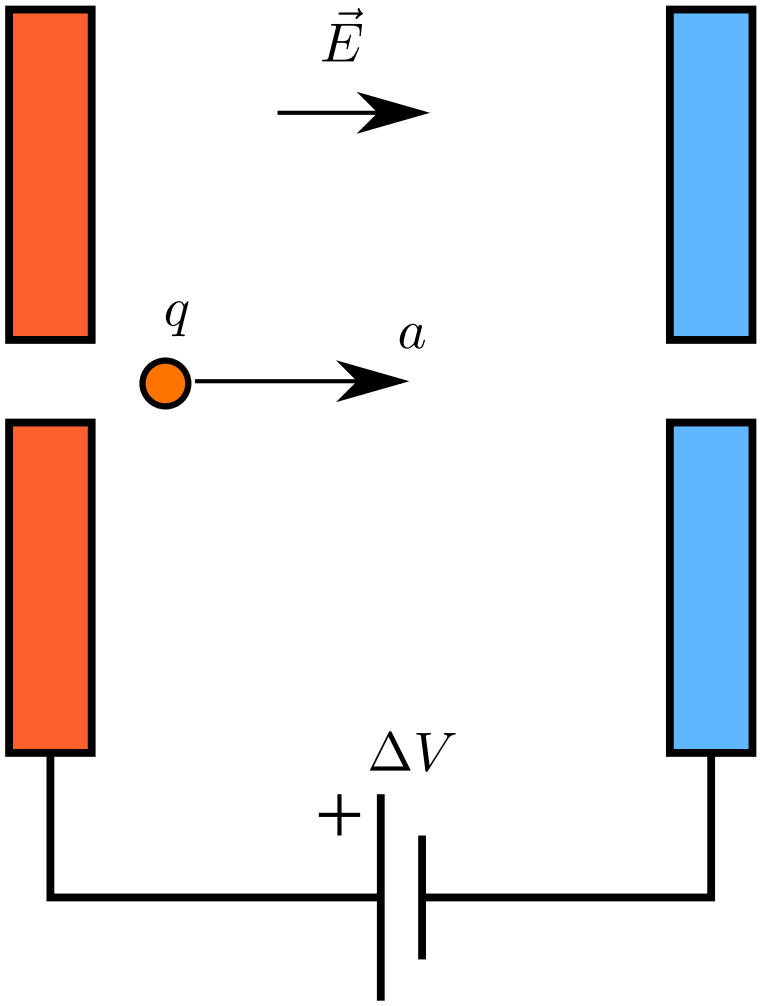

Acceleration using a gap

$$\Delta E_K = q\Delta V \qquad (1)$$

Assuming zero starting velocity

$$E_K = q\Delta V = \frac{1}{2}mv^2. \qquad (2)$$

Velocity of particle accelerated with an electrostatic system

$$v = \sqrt{\frac{2q\Delta V}{m}} \qquad (3)$$

Energy scales

Coulomb potential for two pointlike charges z_1 and z_2 (nucleus)

$$E_U = \frac{z_1 z_2}{4\pi\epsilon_0 r}. \tag{4}$$

On 29 August 2020 we were colliding $^{32}_{16}$S with $^{196}_{78}$Pt. Nuclear reactions start taking place when nuclii collide at a distance of $r_1 + r_2$, where nuclear radii can be estimated with $r = 1.4$ fm $A^{1/3}$.

Reaching such distance needs

$$E_U = \frac{z_1 z_2}{4\pi\epsilon_0 (r_1 + r_2)} \approx 2.29 \cdot 10^{-11} \text{ J} \approx 143 \text{ MeV}. \tag{5}$$

in the center-of-mass (CM) coordinate system.

Energy scales

Center-of-mass velocity with fixed target

$$V_{CM} = \frac{v_1 m_1 + v_2 m_2}{m_1 + m_2} = \frac{v_1 m_1}{m_1 + m_2}. \tag{6}$$

Kinetic energy available in the CM system

$$K_{CM} = \frac{1}{2} m_1 (v_1 - V_{CM})^2 + \frac{1}{2} m_2 V_{CM}^2 \tag{7}$$

leading to

$$K_{\text{beam}} = \frac{1}{2} m_1 v_1^2 = \cdots = \frac{m_1 + m_2}{m_2} K_{CM}. \tag{8}$$

In the example case that is $K_{\text{beam}} = 166$ MeV or about 5.19 MeV/u.

Energy scales

From the ion source the beam is extracted as $^{32}_{16}\mathrm{S}^{7+}$ ion with acceleration potential $\Delta V = 9.46$ kV leading to ion energy of $E_K = q\Delta V = 66.2$ keV.

Typical energy and velocity ranges at the lab

E_K	E_K/m	v	β
66.2 keV	2.07 keV/u	19900 m/s	$6.6 \cdot 10^{-5}$
166 MeV	5.19 MeV/u	$3.16 \cdot 10^7$ m/s	0.11

Producing 166 MeV S^{7+} on a linear accelerator needs a total accelerating potential difference of $\Delta V = E_K/q = 24$ MV!

Producing ions

H, neutral hydrogen atom

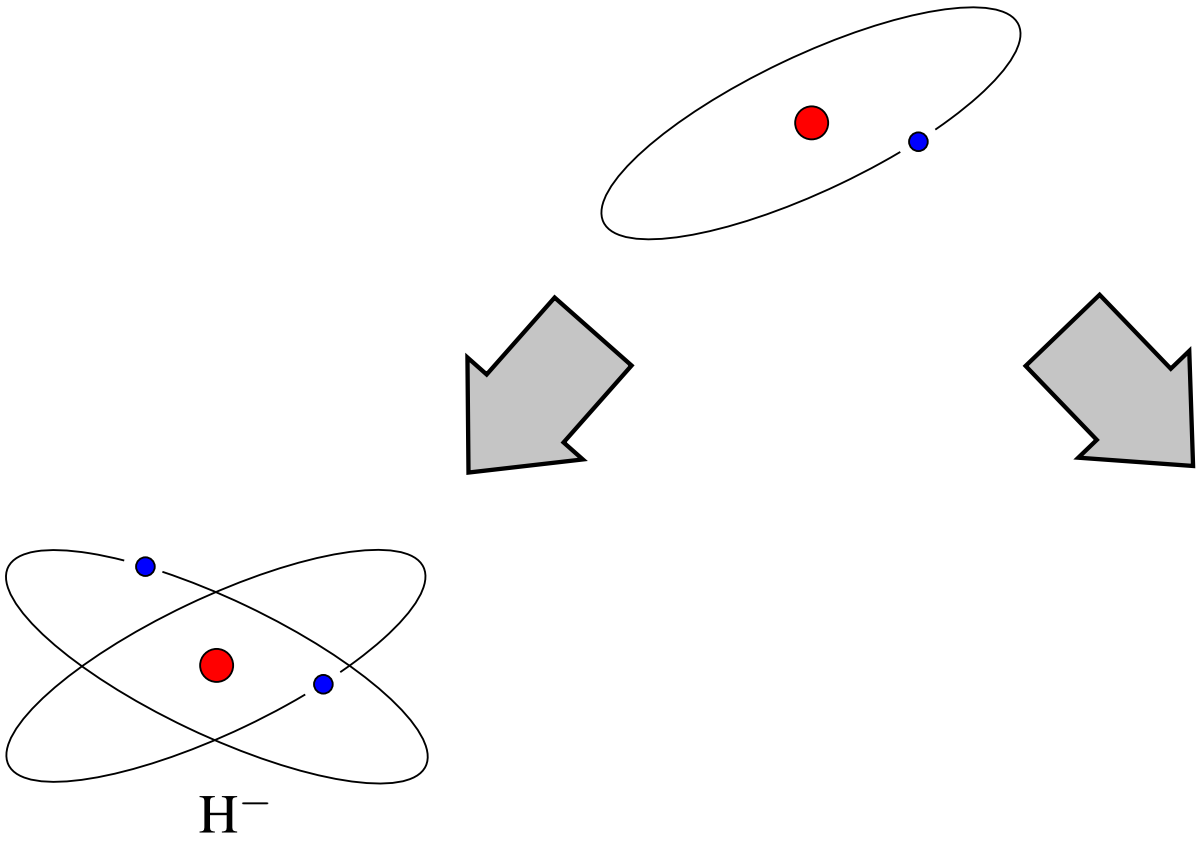

H^-

H^+, proton

Producing ions

H, neutral hydrogen atom

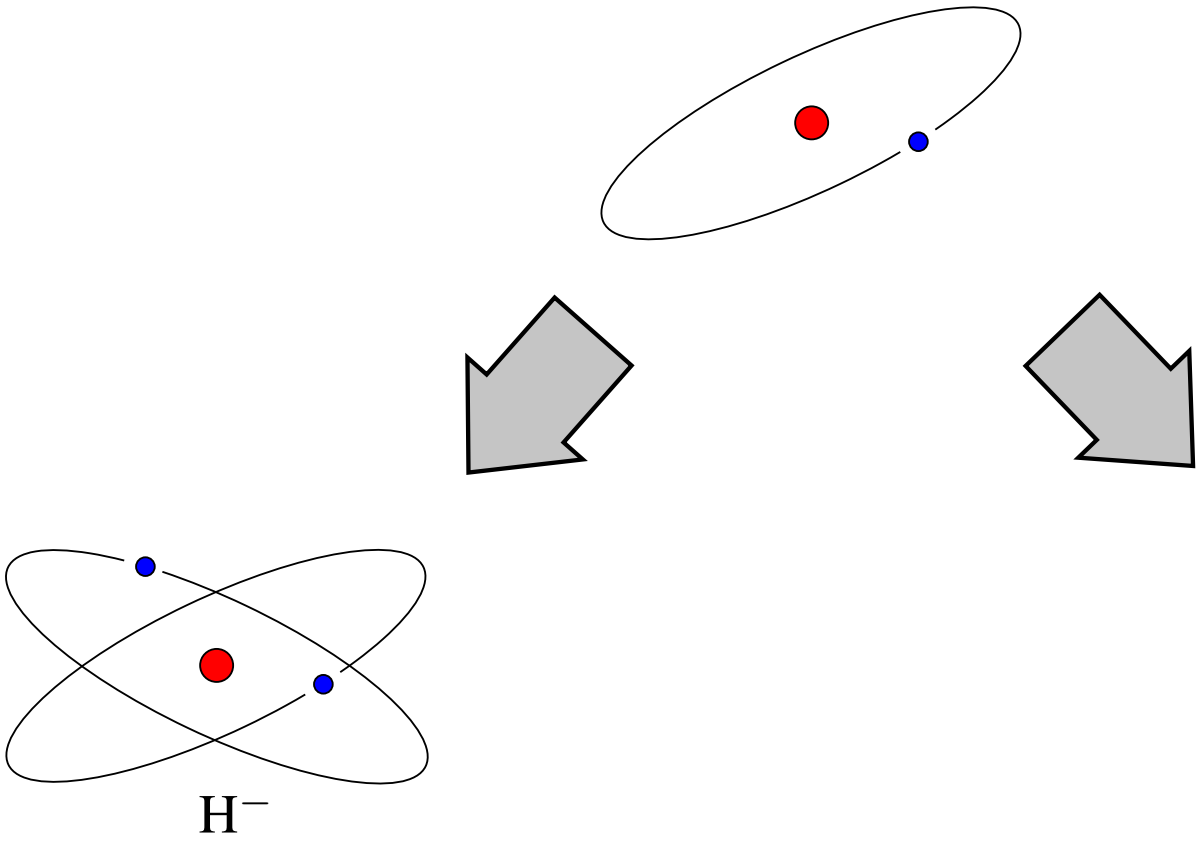

H^-

H^+, proton

High charge states for energy

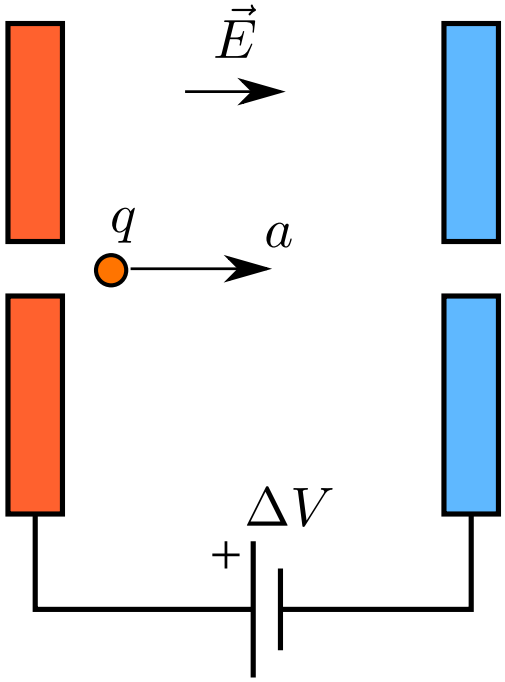

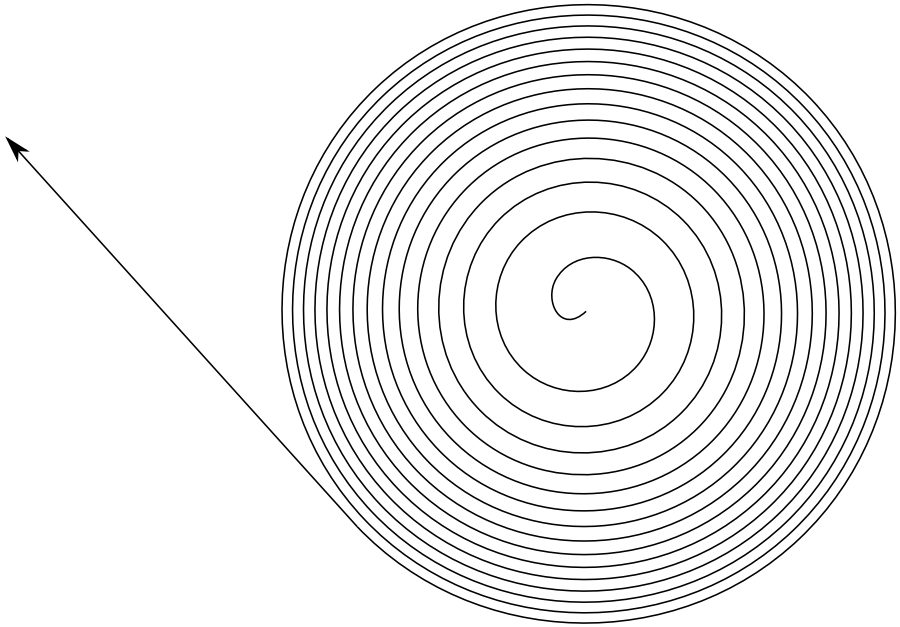

$$\Delta E_K = q\Delta V$$

$$\frac{E_K}{M} = K\left(\frac{Q}{M}\right)^2$$

Negative hydrogen stripping

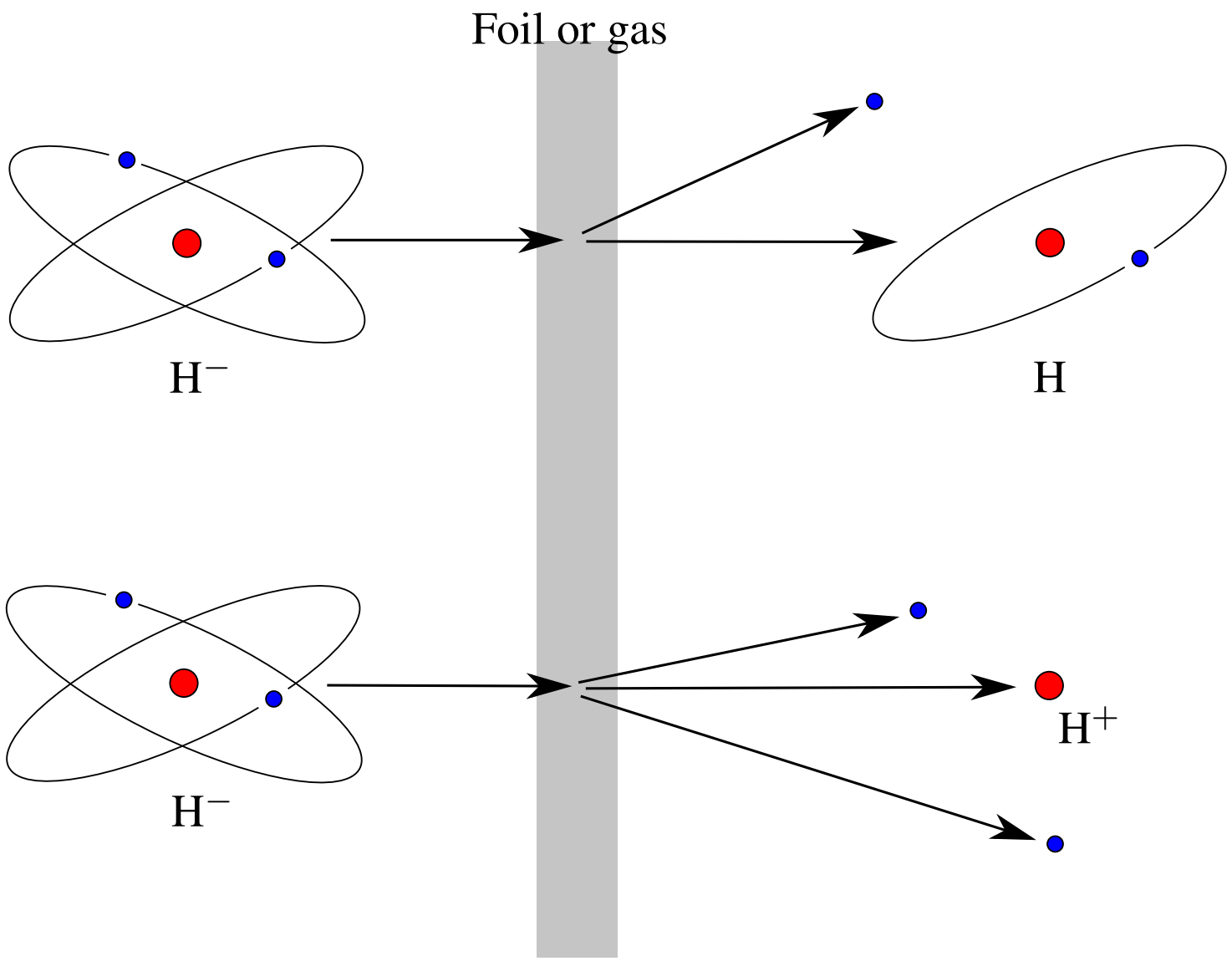

Negative hydrogen stripping in tandem accelerators

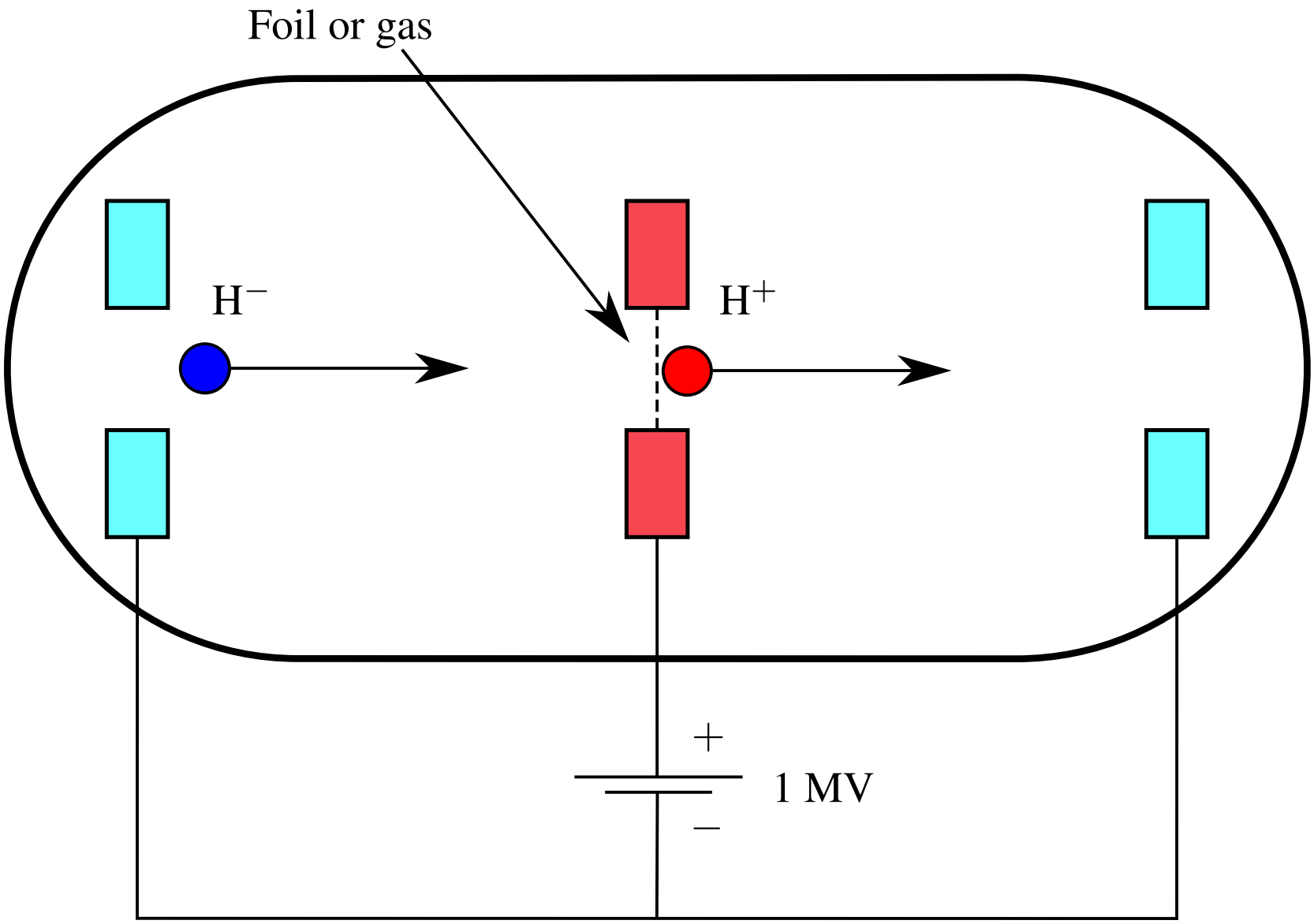

Negative hydrogen stripping in cyclotrons

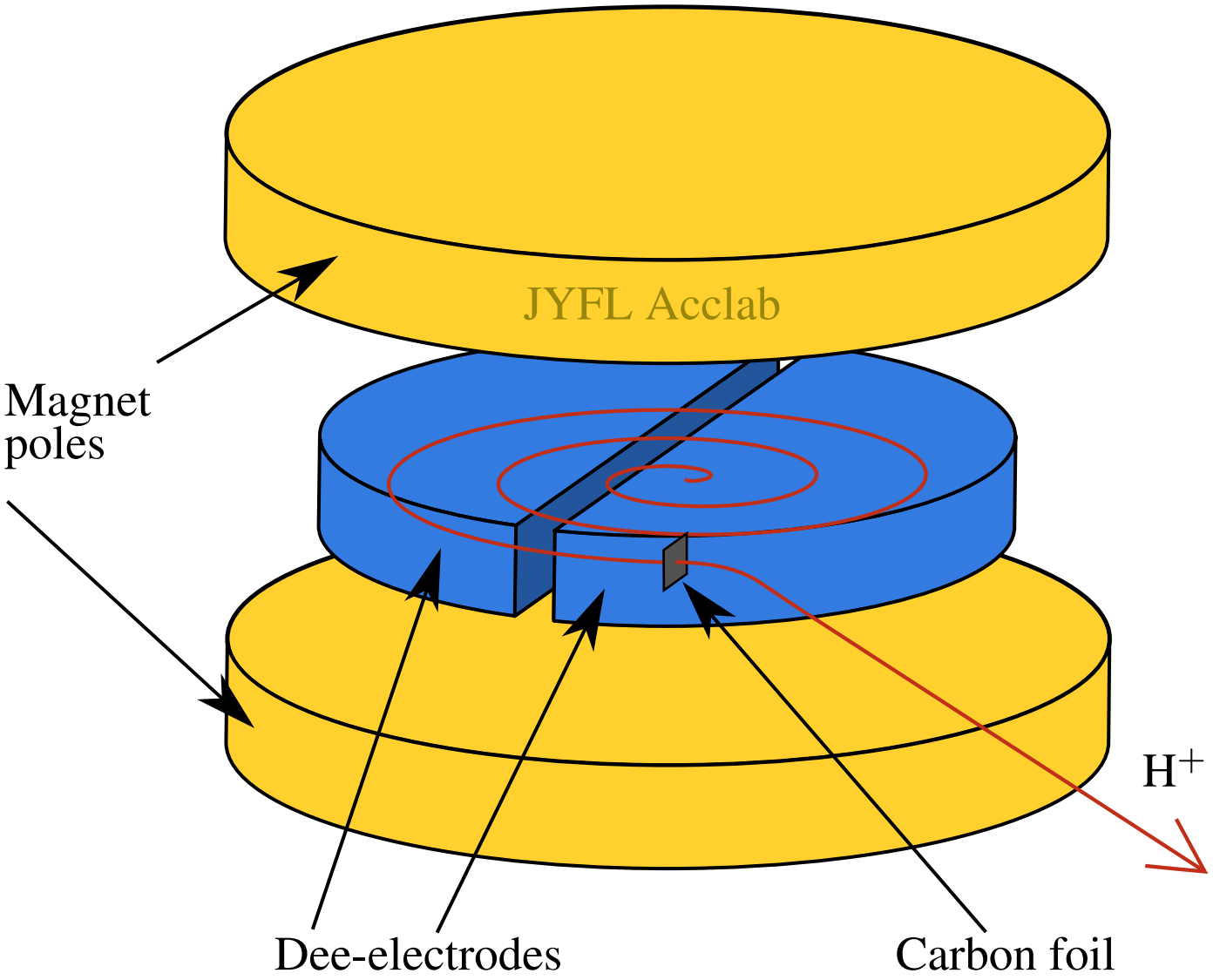

Ion sources

Acclab ion sources

The JYFL Acclab has 3 ion accelerators:

- K130 cyclotron
- MCC30 cyclotron
- Pelletron 1.7 MV linear tandem accelerator

These are injected with:

- Filament-drive multicusp H^- ion sources
- SNICS ion source (Source of Negative Ions by Cesium Sputtering)
- Alphatross, charge exchange cell negative ion source
- Electron Cyclotron Resonance (ECR) ion sources

Filament-drive multicusp H^- ion source

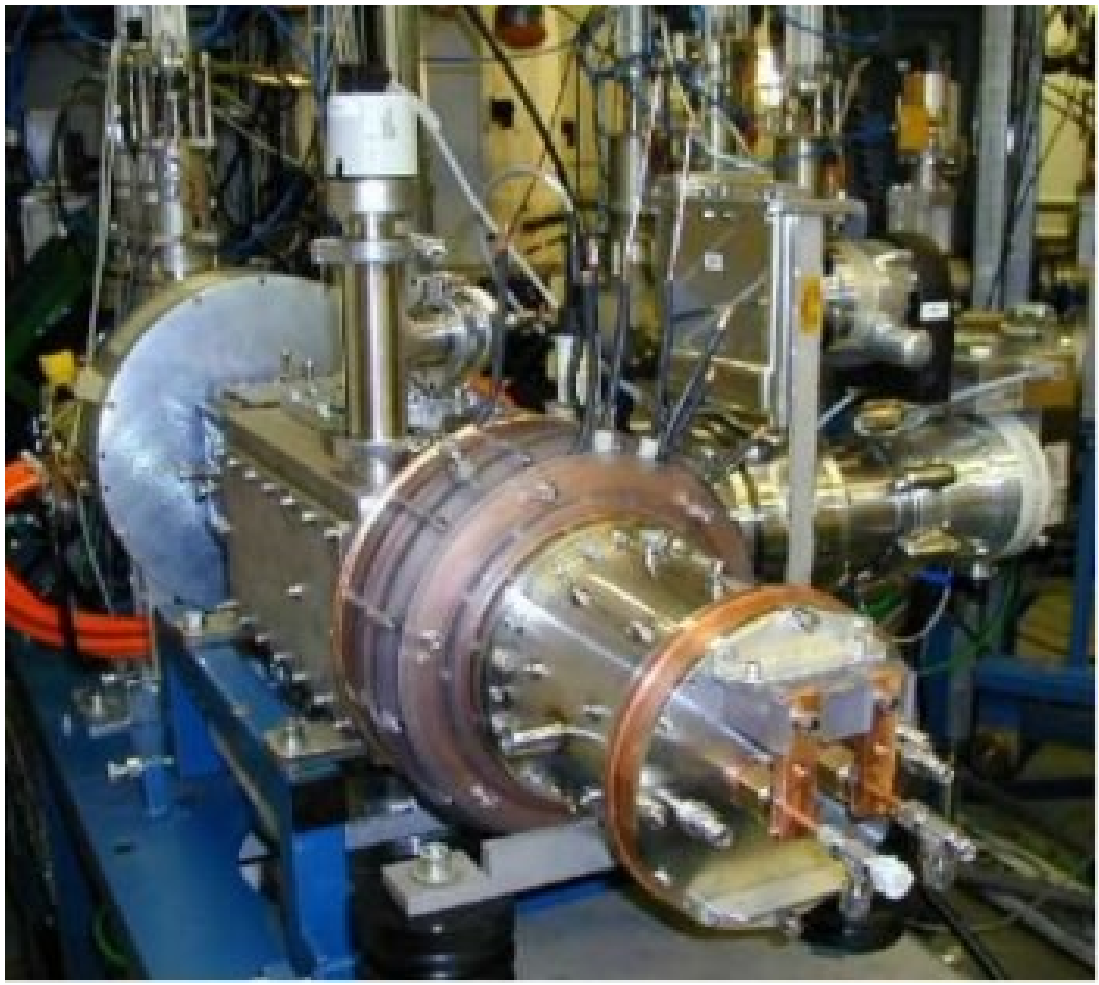

LIISA providing H^- and D^- ion beams to K130 cyclotron.

Filament-drive multicusp H^- ion source

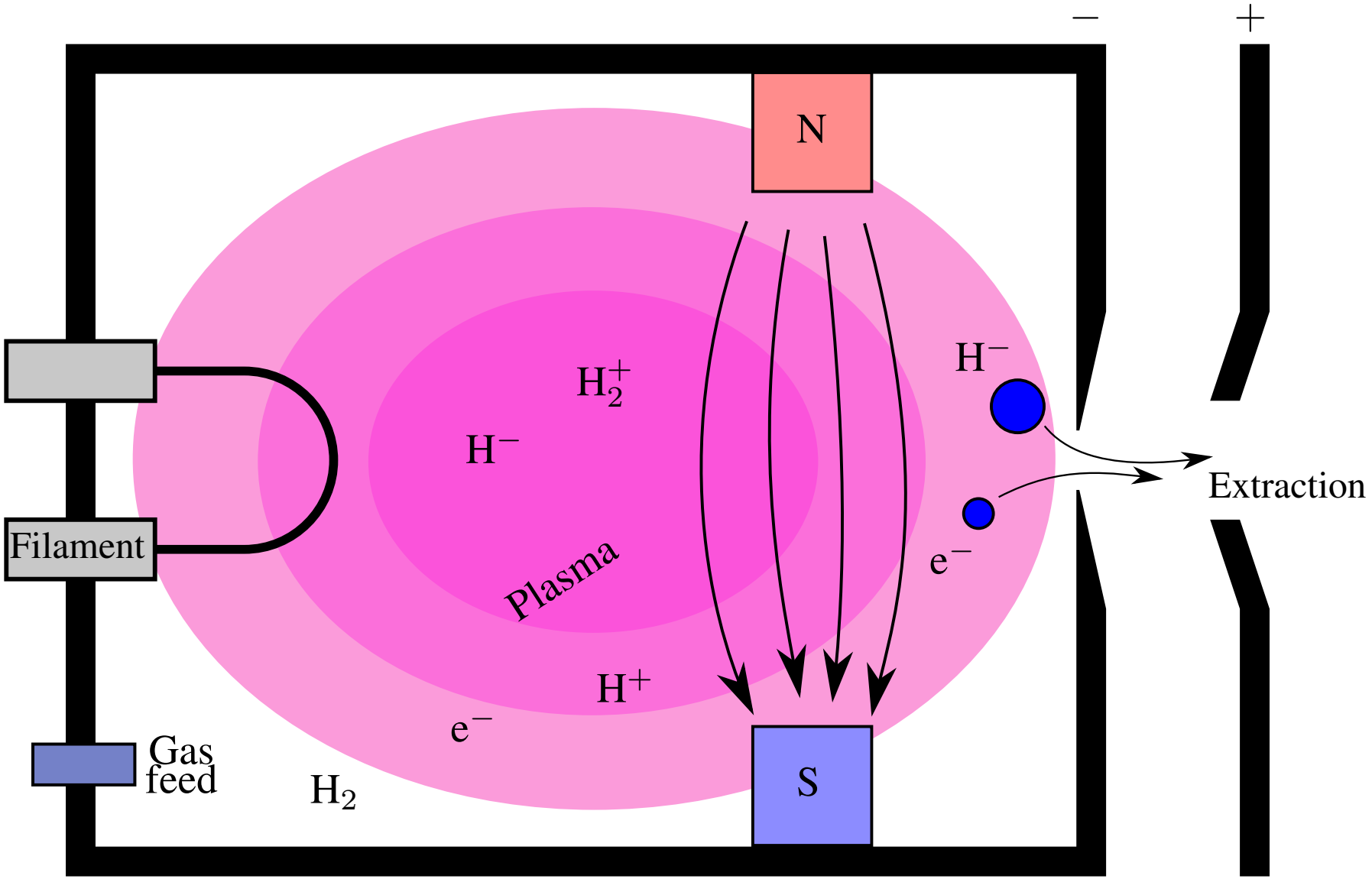

Filament-drive multicusp H^- ion source

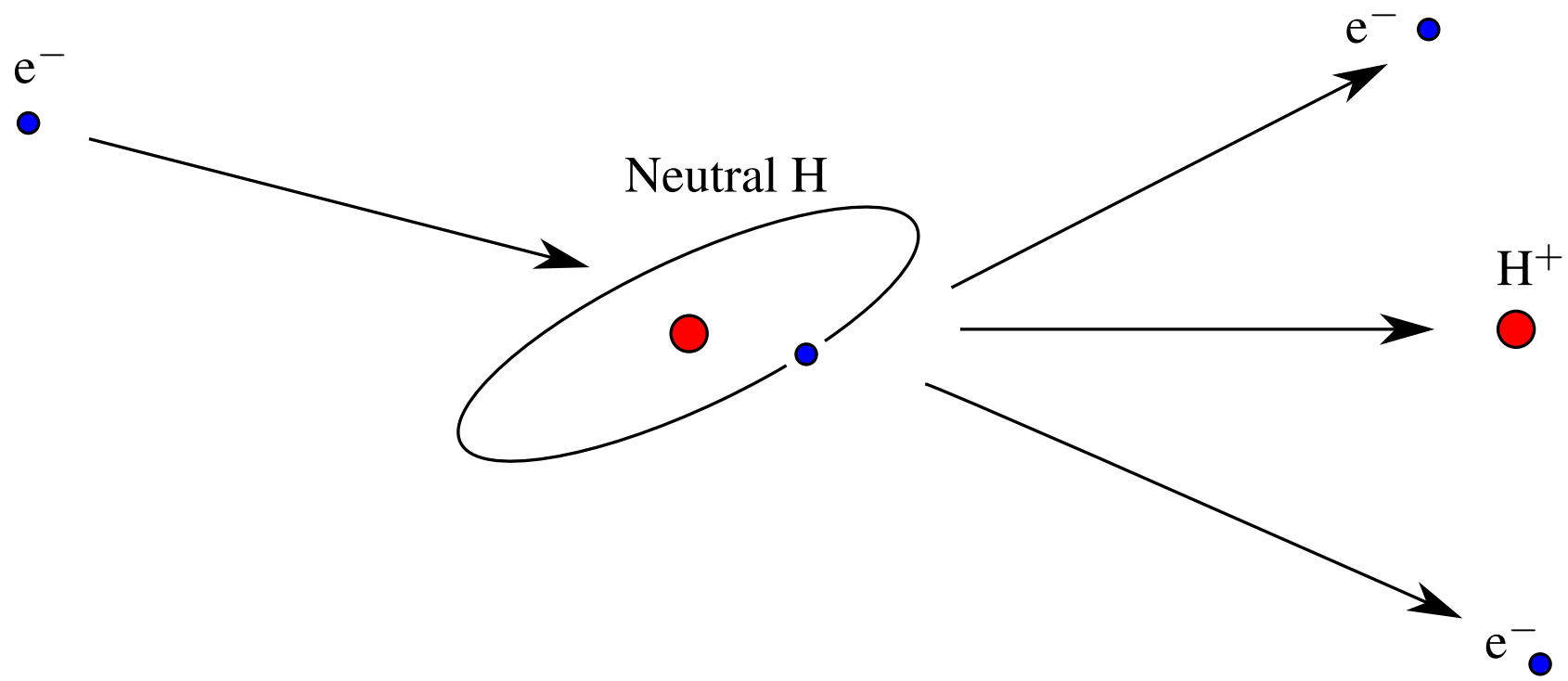

Filament-drive multicusp H^- ion source

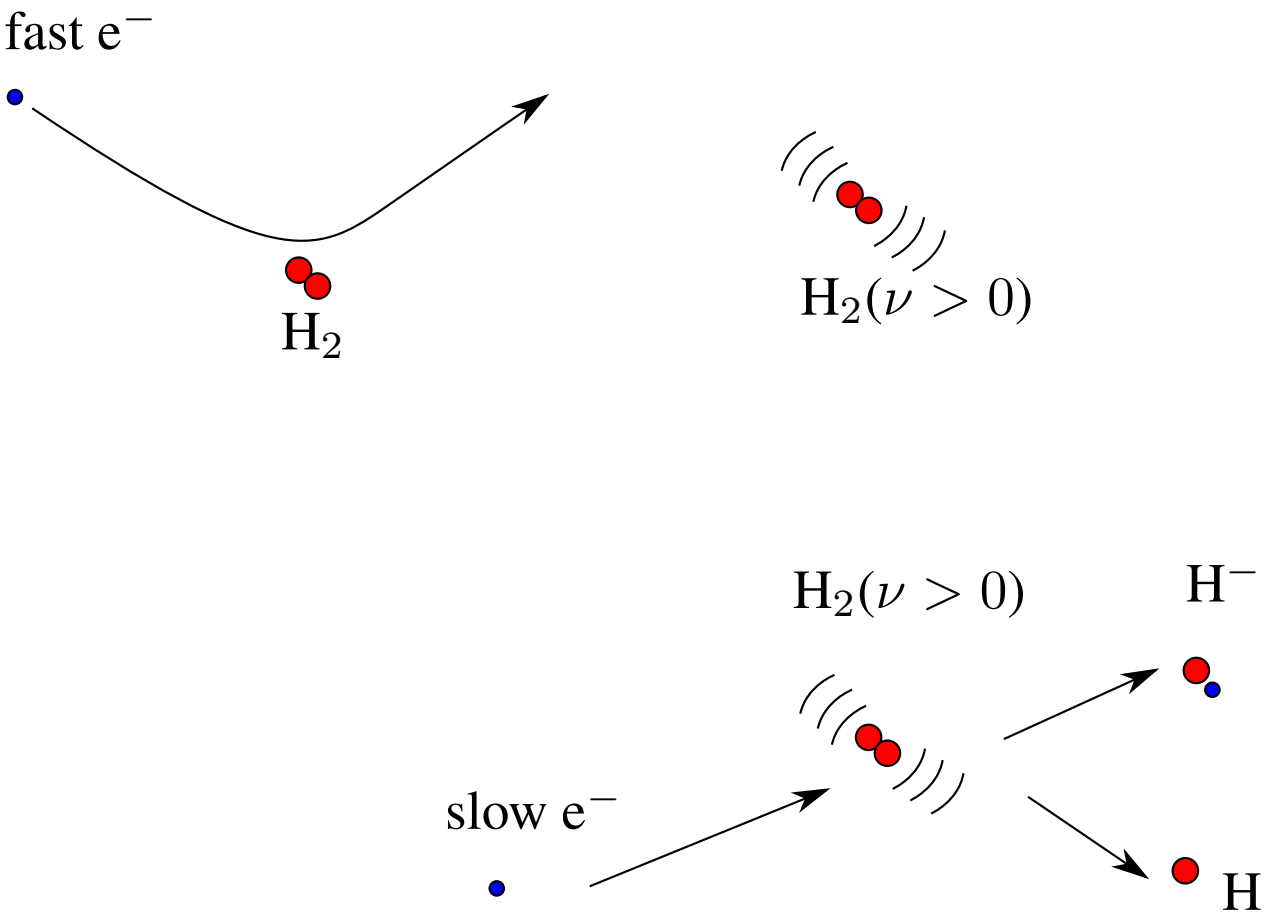

Filament-drive multicusp H^- ion source

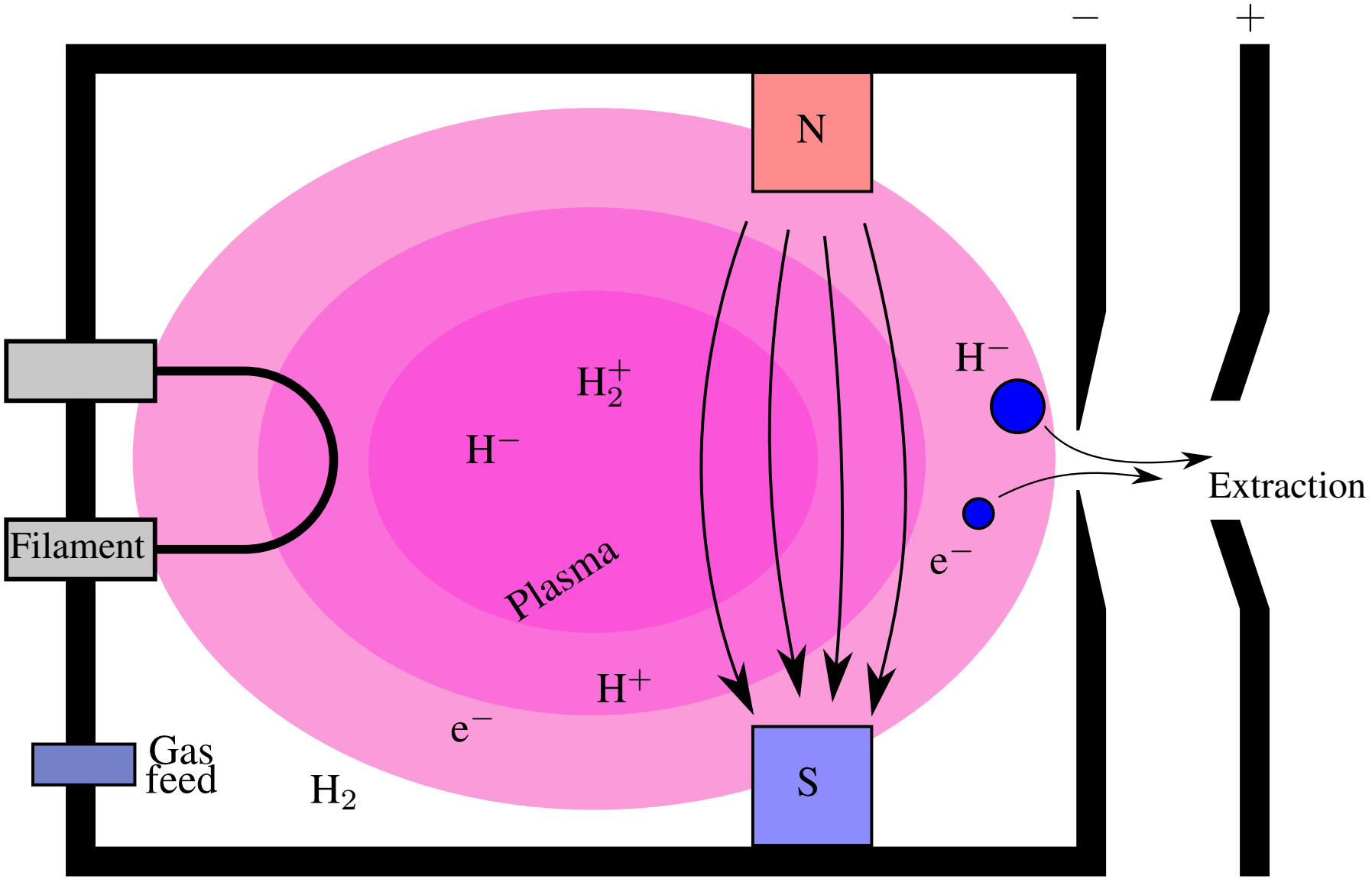

H^- ion source extraction

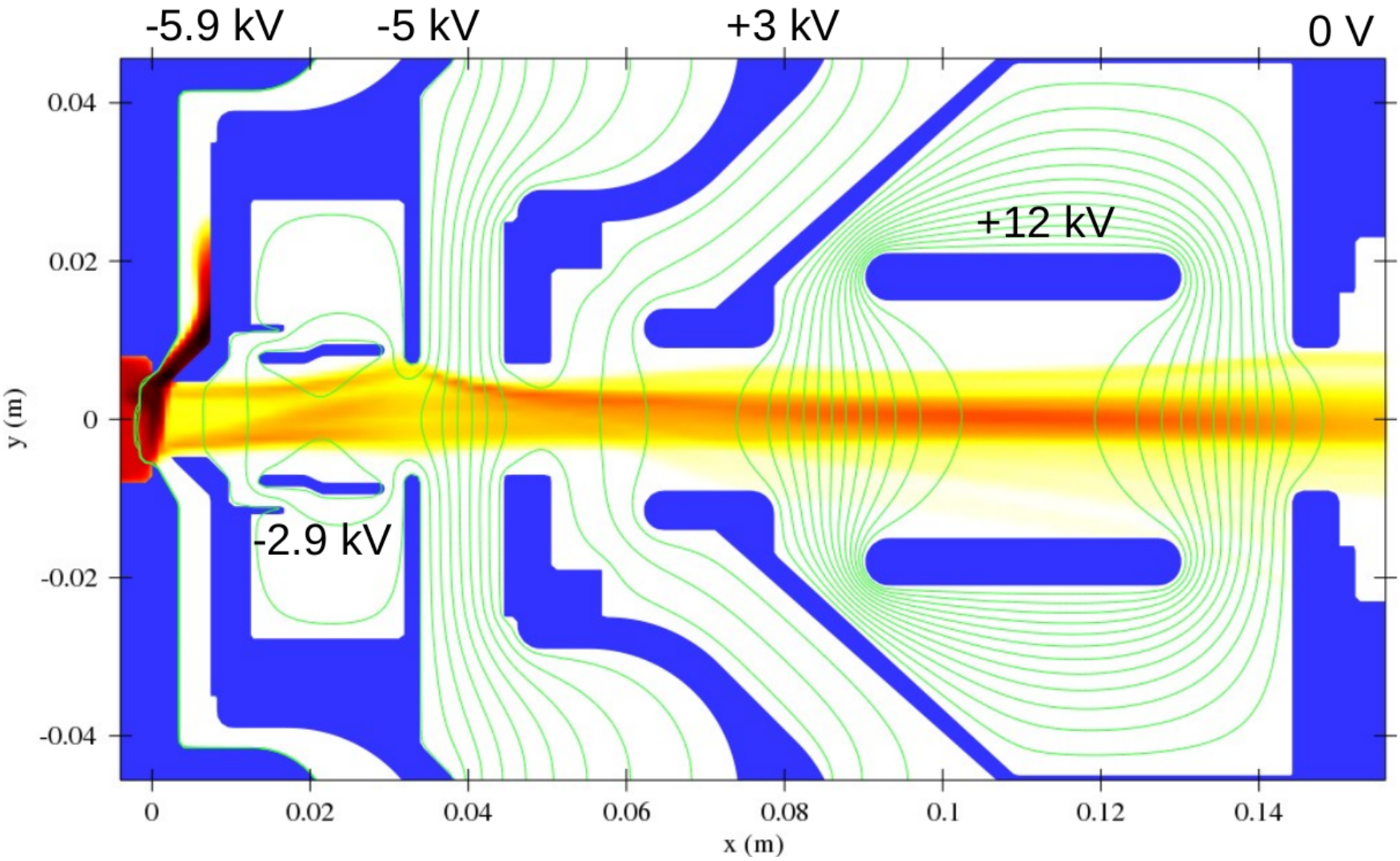

H^- source operational parameters

- Gas feed (source neutral pressure)
- Filament heating current (and voltage)
- Filament discharge voltage (and current)
- Ion source high voltage bias
- Puller/extractor electrode voltage
- Focusing electrode voltages

Very consistent

ECR ion sources

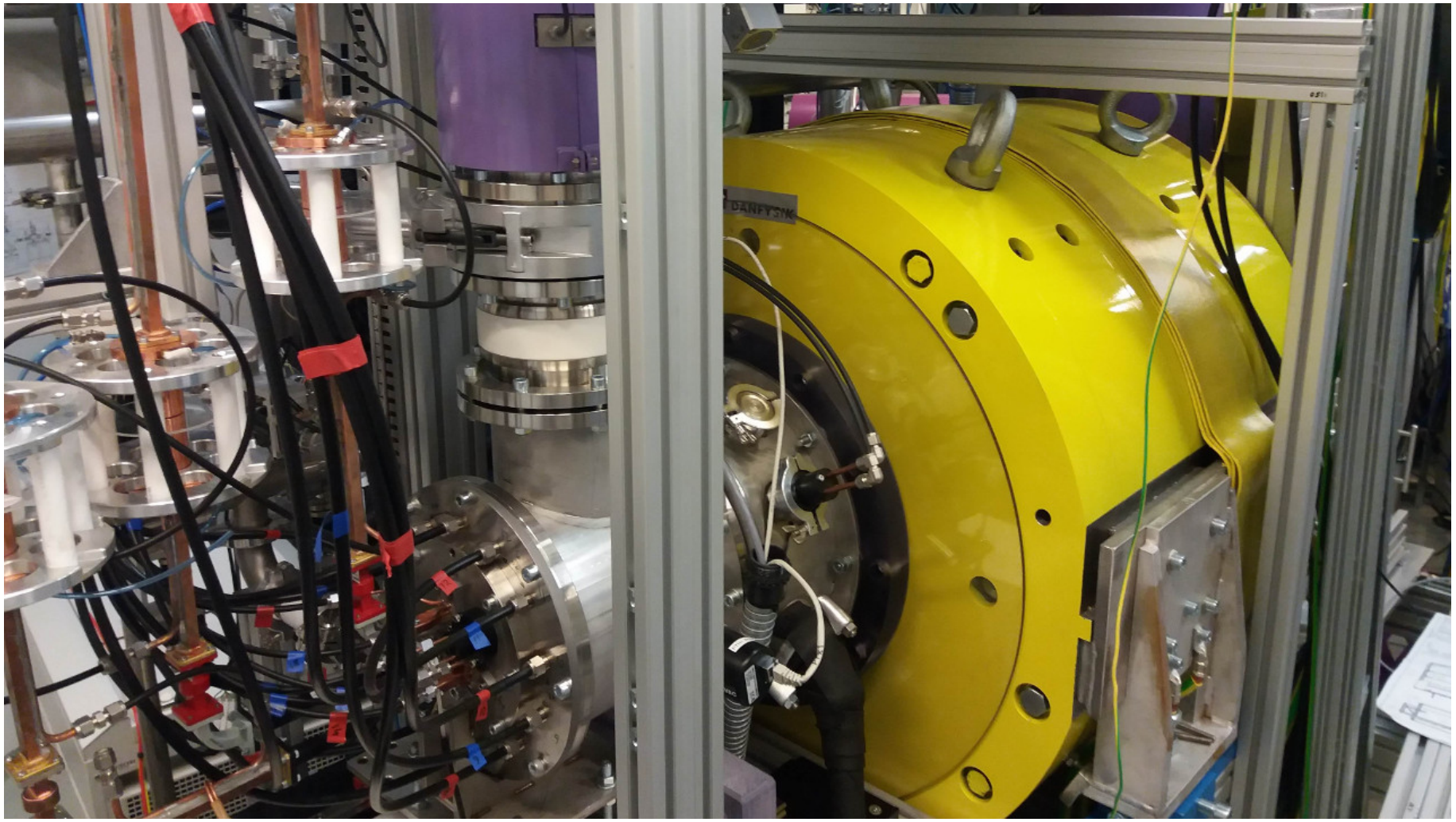

The most powerful room-temperature ECR ion source in the world, HIISI

ECR ion sources

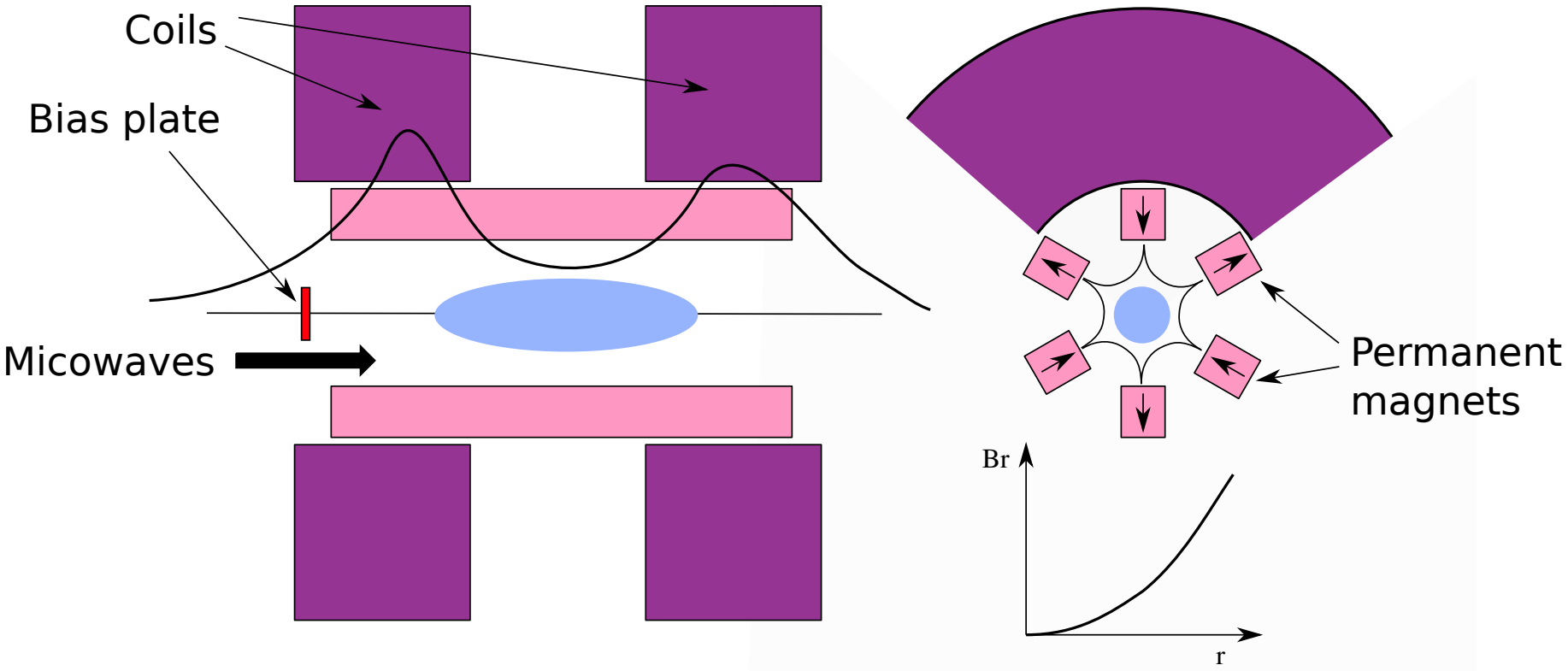

ECR ion sources

1. Magnetic confinement of electrons with microwave resonance for electron heating

$$\omega_{RF} = \omega_c = \frac{qB_{ECR}}{m} \qquad (9)$$

2. Electrostatic confinement of ions within the potential well created by electrons
3. Stepwise ionization of atoms with electron impact processes

$$\mathrm{X}^{Q+} + \mathrm{e} \rightarrow \mathrm{X}^{(Q+1)+} + 2\mathrm{e}$$

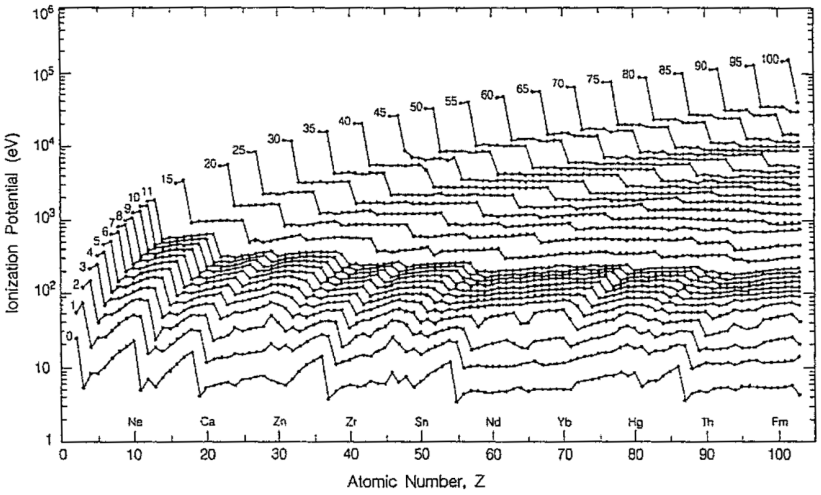

ECRIS beam production

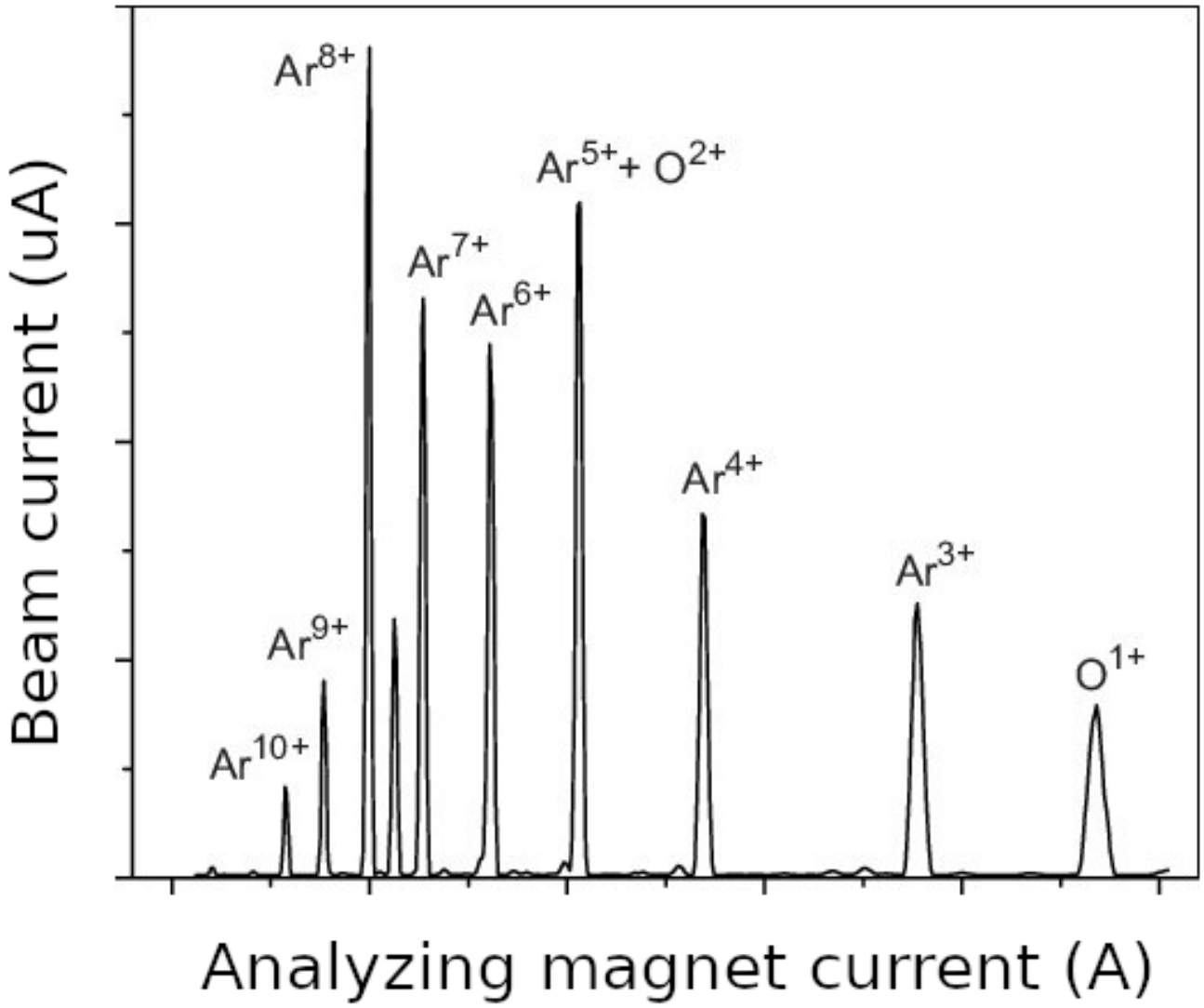

ECRIS beam production

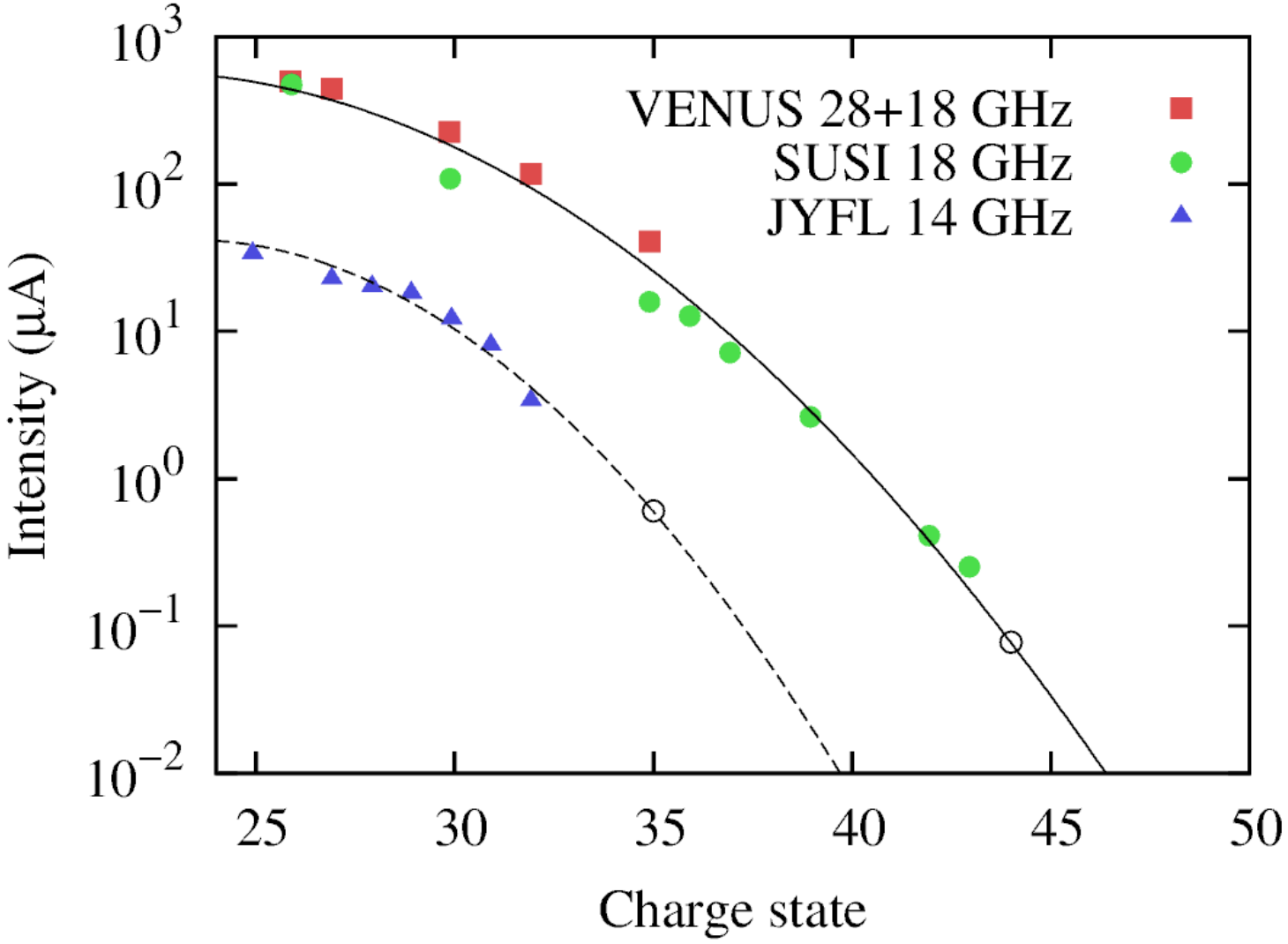

Elements produced at JYFL Acclab

Methods of injection

- Gas
- Sputtering
- Oven
- MIVOC

1 **H** 1.00794																	2 **He** 4.00260
3 **Li** 6.941	4 **Be** 9.01218											5 **B** 10.81	6 **C** 12.011	7 **N** 14.0067	8 **O** 15.9994	9 **F** 18.9984	10 **Ne** 20.179
11 **Na** 22.9898	12 **Mg** 24.305											13 **Al** 26.9815	14 **Si** 28.0855	15 **P** 30.9738	16 **S** 32.06	17 **Cl** 35.453	18 **Ar** 39.945
19 **K** 39.0983	20 **Ca** 40.08	21 **Sc** 44.9559	22 **Ti** 47.88	23 **V** 50.9415	24 **Cr** 51.996	25 **Mn** 54.9380	26 **Fe** 55.847	27 **Co** 58.9332	28 **Ni** 58.69	29 **Cu** 63.546	30 **Zn** 65.38	31 **Ga** 69.72	32 **Ge** 72.59	33 **As** 74.9216	34 **Se** 78.96	35 **Br** 79.904	36 **Kr** 83.80
37 **Rb** 85.4678	38 **Sr** 87.62	39 **Y** 88.9059	40 **Zr** 91.22	41 **Nb** 92.9064	42 **Mo** 95.94	43 **Tc** (98)	44 **Ru** 101.07	45 **Rh** 102.906	46 **Pd** 106.42	47 **Ag** 107.868	48 **Cd** 112.41	49 **In** 114.82	50 **Sn** 118.69	51 **Sb** 121.75	52 **Te** 127.60	53 **I** 126.905	54 **Xe** 131.29
55 **Cs** 132.905	56 **Ba** 137.33	57-71 Lanta-noidit	72 **Hf** 178.49	73 **Ta** 180.948	74 **W** 183.85	75 **Re** 186.207	76 **Os** 190.2	77 **Ir** 192.22	78 **Pt** 195.08	79 **Au** 196.967	80 **Hg** 200.59	81 **Tl** 204.383	82 **Pb** 207.2	83 **Bi** 208.980	84 **Po** (209)	85 **At** (210)	86 **Rn** (222)
87 **Fr** (223)	88 **Ra** 226.025	89-103 Akti-noidit	104 **Rf** (261)	105 **Db** (260)	106 **Sg** (263)	107 **Bh** (262)	108 **Hs** (265)	109 **Mt** (266)									

Lantanoidit	57 **La** 138.906	58 **Ce** 140.12	59 **Pr** 140.908	60 **Nd** 144.24	61 **Pm** (145)	62 **Sm** 150.36	63 **Eu** 151.96	64 **Gd** 157.25	65 **Tb** 158.925	66 **Dy** 162.50	67 **Ho** 164.930	68 **Er** 167.26	69 **Tm** 168.934	70 **Yb** 173.04	71 **Lu** 174.967
Aktinoidit	89 **Ac** 227.028	90 **Th** 232.038	91 **Pa** 231.036	92 **U** 238.029	93 **Np** 237.048	94 **Pu** (244)	95 **Am** (243)	96 **Cm** (247)	97 **Bk** (247)	98 **Cf** (251)	99 **Es** (252)	100 **Fm** (257)	101 **Md** (258)	102 **No** (259)	103 **Lr** (260)

ECRIS operational parameters

- Gas feeds (source neutral pressure)
- Oven/sputter parameters
- Microwave feed
- Coil currents
- Bias plate voltage
- Ion source high voltage bias
- Extraction electrode voltage

Also depends on the phase of the moon, weather, weekday and price of crude oil. Moody!

Ion optics

Example ion optical system

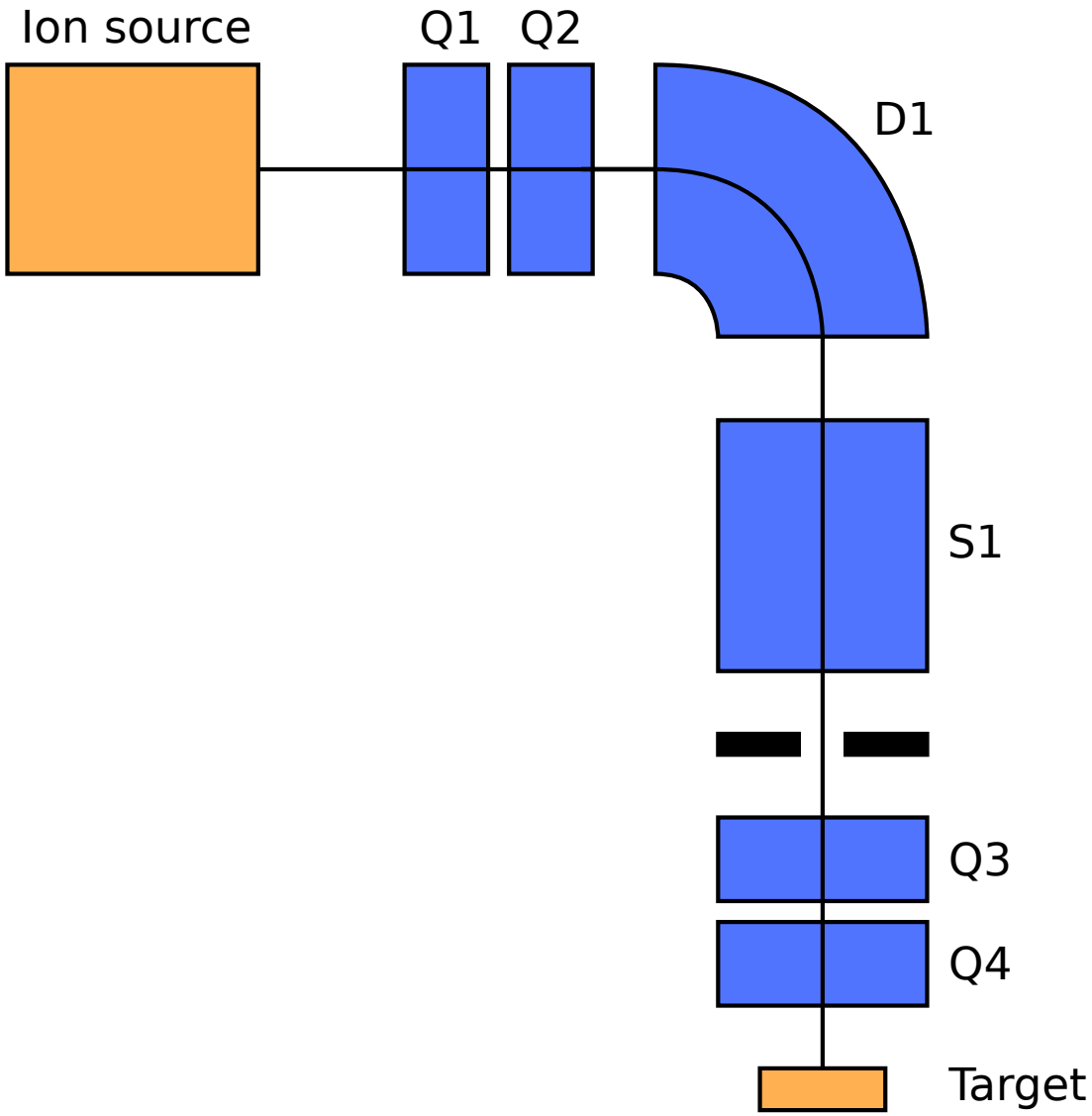

Curvilinear coordinate system

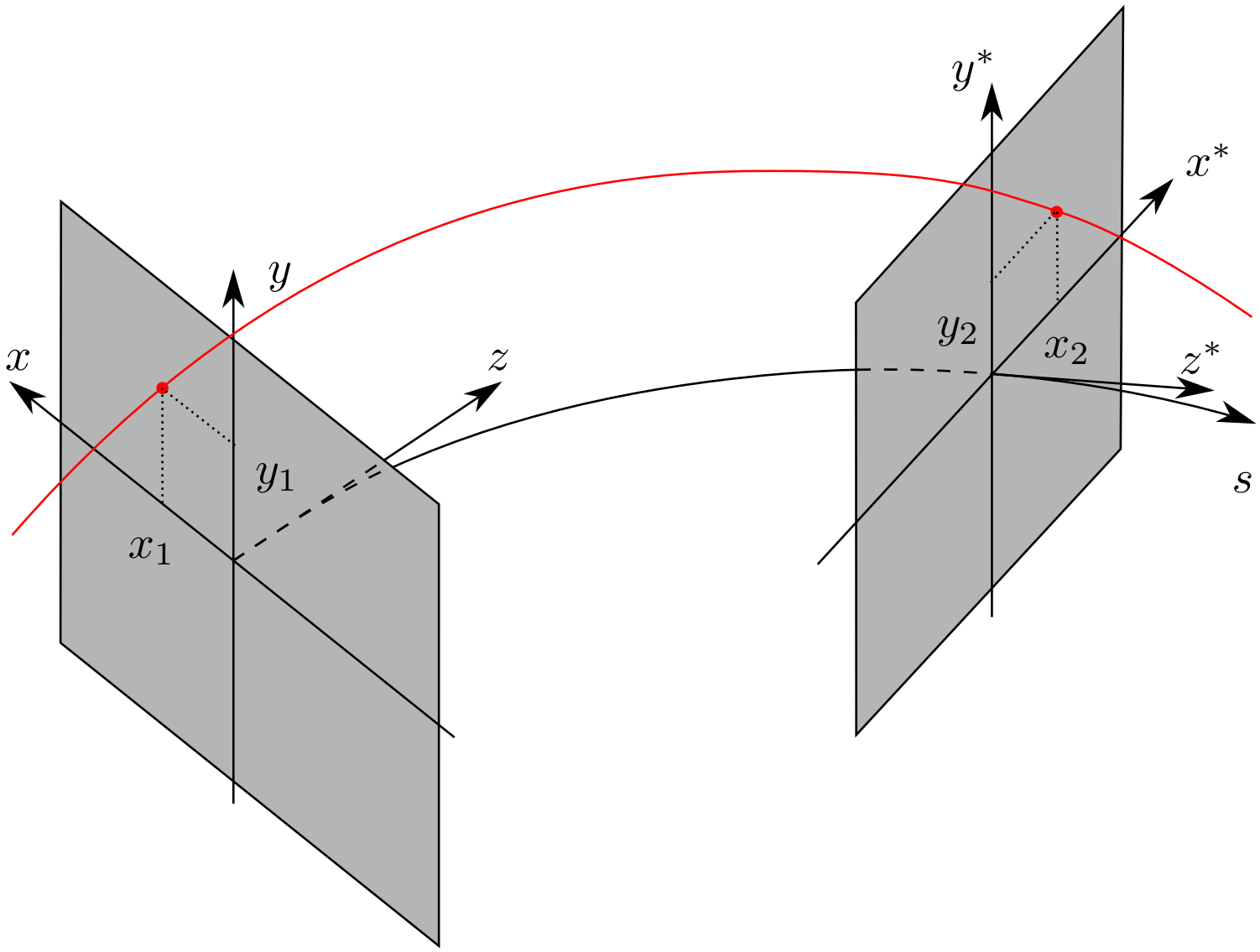

The s-axis is defined by the reference particle and y is "up".

Curvilinear coordinate system

The coordinates of each particle consists of the longitudinal coordinate s, transverse position (x, y) and velocity components (v_x, v_y, v_z).

Also tangents of the trajectory angles, often defined using components of the momentum vector

$$x' = \frac{p_x}{p_z} = \tan(\alpha) \tag{10}$$

$$y' = \frac{p_y}{p_z} = \tan(\beta) \tag{11}$$

are used. Please note that this is not the only convention. Also

$$x' = \frac{p_x}{p_0} \tag{12}$$

is used, where p_0 is the momentum of the reference particle. While x' and y' are not really angles, typically units of rad or mrad are used.

Light optics: ideal thin lens

Why "ion optics"? Ion propagation analogous to propagation of photons in *light optics*, i.e. systems of lenses.

Thin optical lens:

$$\Delta x' = -\frac{x}{f} \tag{13}$$

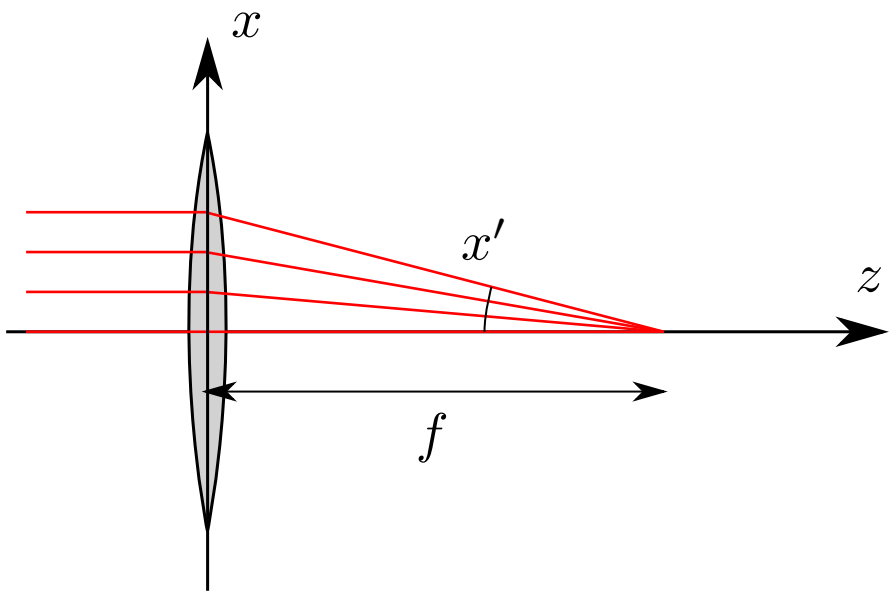

Matrix representation

Each ray of light is described with position x and direction x' conveniently given as components of a vector $\vec{X}$.

As a ray of light passes through elements/matter/anything the results can be described with a function: $\vec{X}_2 = f(\vec{X}_1) = \big(f_1(x, x'), f_2(x, x')\big)$.

According to Taylor, the functions can be represented by an infinite series

$$f_i = a_{i,0} + a_{i,1}x + a_{i,2}x' + a_{i,3}x^2 + a_{i,4}x'^2 + a_{i,5}xx' + \cdots . \tag{14}$$

If coordinate system is chosen wisely, the constant term $a_{i,0} = 0$ and by approximating higher order terms to zero one arrives at a linear model

$$(x_2, x_2') = (a_{1,1}x_1 + a_{1,2}x_1', a_{2,1}x_1 + a_{2,2}x_1') \tag{15}$$

conveniently given by matrix multiplication

$$\vec{X}_2 = \begin{pmatrix} a_{1,1} & a_{1,2} \\ a_{2,1} & a_{2,2} \end{pmatrix} \vec{X}_1. \tag{16}$$

Matrix representation of thin lens

In a thin lens, position of the light ray can not change:

$$x_2 = x_1. \tag{17}$$

The angle changes due to focusing action as given before: $\Delta x' = -x/f$, now written as

$$x_2' = x_1' - x_1/f. \tag{18}$$

These equations can be written as a matrix:

$$\begin{pmatrix} x_2 \\ x_2' \end{pmatrix} = \begin{pmatrix} 1 & 0 \\ -1/f & 1 \end{pmatrix} \begin{pmatrix} x_1 \\ x_1' \end{pmatrix}. \tag{19}$$

Matrix representation of drift space

In empty space of length L, the position of the light ray changes as

$$x_2 = x_1 + x_1' L. \tag{20}$$

The angle does not change.

$$x_2' = x_1'. \tag{21}$$

Equations as a matrix:

$$\begin{pmatrix} x_2 \\ x_2' \end{pmatrix} = \begin{pmatrix} 1 & L \\ 0 & 1 \end{pmatrix} \begin{pmatrix} x_1 \\ x_1' \end{pmatrix}. \tag{22}$$

Transport of light ray using matrices

A light ray passing through an optical system with drift length L_1, a thin lens with focal length f and a drift length L_2 is described by

$$\begin{pmatrix} x_4 \\ x_4' \end{pmatrix} = \begin{pmatrix} 1 & L_2 \\ 0 & 1 \end{pmatrix} \begin{pmatrix} 1 & 0 \\ -1/f & 1 \end{pmatrix} \begin{pmatrix} 1 & L_1 \\ 0 & 1 \end{pmatrix} \begin{pmatrix} x_1 \\ x_1' \end{pmatrix} . \tag{23}$$

According to matrix algebra we can evaluate the matrix multiplications giving

$$\begin{pmatrix} x_4 \\ x_4' \end{pmatrix} = \begin{pmatrix} 1 - L_2/f & L_1 + L_2 - L_1 L_2/f) \\ -1/f & 1 - L_1/f \end{pmatrix} \begin{pmatrix} x_1 \\ x_1' \end{pmatrix} . \tag{24}$$

What does this mean?

Meaning of matrix elements

Earlier we presented the matrix transport equation as

$$\begin{pmatrix} x_2 \\ x_2' \end{pmatrix} = \begin{pmatrix} a_{1,1} & a_{1,2} \\ a_{2,1} & a_{2,2} \end{pmatrix} \begin{pmatrix} x_1 \\ x_1' \end{pmatrix} . \tag{25}$$

What are these $a_{i,j}$ *transfer coefficients*? Often used nomenclature uses $(x|x')$ to mark the effect of x' to x. The whole transport equation then becomes

$$\begin{pmatrix} x_2 \\ x_2' \end{pmatrix} = \begin{pmatrix} (x|x) & (x|x') \\ (x'|x) & (x'|x') \end{pmatrix} \begin{pmatrix} x_1 \\ x_1' \end{pmatrix} . \tag{26}$$

Meaning of matrix elements

Useful special cases, where one of the elements is zero

$(x|x') = 0$

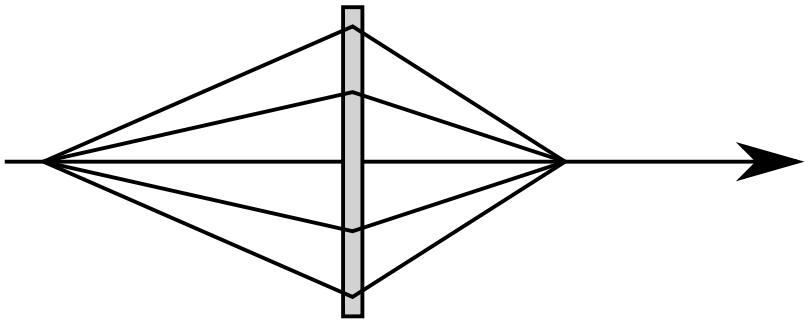

$(x'|x) = 0$

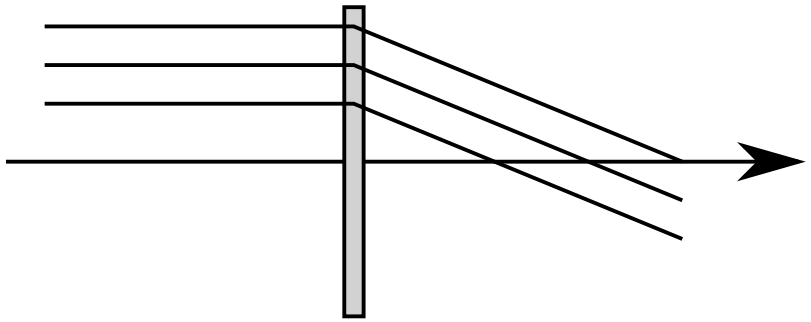

$(x|x) = 0$

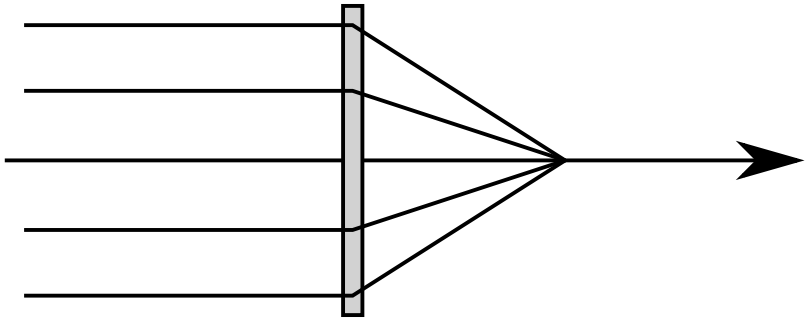

$(x'|x') = 0$

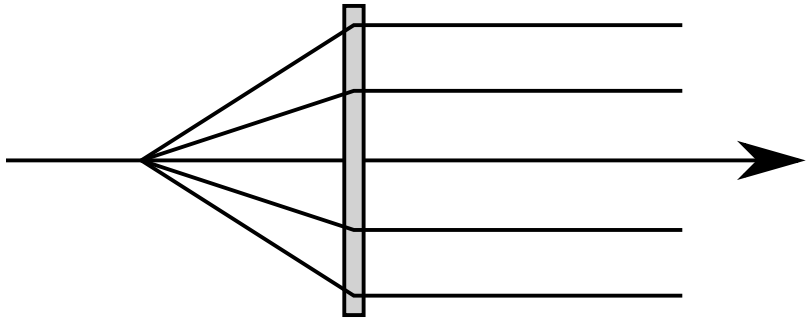

Back to the lens system

Requiring point-to-point focusing, $(x|x') = 0$ on matrix Eq. (24):

$$\begin{pmatrix} x_4 \\ x_4' \end{pmatrix} = \begin{pmatrix} 1 - L_2/f & L_1 + L_2 - L_1 L_2/f) \\ -1/f & 1 - L_1/f \end{pmatrix} \begin{pmatrix} x_1 \\ x_1' \end{pmatrix}.$$

is

$$L_1 + L_2 - L_1 L_2/f = 0, \tag{27}$$

which can also be written more familiarly as

$$\frac{1}{L_1} + \frac{1}{L_2} = \frac{1}{f}, \tag{28}$$

i.e. *the lens equation*. In that case, the first line of the matrix equation

$$x_4 = 1 - \frac{L_2}{f} x_1 \tag{29}$$

gives the magnification of the lens system.

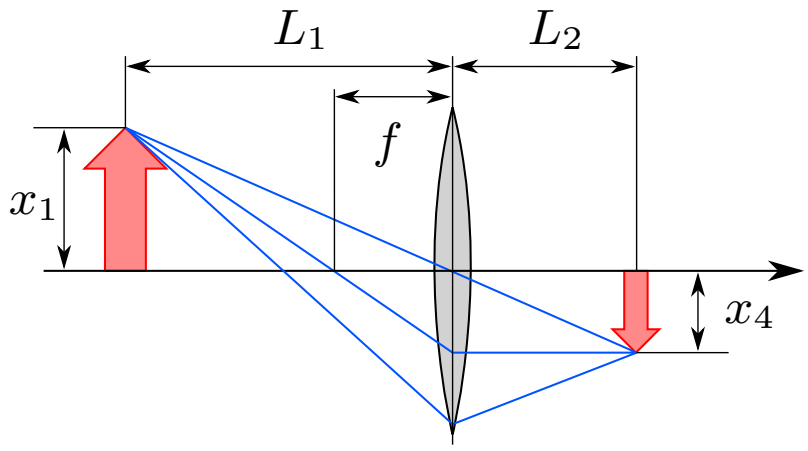

Ion optical elements

- Consists of electric and magnetic fields
- Particle trajectories from Lorentz force: $\vec{F} = q(\vec{E} + \vec{v} \times \vec{B})$
- Fields usually from a mathematically simple set and assumed to be confined within a finite length L from s_1 to s_2.
- Perform the needed operations: bending, focusing, accerating, separating, ...
- Majority of ion optical elements are so-called transverse field or *multipole* elements with $B_z = E_z = 0$.
- First: electrostatic gap lenses

Particle trajectories in uniform electrostatic field

Charged particle is accelerated through a uniform electric field.

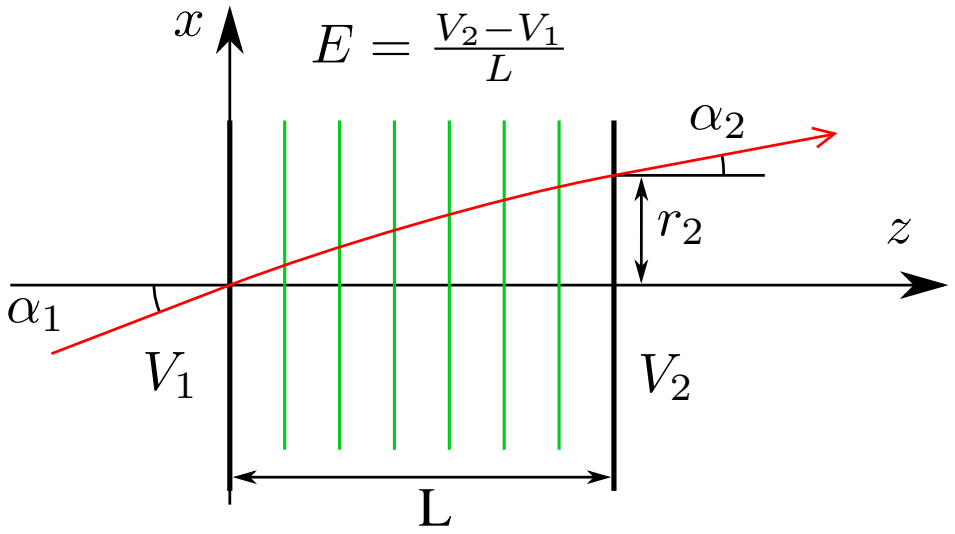

Equations of motion are (assuming $z_1 = 0$ and $x_1 = 0$ at $t = 0$):

$$a_z = \frac{qE}{m} \tag{30}$$

$$v_z = v_1 \cos\alpha_1 + \frac{qE}{m}t \tag{31}$$

$$z = v_1 \cos\alpha_1 \cdot t + \frac{qE}{2m}t^2 \tag{32}$$

$$x = v_1 \sin\alpha_1 \cdot t \tag{33}$$

Particle trajectories in uniform electrostatic field

Solving the quadratic for t gives

$$t = \frac{mv_1}{qE}\left(\sqrt{\cos^2\alpha_1 + \frac{2qE}{mv_1}z} - \cos\alpha_1\right) \tag{34}$$

and therefore (using $v_1 = \sqrt{\frac{2qV_1}{m}}$):

$$x = \frac{2V_1}{E}\sin\alpha_1\left(\sqrt{\frac{E}{V_1}z\cos^2\alpha_1} - \cos\alpha_1\right). \tag{35}$$

Here

$$\frac{E}{V_1} = \frac{V_2 - V_1}{L}\frac{1}{V_1} = \frac{1}{L}\left(\frac{V_2}{V_1} - 1\right) \tag{36}$$

and thus at $z = L$,

$$x_2 = \frac{2L\sin\alpha_1}{\frac{V_2}{V_1} - 1}\left(\sqrt{\frac{V_2}{V_1} - \sin^2\alpha_1} - \cos\alpha_1\right). \tag{37}$$

Particle trajectories in uniform electrostatic field

The slope is found by differentiating eq. (35):

$$x' = \frac{dx}{dz} = \sin\alpha_1 \left(\frac{E}{V_1} z + \cos^2 \alpha_1 \right)^{-1/2} . \tag{38}$$

and thus

$$x'_2 = \frac{dx}{dz} = \sin\alpha_1 \left(\frac{V_2}{V_1} - \sin^2 \alpha_1 \right)^{-1/2} . \tag{39}$$

From these results one can define the *refractive index* for electric field:

$$\frac{\sin\alpha_2}{\sin\alpha_1} = \sqrt{\frac{V_1}{V_2}} \tag{40}$$

Particle trajectories in uniform electrostatic field

In the *paraxial approximation* ($\alpha_i \ll 1$): $\sin\alpha_1 \approx x_1'$, $\cos\alpha_1 \approx 1$ and $x_1' \ll \frac{V_2}{V_1}$:

$$x_2 \approx \frac{2Lx_1'}{\frac{V_2}{V_1}-1}\left(\sqrt{\frac{V_2}{V_1}}-1\right) = \frac{2L}{\sqrt{\frac{V_2}{V_1}}+1}\,x_1' \tag{41}$$

and

$$x_2' \approx \sqrt{\frac{V_1}{V_2}}\,x_1'. \tag{42}$$

In the transfer matrix form one can represent the result as

$$\begin{pmatrix} x_2 \\ x_2' \end{pmatrix} = \begin{pmatrix} 1 & \frac{2L}{\sqrt{V_1/V_2}+1} \\ 0 & \sqrt{V_1/V_2} \end{pmatrix} \begin{pmatrix} x_1 \\ x_1' \end{pmatrix} \tag{43}$$

Passage through an aperture

Acceleration gap presented above was ideal. Real gaps have apertures for the beam to pass.

Equipotential surfaces bulge through the aperture causing radial field components.

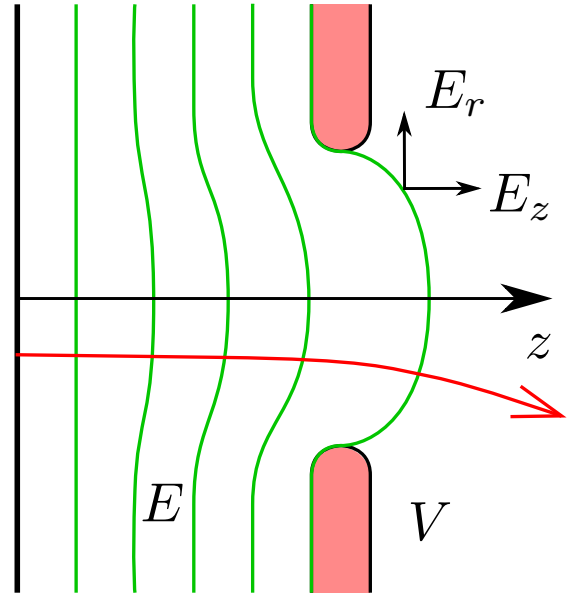

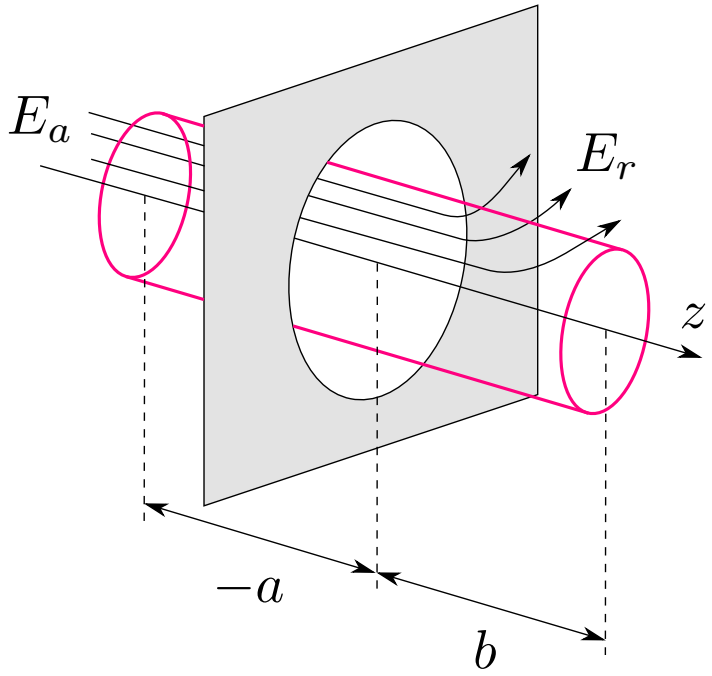

From Gauss law (no charges):

$$\pi r^2 E_a = 2\pi r \int_{z=-a}^{b} E_r dz \qquad (44)$$

A particle passing at distance r from axis experiences a radial impulse leading to

$$mv_r = \int F_r dt \qquad (45)$$

Passage through an aperture

A change of variables from $v_z = dz/dt \Leftrightarrow dt = dz/v_z$ transforms the integral to

$$mv_r = \int F_r dt = \int_{z=-a}^{b} \frac{qE_r}{v_z} dz. \tag{46}$$

In the paraxial approximation the v_z is constant near the aperture and thus we obtain

$$mv_r = \frac{q}{v_z} \int_{z=-a}^{b} E_r dz = \frac{q}{v_z} \frac{rE_a}{2}. \tag{47}$$

The particle trajectory suffers a kink (thin lens approximation)

$$\Delta r' = \frac{v_r}{v_z} = \frac{qE_a}{2mv_z^2} r = \frac{E_a}{4V} r \tag{48}$$

at the aperture.

Passage through an aperture

The general case (not derived) is one, where the aperture is separating two regions of different field strengths.

In such case the focusing action is described with

$$\Delta r' = \frac{E_2 - E_1}{4V} r \tag{49}$$

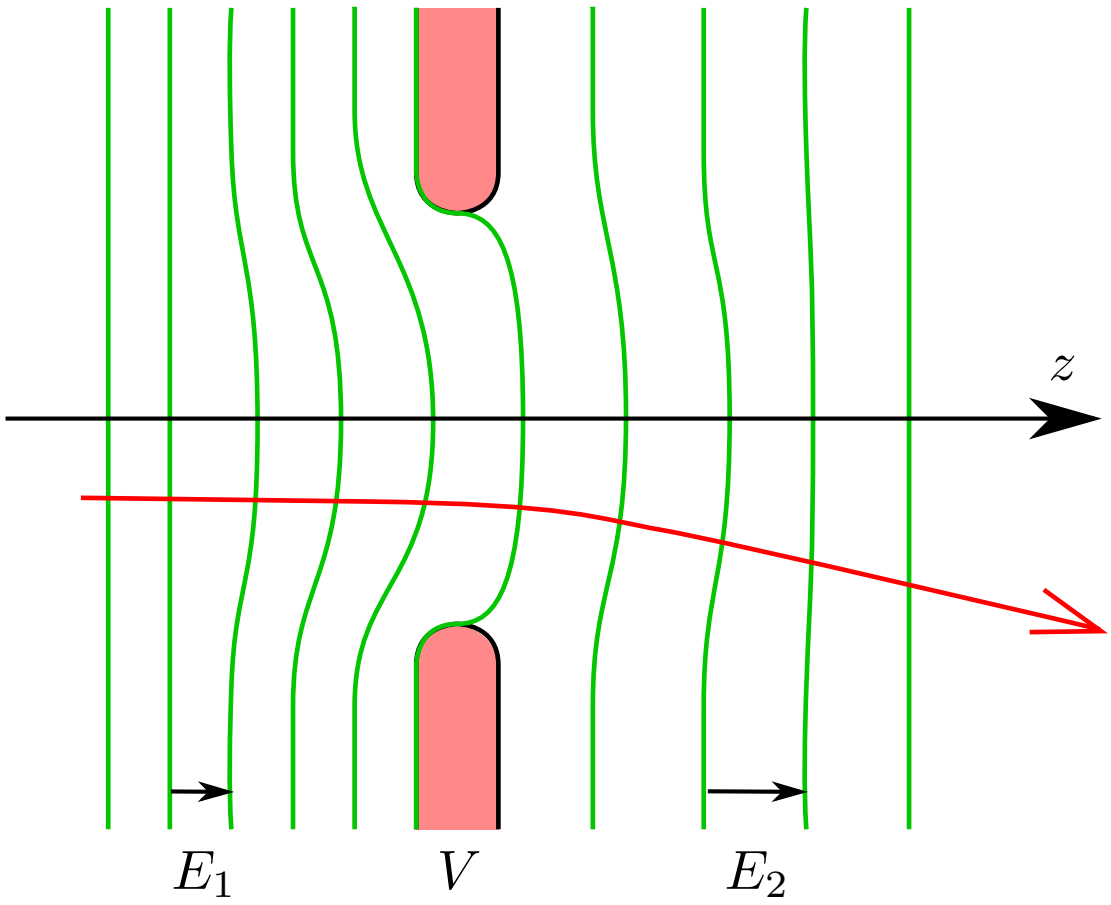

Immersion/Gap lens

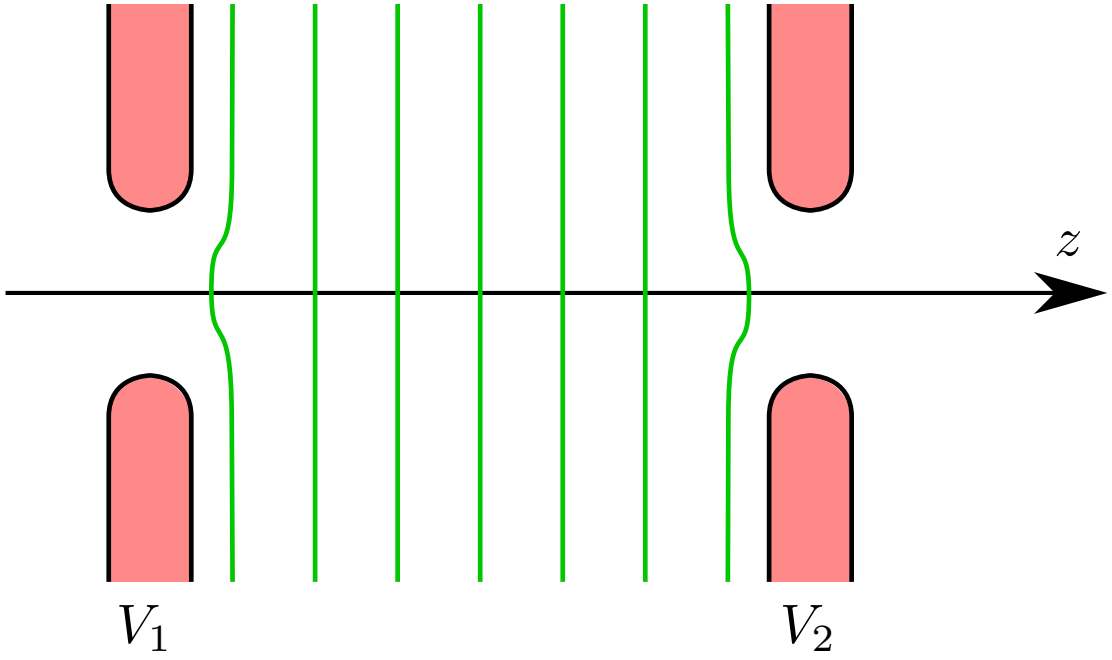

$$\begin{pmatrix} r_2 \\ r_2' \end{pmatrix} = M_{\text{aperture1}} M_{\text{field}} M_{\text{aperture2}} \begin{pmatrix} r_1 \\ r_1' \end{pmatrix}$$

$$\begin{pmatrix} r_2 \\ r_2' \end{pmatrix} = \begin{pmatrix} 1 & 0 \\ \frac{V_2 - V_1}{4V_1 L} & 1 \end{pmatrix} \begin{pmatrix} 1 & \frac{2L}{\sqrt{V_1/V_2}+1} \\ 0 & \sqrt{V_1/V_2} \end{pmatrix} \begin{pmatrix} 1 & 0 \\ \frac{V_1 - V_2}{4V_2 L} & 1 \end{pmatrix} \begin{pmatrix} r_1 \\ r_1' \end{pmatrix} \quad (50)$$

Einzel lens

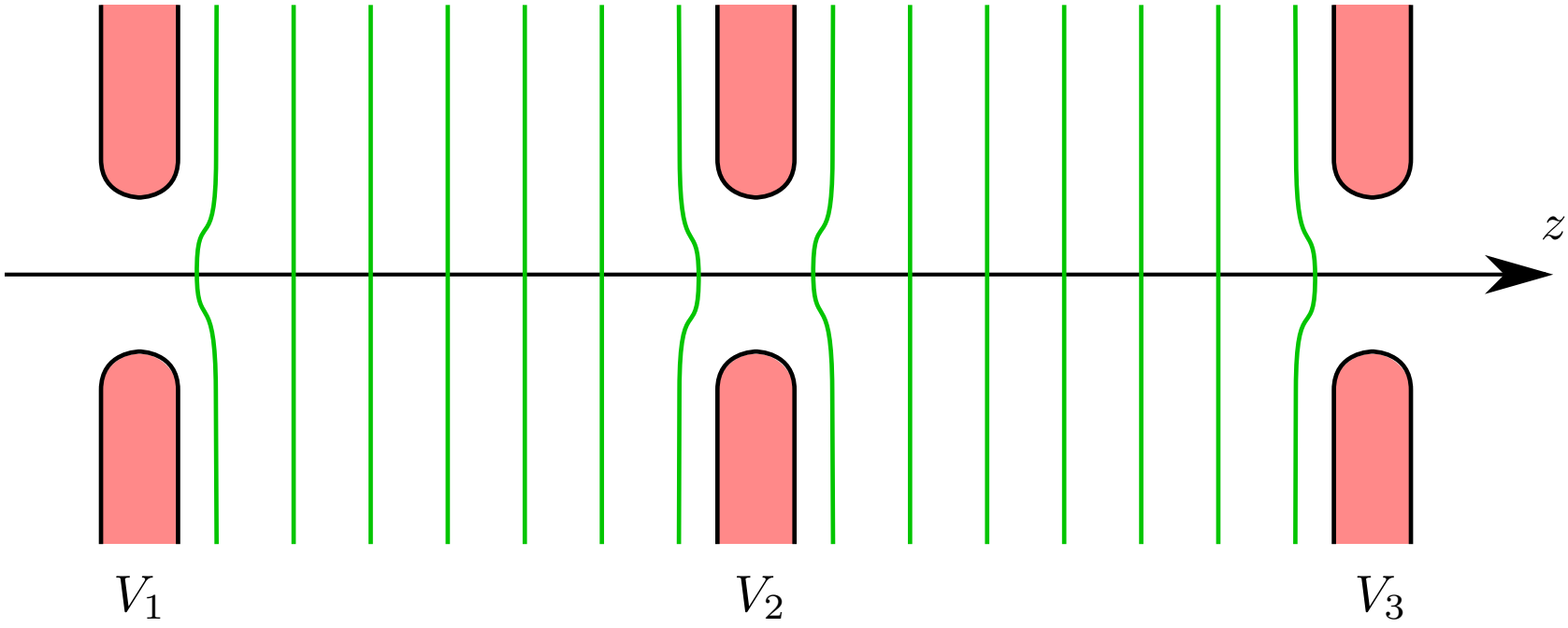

$$\begin{pmatrix} r_2 \\ r_2' \end{pmatrix} = \begin{pmatrix} 1 & 0 \\ \frac{V_2 - V_1}{4V_1 L} & 1 \end{pmatrix} \begin{pmatrix} 1 & \frac{2L}{\sqrt{V_1/V_2}+1} \\ 0 & \sqrt{V_1/V_2} \end{pmatrix} \begin{pmatrix} 1 & 0 \\ \frac{V_3 + V_1 - 2V_2}{4V_2 L} & 1 \end{pmatrix}$$
$$\begin{pmatrix} 1 & \frac{2L}{\sqrt{V_2/V_3}+1} \\ 0 & \sqrt{V_2/V_3} \end{pmatrix} \begin{pmatrix} 1 & 0 \\ \frac{V_3 - V_2}{4V_3 L} & 1 \end{pmatrix} \begin{pmatrix} r_1 \\ r_1' \end{pmatrix} \quad (51)$$

Practical electrostatic lenses

In practice, most electrostatic lenses are not well described by analytic formalism.

Modelling usually based on *ray tracing*:

- Calculation of potential map $\phi(x, y, z)$ from geometrical constraints using Poisson equation $\nabla^2 \phi_E = 0$.
- Calculation of fields from potential: $\vec{E} = -\nabla \phi_E$.
- Calculation of particle trajectories with numerical integration of the equations of motion: $\frac{d^2\vec{r}}{dt^2} = \frac{q}{m}\left(\vec{E} + \vec{v} \times \vec{B}\right)$.

NOTE: Calculation of test particles in any field can lead to formation of matrices by fitting of Taylor series coefficients (up to any order).

Practical einzel lenses

Einzel is a cylindrically symmetric focusing lens, which is characterized by voltage ratio

$$R = \frac{V_{\text{einzel}} - V_{\text{tube}}}{V_{\text{tube}}}, \tag{52}$$

where V_{einzel} is the center electrode potential, V_{tube} is the beam tube potential and $V = 0$ is the potential where particle kinetic energy is zero. The einzel lens can be accelerating ($R > 0$) or decelerating ($R < 0$).

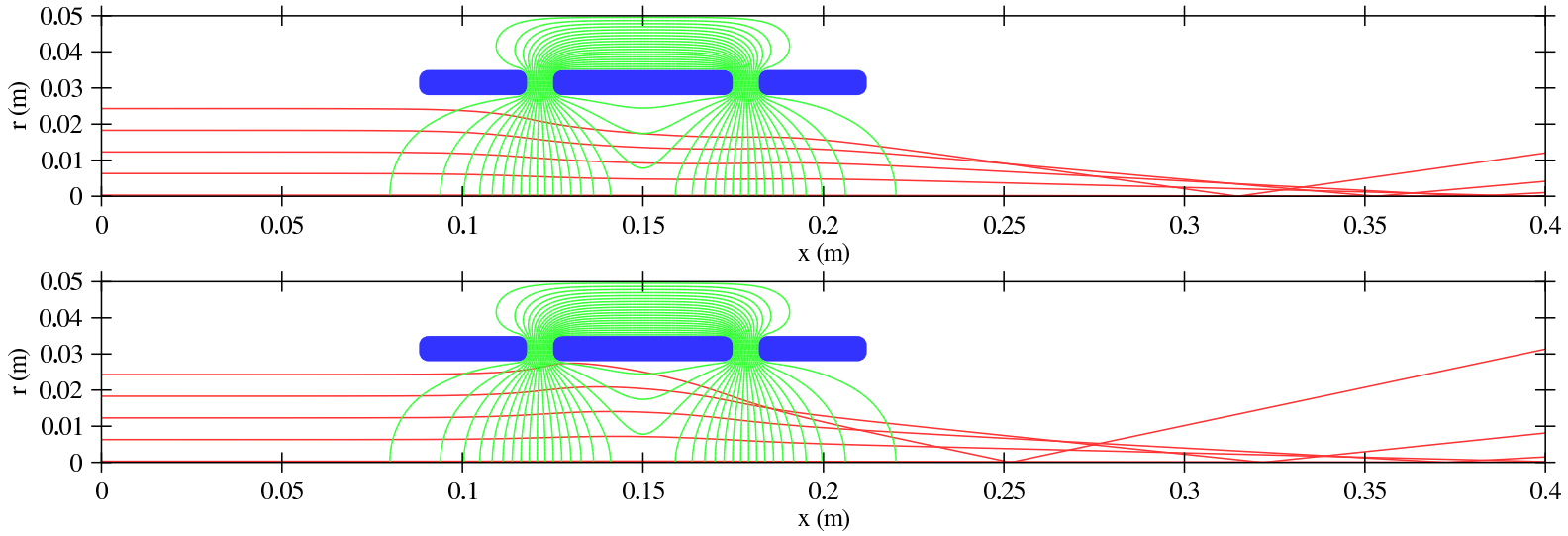

Images from Ion Beam Simulator, IBSimu

Practical einzel lenses

Focusing power as a function of R.

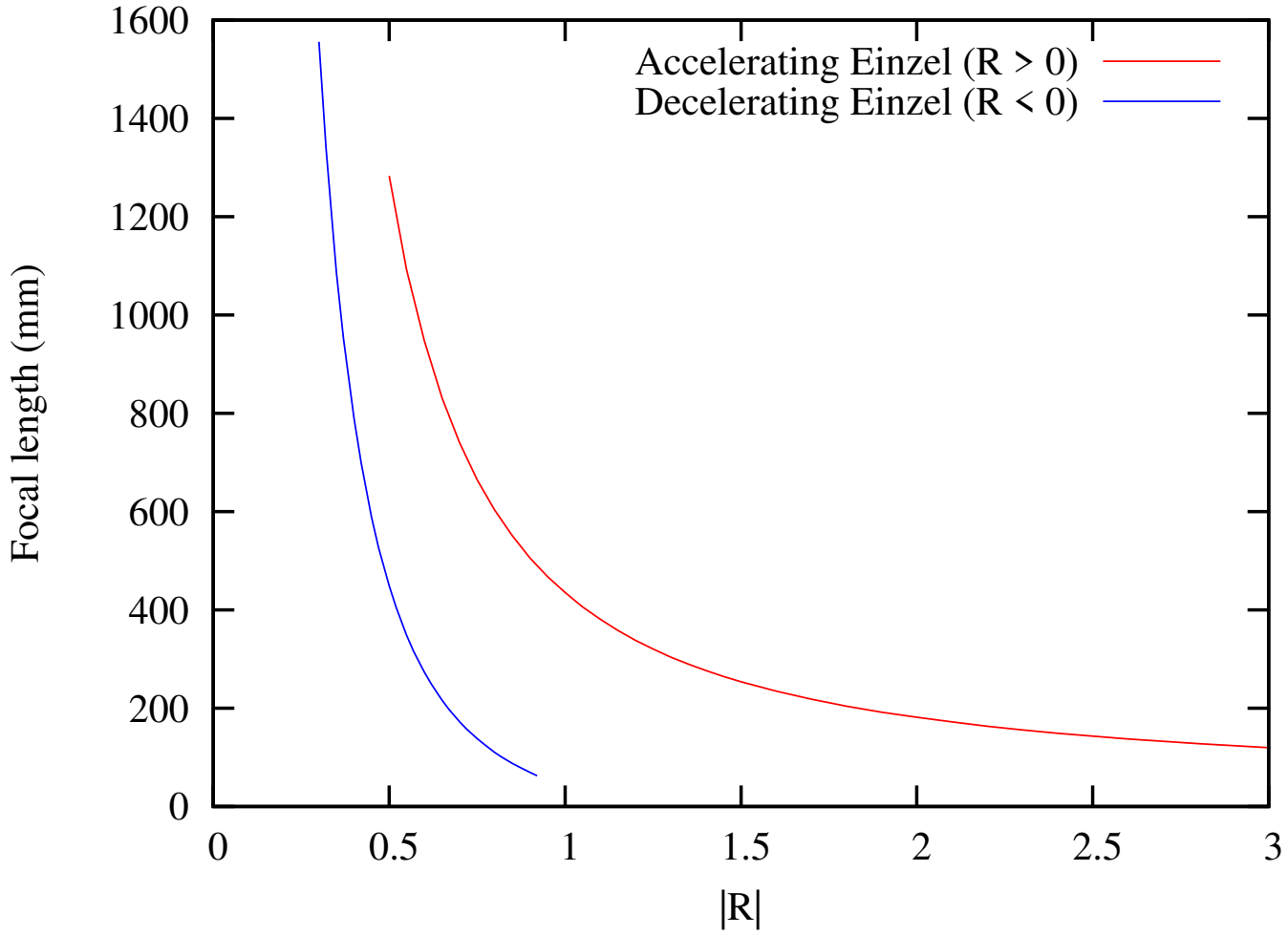

Einzel aberrations

Focal length changes with particle radius

Accelerating

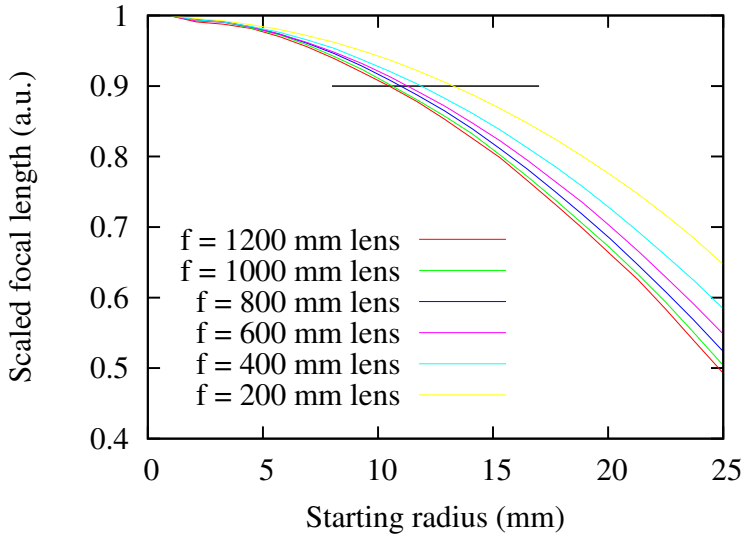

Decelerating

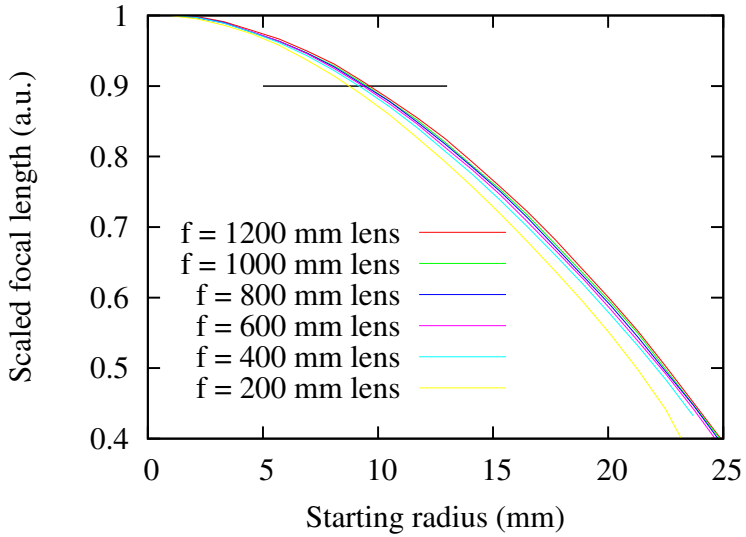

- Beam should fill less than half of the einzel radius (28 mm in the example case).
- Accelerating should be preferred if not voltage/E-field limited (less aberrations, limits space charge compensation leakage)

Multipole expansion for transverse field elements

Electric potential and magnetic potential (marked here with ϕ) in absence of charges and currents fulfill Laplace's equation

$$\nabla^2\phi = 0 \tag{53}$$

with fields solved by

$$\vec{B} = -\nabla\phi_B \qquad \text{and} \qquad \vec{E} = -\nabla\phi_E. \tag{54}$$

In 2D, all physically realizable solutions are represented as

$$\phi = \sum_{n=1}^{\infty}(J_n r^n \cos n\theta + K_n r^n \sin n\theta). \tag{55}$$

Thus, the field components (for $\vec{B}$) are

$$B_r = -\sum_{n=1}^{\infty}(nJ_n r^{n-1} \cos n\theta + nK_n r^{n-1} \sin n\theta) \tag{56}$$

$$B_\theta = -\sum_{n=1}^{\infty}(-nJ_n r^{n-1} \sin n\theta + nK_n r^{n-1} \cos n\theta) \tag{57}$$

Multipole expansion

These infinite series represent all possible field configurations in absence of currents and charges in cylindrical coordinates.

Coefficients J_n and K_n are determined by geometry, i.e. steel and coils for magnets and electrode geometry for electric fields.

Convenient and practical *multipole elements* can be constructed, for which the field consist primarily of single order (n) terms.

In cartesian coordinates, the components are

$$B_x = B_r \cos\theta - B_\theta \sin\theta \tag{58}$$

$$B_y = B_r \sin\theta + B_\theta \cos\theta \tag{59}$$

Dipole, $n = 1$

Cylindrical:

$$B_r = J_1 \cos\theta + K_1 \sin\theta \tag{60}$$

$$B_\theta = -J_1 \sin\theta + K_1 \cos\theta \tag{61}$$

$$\phi = J_1 r \cos\theta + K_1 r \sin\theta \tag{62}$$

Cartesian:

$$B_x = J_1 \tag{63}$$

$$B_y = K_1 \tag{64}$$

$$\phi = J_1 x + K_1 y \tag{65}$$

Choosing $J_1 = 0$ gives vertical magnetic dipole field:

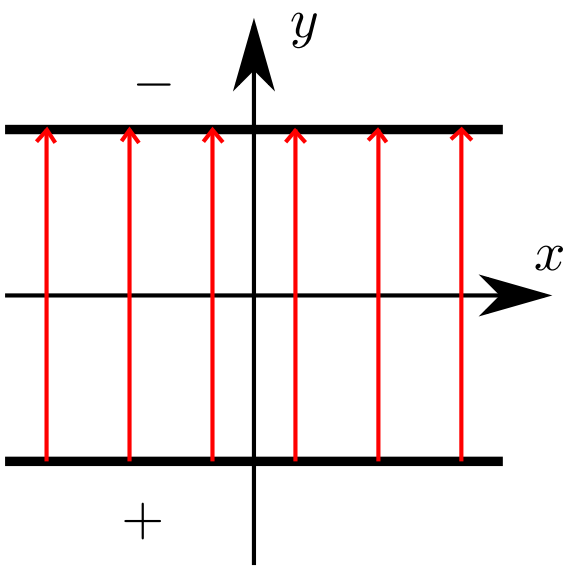

Quadrupole, $n = 2$

Cylindrical:

$$B_r = 2J_2 r \cos 2\theta + 2K_2 r \sin 2\theta \tag{66}$$

$$B_\theta = -2J_2 r \sin 2\theta + 2K_2 r \cos 2\theta \tag{67}$$

$$\phi = J_2 r^2 \cos 2\theta + K_2 r^2 \sin 2\theta \tag{68}$$

Cartesian:

$$B_x = 2(J_2 x + K_2 y) \tag{69}$$

$$B_y = 2(-J_2 y + K_2 x) \tag{70}$$

$$\phi = J_2(x^2 + y^2) + 2K_2 xy \tag{71}$$

Choosing $J_2 = 0$ gives xy magnetic quadrupole field:

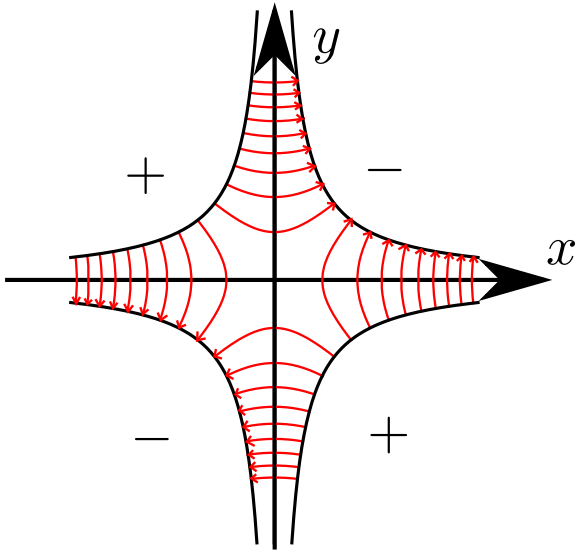

Sextupole, $n = 3$

Cylindrical:

$$B_r = 3J_3 r^2 \cos 3\theta + 3K_3 r^2 \sin 3\theta \tag{72}$$

$$B_\theta = -3J_3 r^2 \sin 3\theta + 3K_3 r^2 \cos 3\theta \tag{73}$$

$$\phi = J_3 r^3 \cos 3\theta + K_3 r^3 \sin 3\theta \tag{74}$$

Cartesian:

$$B_x = 3\big(J_3(x^2 - y^2) + 2K_3 xy\big) \tag{75}$$

$$B_y = 3\big(-2J_3 xy + K_3(x^2 - y^2)\big) \tag{76}$$

$$\phi = J_3(x^3 - 3y^2 x) + K_3(3yx^2 - y^3) \tag{77}$$

Choosing $J_3 = 0$ gives "normal" magnetic sextupole field:

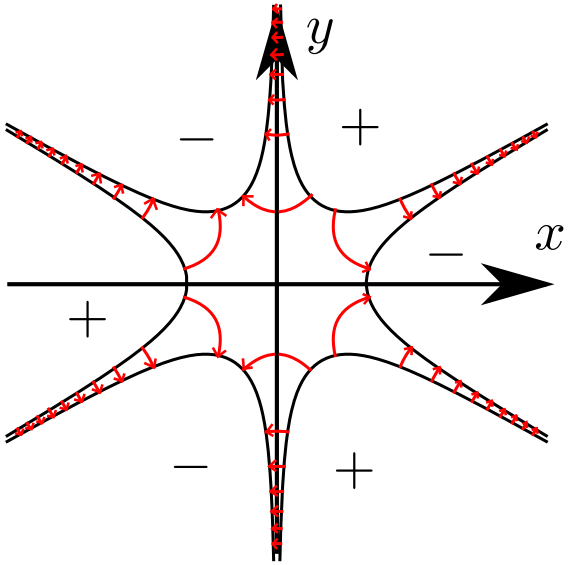

Magnetic steering (dipole)

Constant $\vec{B} = B_0\hat{y}$ at right angle to velocity causes circular particle motion with radius

$$r = \frac{mv}{qB}. \tag{78}$$

The beam bend θ depends on the radius of curvature via

$$L = r\sin\theta \approx r\theta \tag{79}$$

and thus

$$\theta \approx \frac{qBL}{mv} \tag{80}$$

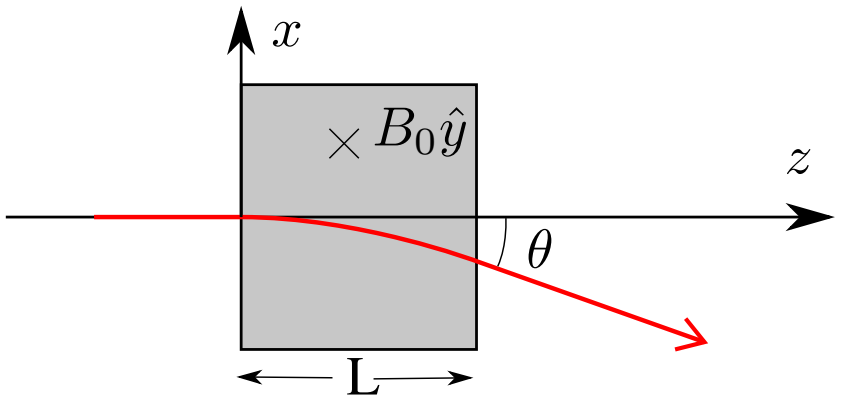

JYFL injection line XY steering magnets

Coils consist of 2×94 rounds of $\varnothing 2$ mm copper wire wound around regular low-grade (AISI 1010) steel.

FEMM 2D simulation: A 10 A excitation produces an ~ 18 mT field.

Ar^{8+} with source potential $U_0 = 10$ kV:

$$\theta = \frac{qBL}{mv} = \frac{qBL}{m}\sqrt{\frac{m}{2qU_0}} = BL\sqrt{\frac{q}{2mU_0}} \tag{81}$$

$$= 18\ \text{mT} \cdot 0.1\ \text{m}\sqrt{\frac{8\text{e}}{2 \cdot 40\text{u} \cdot 10\ \text{kV}}} \approx 56\ \text{mrad} \approx 3.2^\circ \tag{82}$$

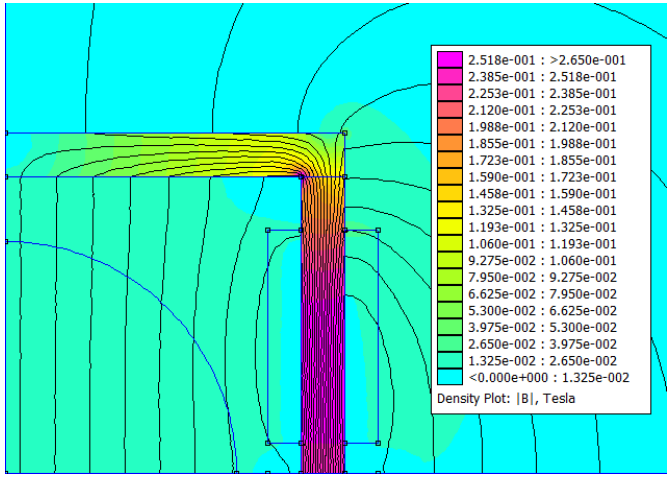

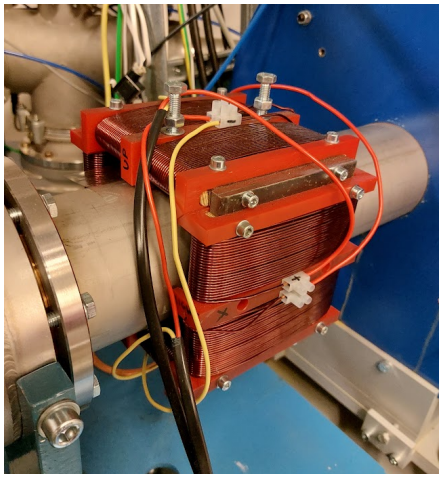

Parallel plates for beam deflection

Simplest possible electrostatic dipole

$$v_z^2 = 2\frac{q}{m}U_0$$

$$v_x = a_x \Delta t = \frac{q}{m}E_x\frac{L}{v_z}$$

$$\theta \approx \frac{v_x}{v_z} = \frac{q}{m}E_x\frac{L}{v_z^2}$$

$$\theta = \frac{U_{\text{plate}}L}{U_0}d$$

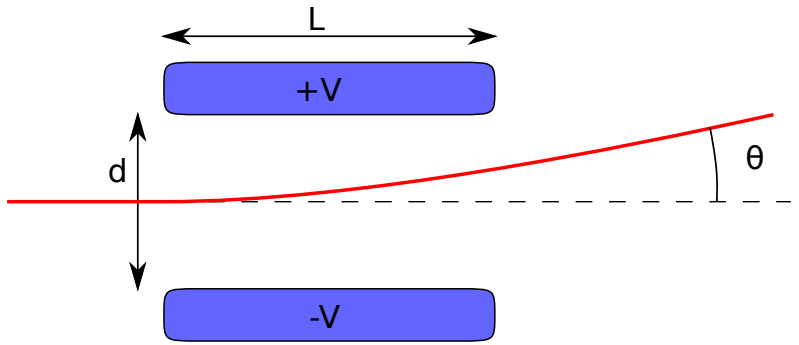

Good example: q and m do not effect trajectories in electrostatic systems.

Trajectories are defined by geometry and relative potentials.

Electrostatic vs. magnetic optics

- Electrostatic fields do not separate ion species.
  - Same focusing for all species.
  - Magnetic: separation of relevant beam.
- Electrostatic lenses are more compact.
- Power efficiency: electrostatic $\sim$1 W, magnetic $\sim$1000 W,
  water cooling usually required for magnetic elements.
- Space charge compensation can be conserved in magnetic lenses.
- Magnets are spark-free.
- Bending power: $\vec{F}_{\mathrm{E}} = q\vec{E}$ vs $\vec{F}_{\mathrm{b}} = q\vec{v} \times \vec{B}$. Typically electrostatic systems have max. 10 MV/m, conventional magnets max. 1.5 T. Magnetic optics is more suitable for high energy beams.
  Forces are equal at $v = \frac{E}{B} = 7 \cdot 10^6$ m/s (200 keV/u).

Magnetic dipole lenses

In addition to bending, homogenous sector magnet focuses in bending plane (x)

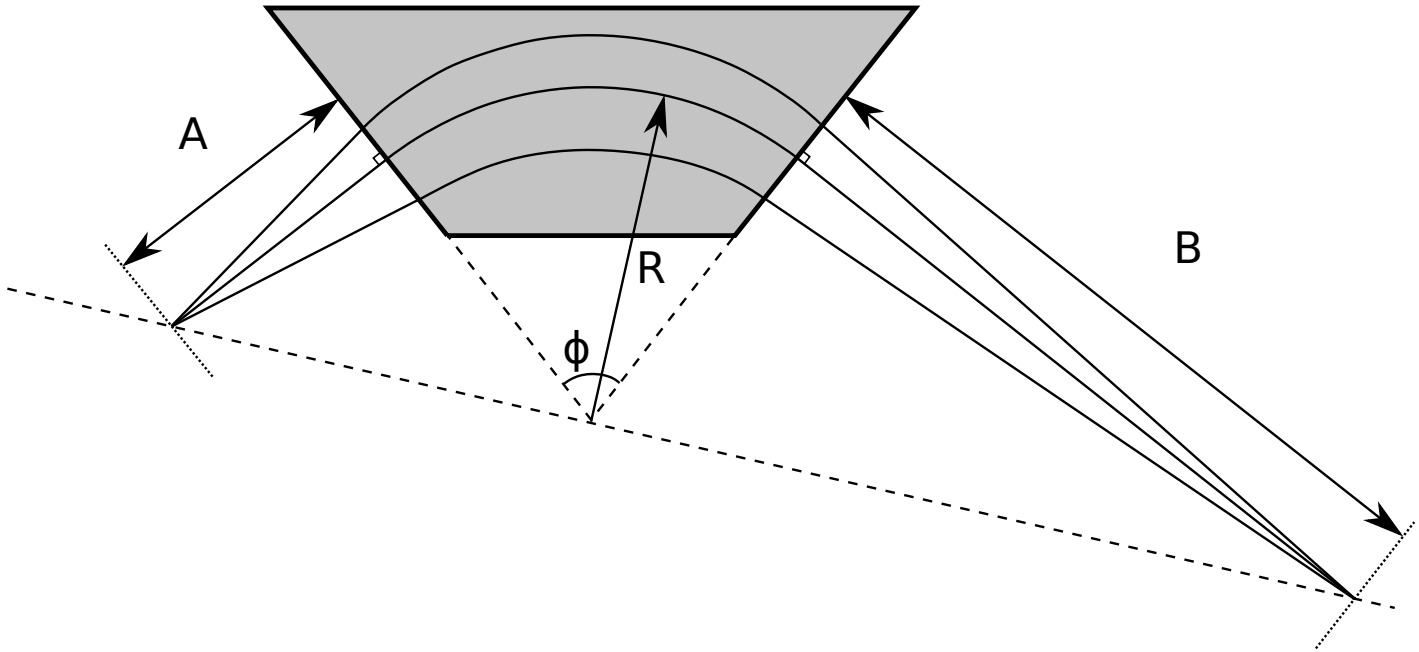

Barber's rule: center of curvature and two focal points are on a straight line

For symmetric setup: $A = B = R/\tan(\frac{\phi}{2})$
For a 90 degree magnet: $A = B = R$

No focusing power in transverse plane (y)

Magnetic dipole lenses

If magnet edge angles deviate from $90°$, the focusing power in x-direction can be adjusted.

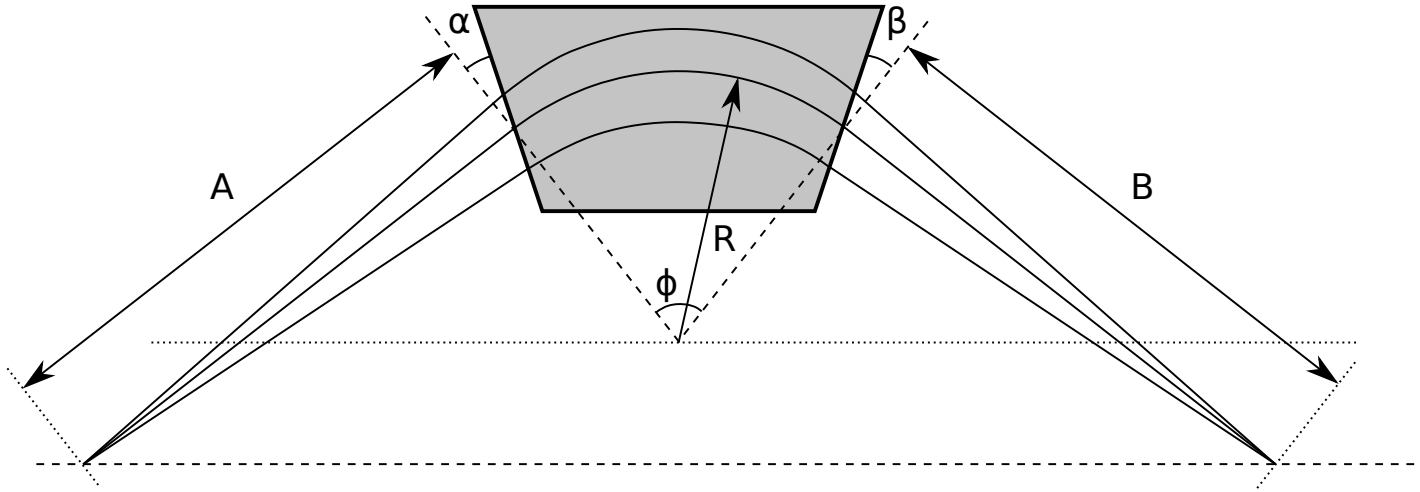

Positive angle (as shown in figure) $\Rightarrow$ less focusing power in x-direction.
Negative angle $\Rightarrow$ more focusing power in x-direction.

Magnetic dipole lenses

The fringing fields provide focusing in y-direction if edge angle (α and β) positive.

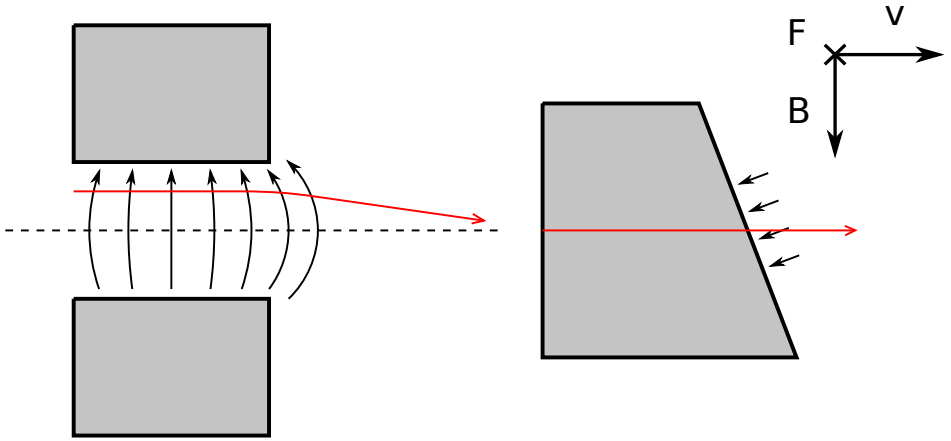

Focusing in x-direction can be traded for y-focusing: $f_y = \frac{R}{\tan(\alpha)}$

Important case: symmetric (same focal length in x and y) double focusing dipole:

$$2\tan(\alpha) = 2\tan(\beta) = \tan(\frac{\phi}{2})$$

$$A = B = \frac{2R}{\tan(\frac{\phi}{2})}$$

For $\phi = 90^\circ$, $\alpha = \beta = 26.6^\circ$ and $A = B = 2R$.

Magnetic dipole applications

Important applications for magnetic dipoles

- Bending
- Species analysis/selection
- Switching magnets

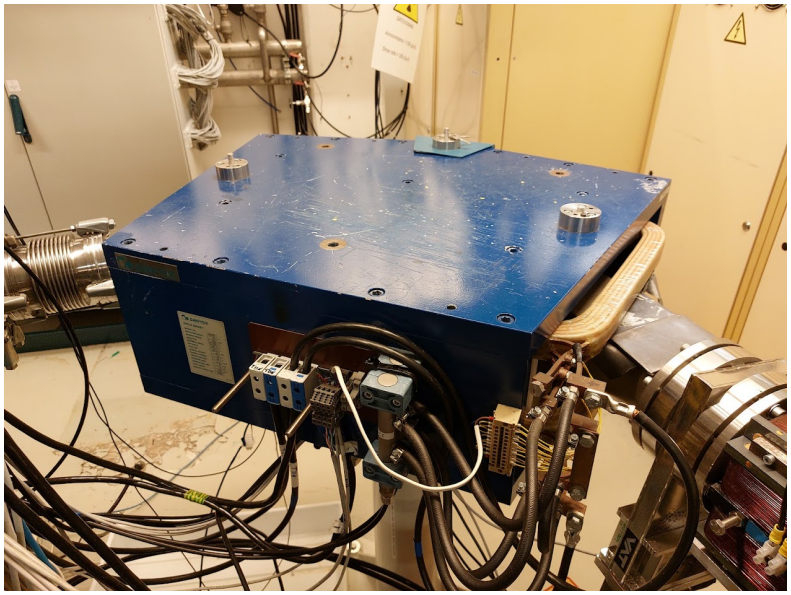

DJ1 dipole (JYFL-ECR2)

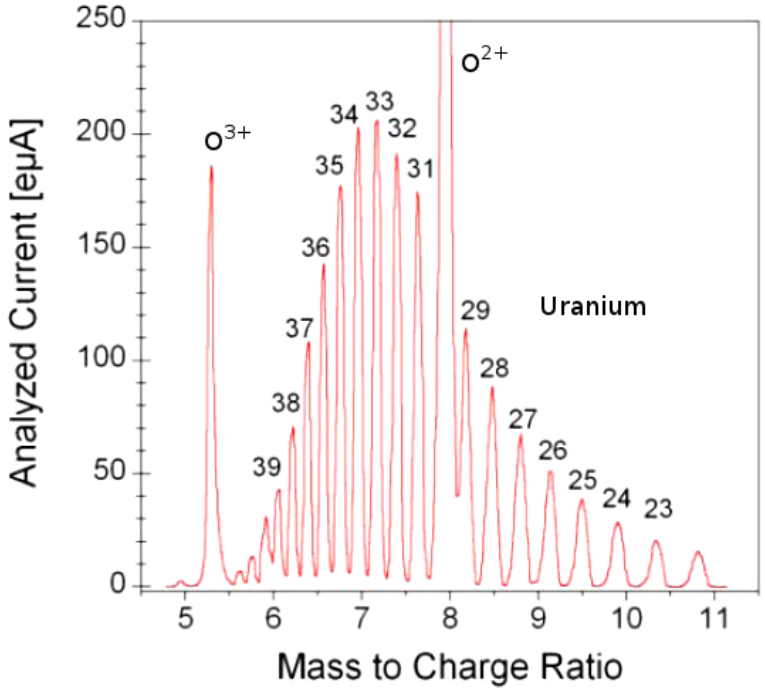

Image from D. Leitner, BIW 2010

Quadrupole focusing

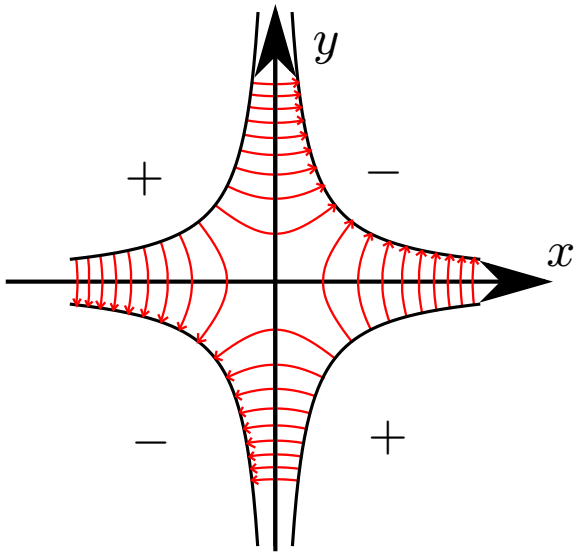

From page 62:

$$B_x = B_0 \frac{y}{r_0} \tag{83}$$

$$B_y = B_0 \frac{x}{r_0} \tag{84}$$

First approximation: velocity in z-direction

$$\vec{F} = q\vec{v} \times B = qv_z(B_x\hat{y} - B_y\hat{x}) = qv_z \frac{B_0}{r_0}(y\hat{y} - x\hat{y}) \tag{85}$$

Linear dependency on position just like a thin lens!

Focusing in x, defocusing in y (or other way round if $B_0 < 0$)!

Quadrupole transfer matrix

Starting from the equations of motion

$$m\frac{d^2x}{dt^2} = -qv_z\frac{B_0}{r_0}x \qquad \text{and} \qquad m\frac{d^2y}{dt^2} = qv_z\frac{B_0}{r_0}y, \tag{86}$$

changing variables with the chain rule

$$\frac{d^2x}{dt^2} = \frac{d^2x}{dz^2}\frac{d^2z}{dt^2} = \frac{d^2x}{dz^2}\left(\frac{dz}{dt}\right)^2 = x''v_z^2 \tag{87}$$

one arrives at

$$x'' = -k^2x \qquad \text{and} \qquad y'' = k^2y, \tag{88}$$

where

$$k^2 = \frac{qB_0}{r_0mv_z} \tag{89}$$

For positive k^2 the solution is

$$x(z) = c_1\cos(kz) + s_1\sin(kz) \tag{90}$$

$$y(z) = c_2\cosh(kz) + s_2\sinh(kz) \tag{91}$$

Quadrupole transfer matrix

Further, by using the initial conditions for the trajectory (x, x', y and y') one can solve the unknown coefficients and arrives at

$$\begin{pmatrix} x_2 \\ x_2' \end{pmatrix} = \begin{pmatrix} \cos(kL) & \frac{1}{k}\sin(kL) \\ -k\sin(kL) & \cos(kL) \end{pmatrix} \begin{pmatrix} x_1 \\ x_1' \end{pmatrix} \tag{92}$$

$$\begin{pmatrix} y_2 \\ y_2' \end{pmatrix} = \begin{pmatrix} \cosh(kL) & \frac{1}{k}\sinh(kL) \\ k\sinh(kL) & \cosh(kL) \end{pmatrix} \begin{pmatrix} y_1 \\ y_1' \end{pmatrix}, \tag{93}$$

where L is the length of the quadrupole in z-direction.

Quadrupole focusing

How to achieve focusing in both directions: Quadrupole doublet!

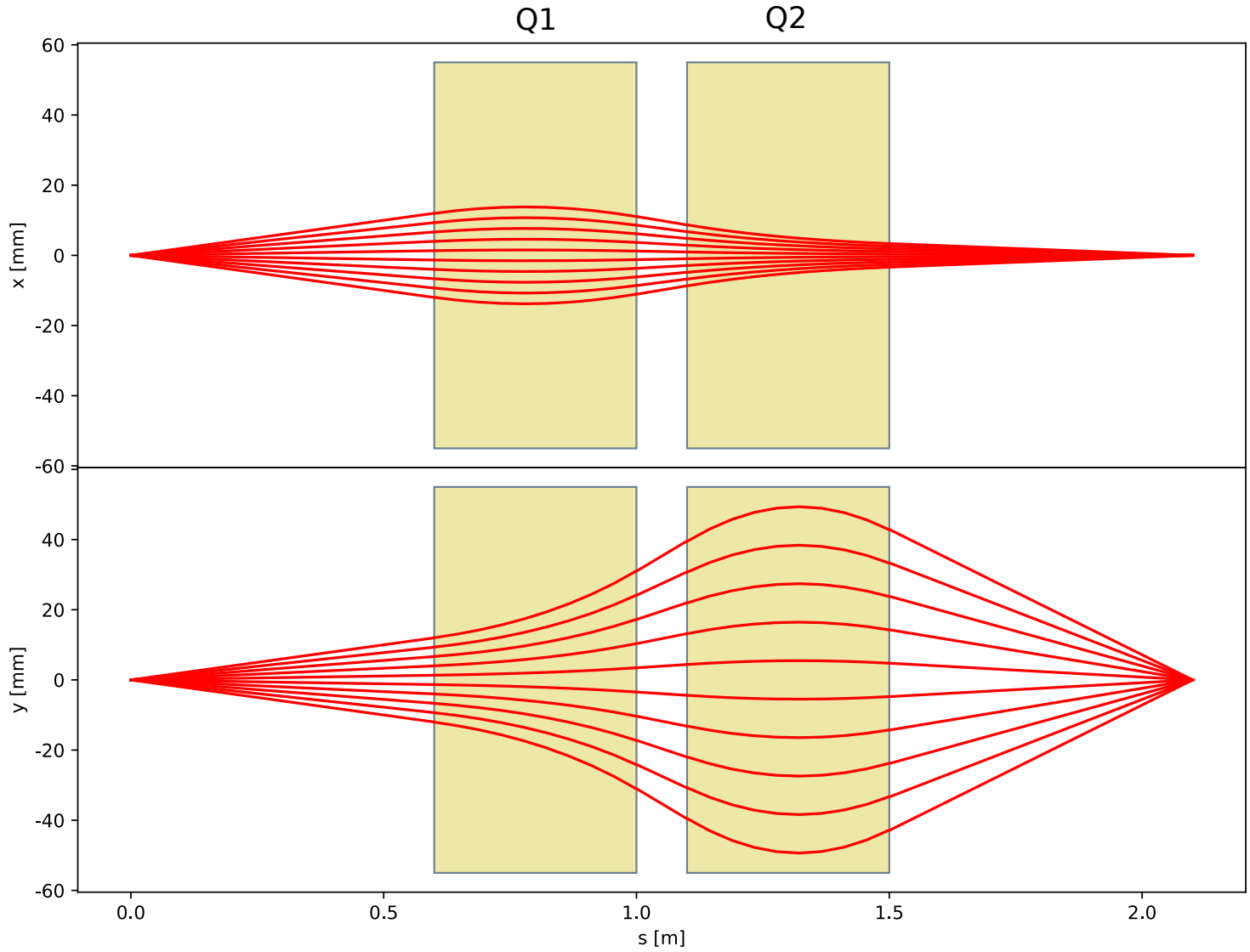

Image from Python Ion Optics Library, PIOL

Quadrupole focusing

Other alternative: quadrupole triplet!

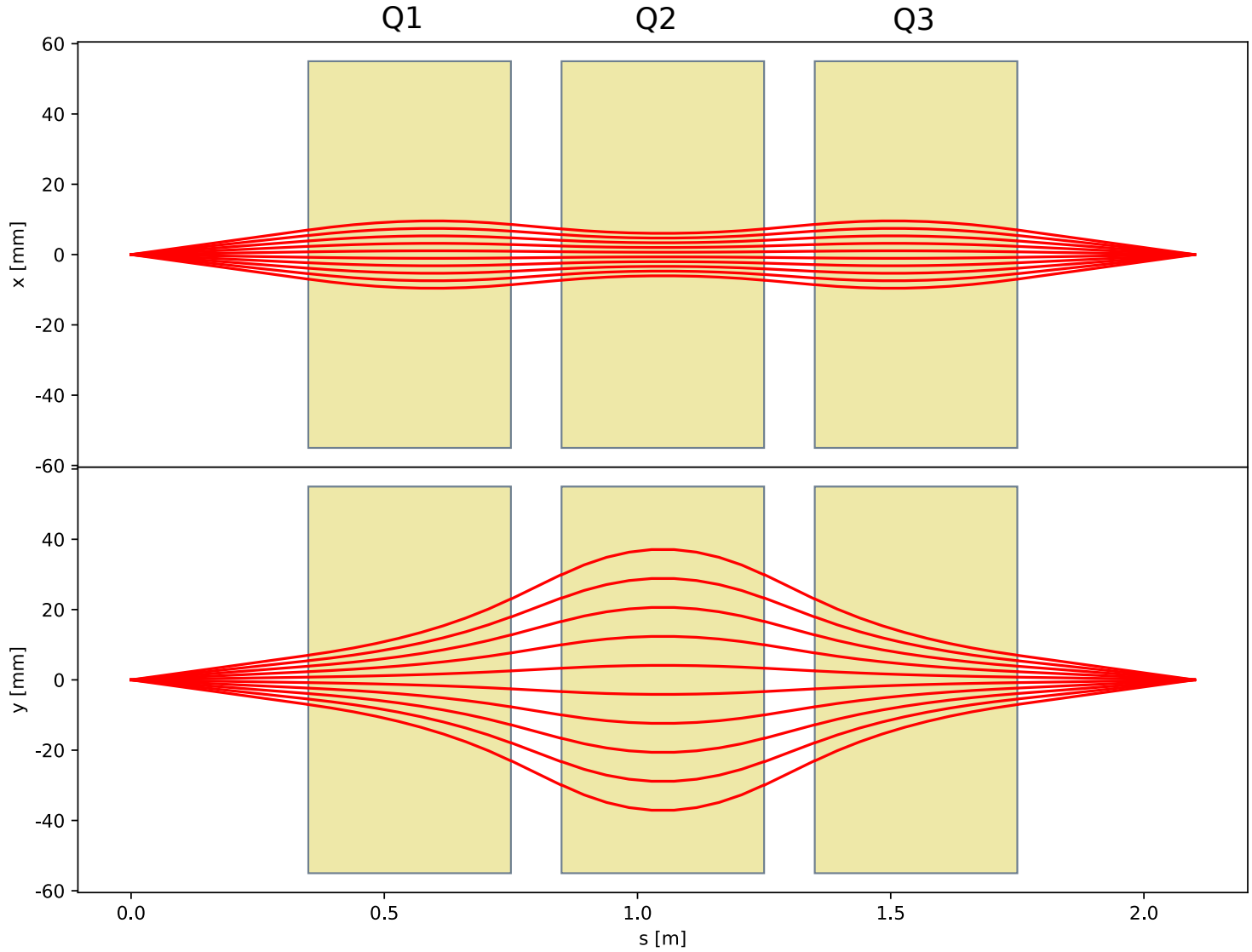

Image from Python Ion Optics Library, PIOL

Magnetic solenoid lens

Cylindrically symmetric magnetic lens.

Winding around beam tube

Solenoid field using on-axis field:

$$\begin{aligned} B_z(r,z) &\approx B_0(z) \\ B_r(r,z) &\approx -\frac{1}{2}B_0(z)'r \end{aligned}$$

Focal length of thin solenoid

$$\frac{1}{f} = \frac{q^2}{8Em}\int_z B_0(z)^2 dz$$

Focusing is a second order effect. Weaker than a quadrupole. Mainly used at low energies.

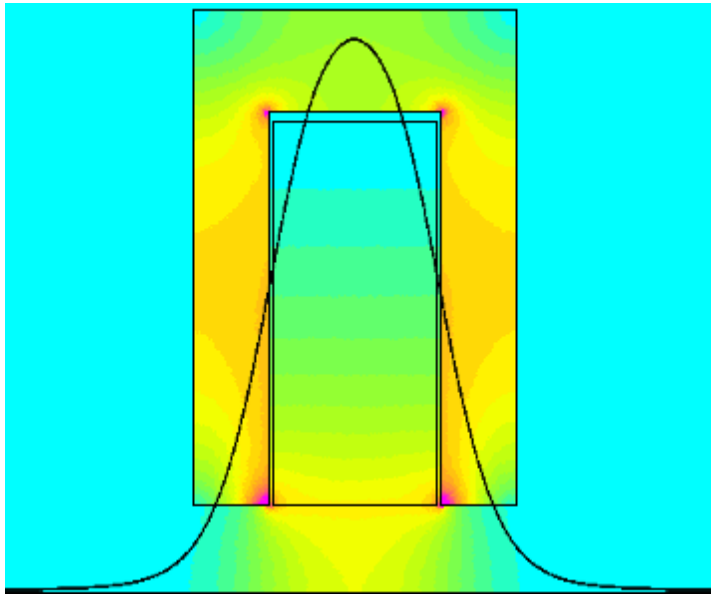

Magnetic solenoid lens

Solenoid spherical aberrations

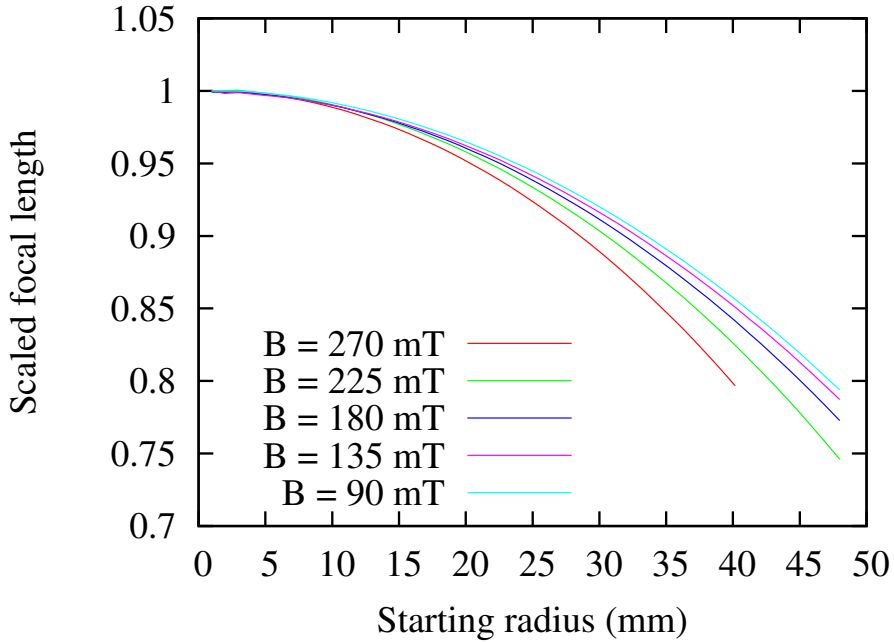

Filling about half of the bore leads to ∼5–10 % focal length variation.

More about ion beams

Beam distributions

Previously we concentrated on how the fields of ion optical elements act on **individual** particles with charge q, mass m, position (x, y, z) and momentum (p_x, p_y, p_z).

In many cases it is relevant to also discuss the particle distributions of the ion beam bunch, the 6-dimensional $f(x, p_x, y, p_y, z, p_z)$ in the general case or lower-dimensional reductions such as $f(x, x', y, y')$, $f(x, x')$, ...

From these distributions one can calculate physical beam size

$$x_{\text{rms}} = \sqrt{\frac{\int x^2 f(x) dx}{\int f(x) dx}} \tag{94}$$

and other *statistical measures* of the distribution.

Phase space plots

The (x, y) is known as *real space* while (x, x') and (y, y') are *phase spaces*.

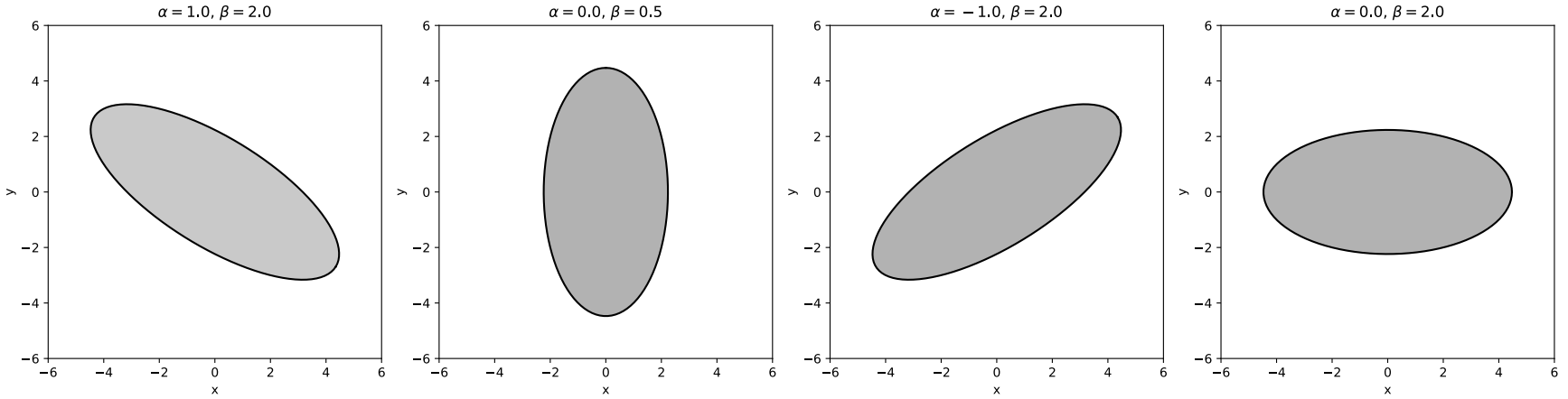

Converging Waist Diverging Parallel

Emittance

In addition to separate rms-sizes, the *emittance* is the most important measure describing **beam quality**.

Traditionally the emittance is defined as the 6-dimensional volume limited by a countour of particle density in the (x, p_x, y, p_y, z, p_z) phase space. This volume obeys the Liouville theorem and is constant in conservative fields.

With practical accelerators a more important beam quality measure is the volume (area) of the elliptical envelope of the beam bunch. This is not conserved generally — only in the case where forces are linear.

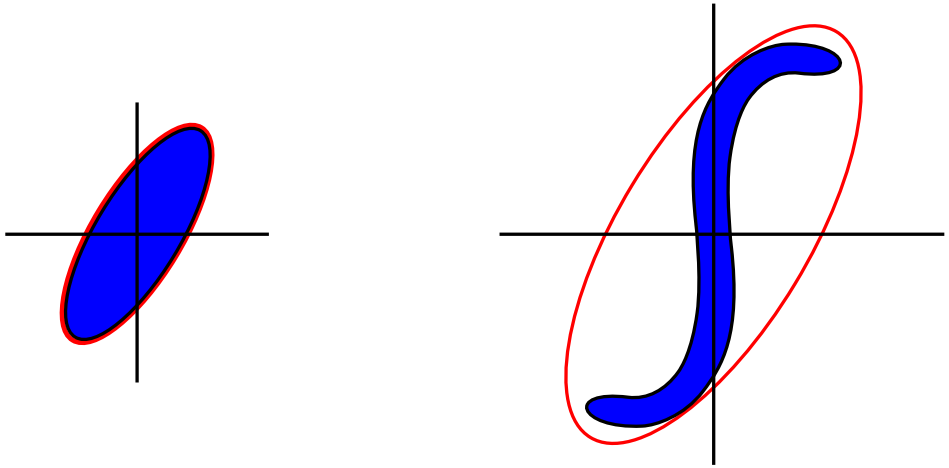

Transverse emittance

Often the transverse direction is more relevant for beam transport.

The transverse distributions in 4- and 2-dimensions are can generally be whatever, but often tend towards Gaussian/elliptical shapes. Therefore the ellipse is the most commonly used *model* for the beam distribution shape.

The 2D emittance ellipse is described by

$$\gamma x^2 + 2\alpha x x' + \beta x'^2 = \epsilon_x,$$

where scaling

$$\beta\gamma - \alpha^2 = 1$$

is chosen. The ϵ_x is the product of the half-axes of the ellipse (A/π) and α, β and γ are known as the *Twiss parameters* defining the ellipse orientation and aspect ratio.

Ellipse geometry

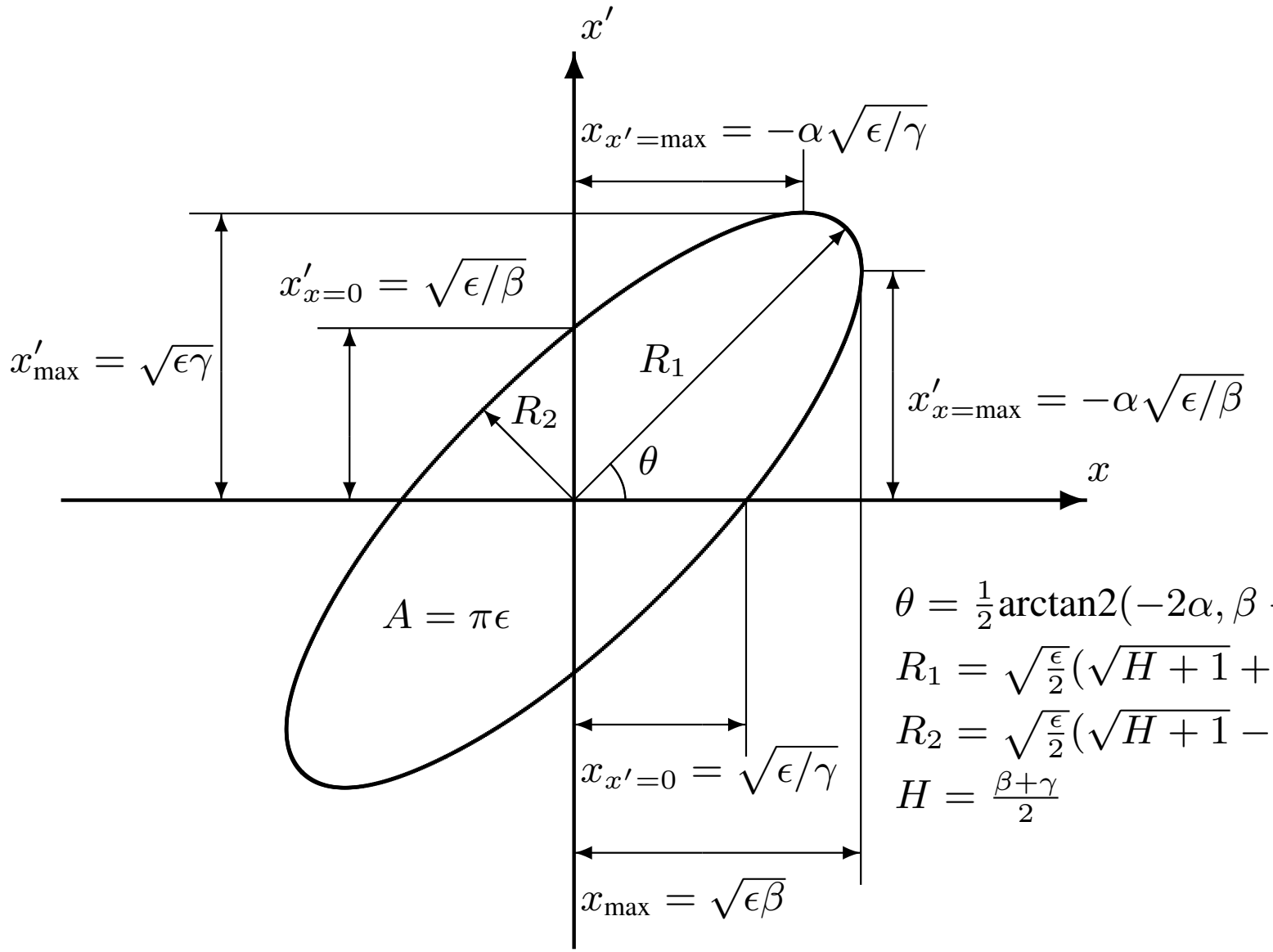

$$\theta = \tfrac{1}{2}\text{arctan2}(-2\alpha, \beta - \gamma)$$
$$R_1 = \sqrt{\tfrac{\epsilon}{2}}(\sqrt{H+1} + \sqrt{H-1})$$
$$R_2 = \sqrt{\tfrac{\epsilon}{2}}(\sqrt{H+1} - \sqrt{H-1})$$
$$H = \tfrac{\beta+\gamma}{2}$$

RMS emittance

Numerous algorithms exist for defining the ellipse from beam data. Often a minimum area ellipse containing some fraction of the beam is wanted (e.g. $\epsilon_{90\%}$). Unfortunately this is difficult to produce in a robust way.

A well-defined way for producing the ellipse is the rms emittance:

$$\epsilon_{\text{rms}} = \sqrt{\langle x'^2 \rangle \langle x^2 \rangle - \langle x x' \rangle^2},$$

and similarly the Twiss parameters

$$\begin{aligned} \alpha &= -\frac{\langle x x' \rangle}{\epsilon}, \\ \beta &= \frac{\langle x^2 \rangle}{\epsilon}, \\ \gamma &= \frac{\langle x'^2 \rangle}{\epsilon}, \end{aligned}$$

where

$$\begin{aligned} \langle x^2 \rangle &= \frac{\iint x^2 I(x,x') \mathrm{d}x \mathrm{d}x'}{\iint I(x,x') \mathrm{d}x \mathrm{d}x'}, \\ \langle x'^2 \rangle &= \frac{\iint x'^2 I(x,x') \mathrm{d}x \mathrm{d}x'}{\iint I(x,x') \mathrm{d}x \mathrm{d}x'}, \\ \langle x x' \rangle &= \frac{\iint x x' I(x,x') \mathrm{d}x \mathrm{d}x'}{\iint I(x,x') \mathrm{d}x \mathrm{d}x'}. \end{aligned}$$

Assuming $\langle x \rangle = 0$ and $\langle x' \rangle = 0$.

Normalization of emittance

The transverse emittance defined in this way is dependent on the beam energy. If p_z increases, $x' = p_x/p_z$ decreases.

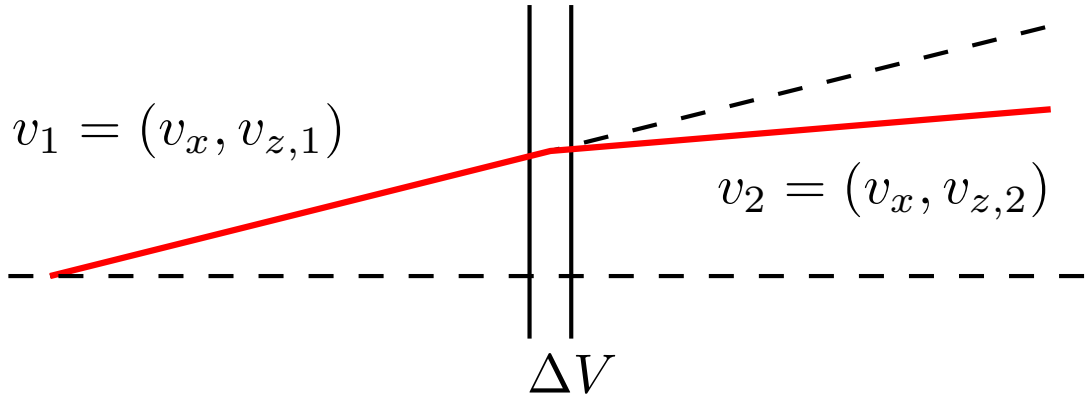

The effect is eliminated by normalizing the velocity to c, which gives

$$x'_n = \frac{p_x}{p_{z1}}\frac{v_{z1}}{c} = \frac{v_x}{c} = \frac{p_x}{p_{z2}}\frac{v_{z2}}{c}.$$

Normalized emittance is

$$\epsilon_n = \epsilon\frac{v_z}{c}$$

RMS emittance example

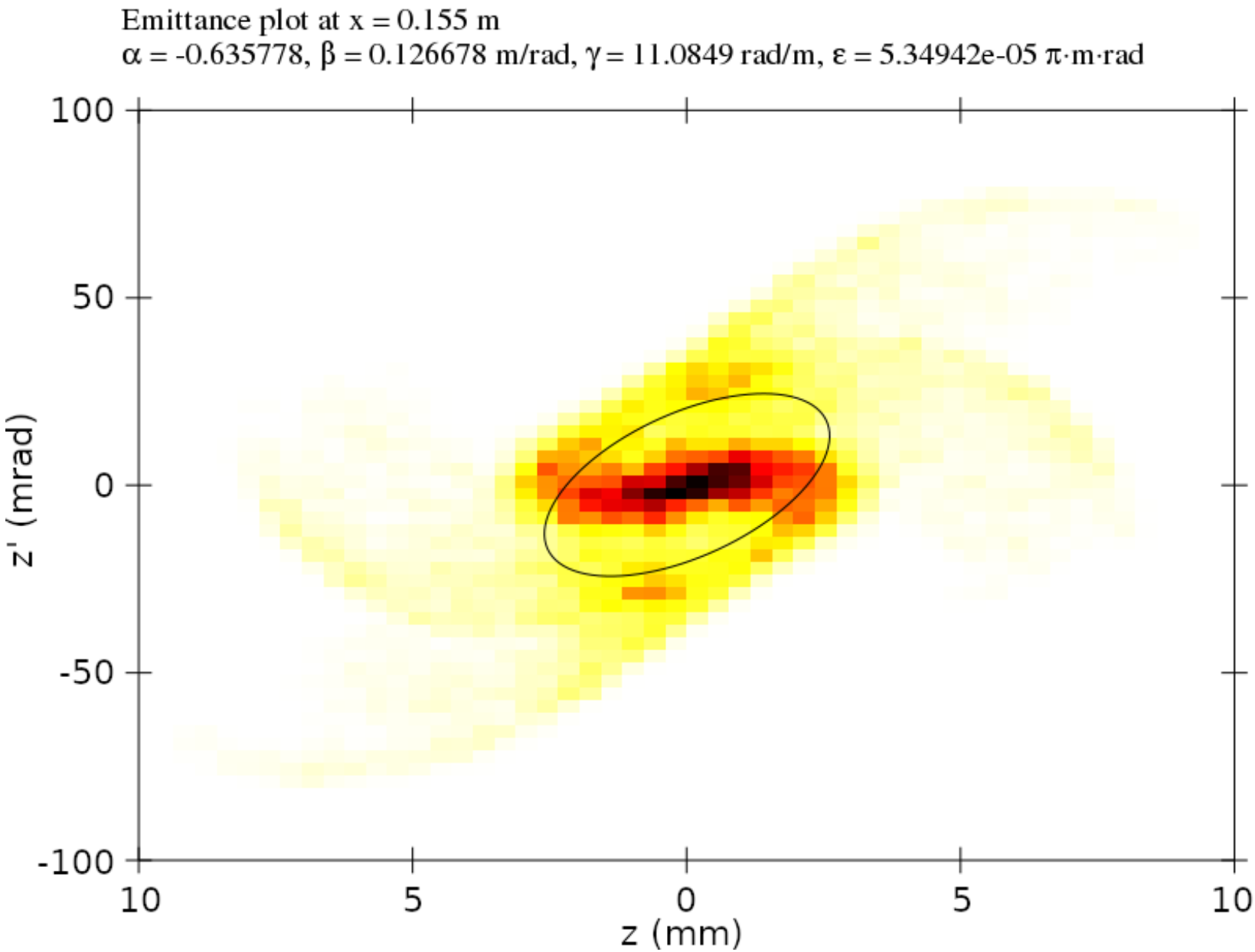

Model distributions

Kapchinskij-Vladimirskij (KV)

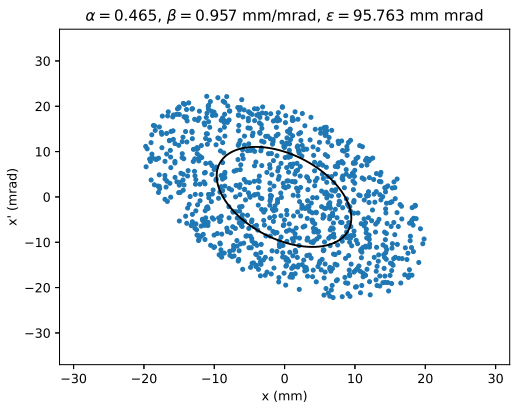

Waterbag distribution

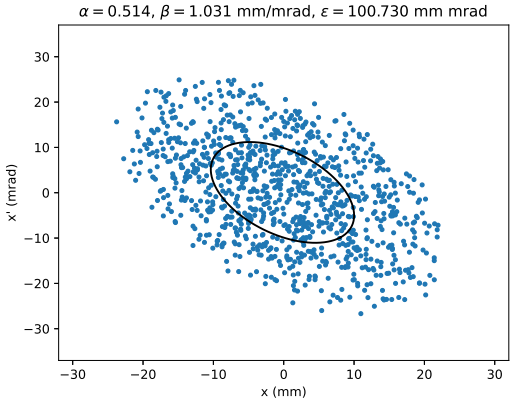

Gaussian distribution

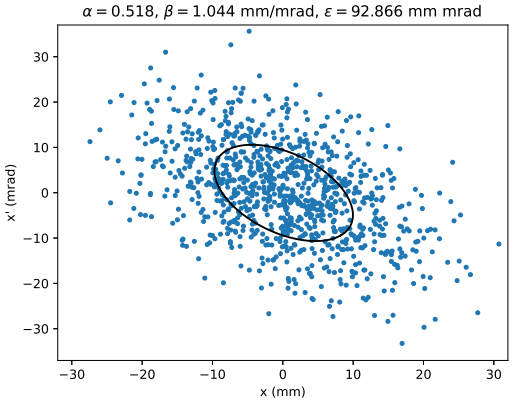

How much beam does the rms ellipse contain?

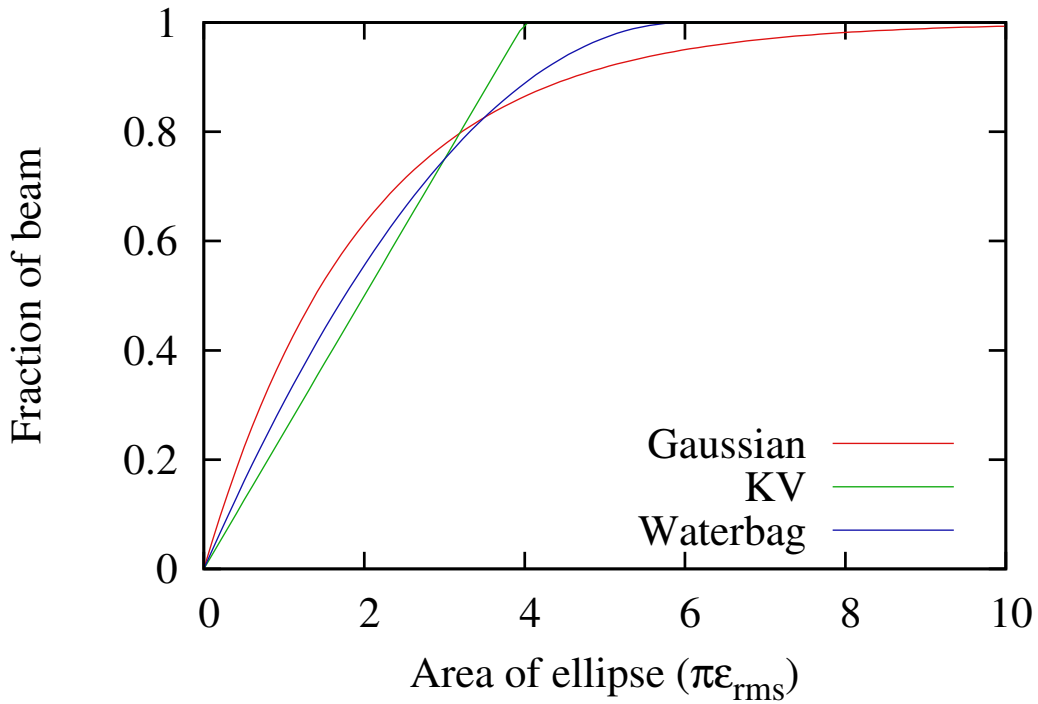

Acceptance

What portion of the beam fits inside a phase space acceptance of some device?

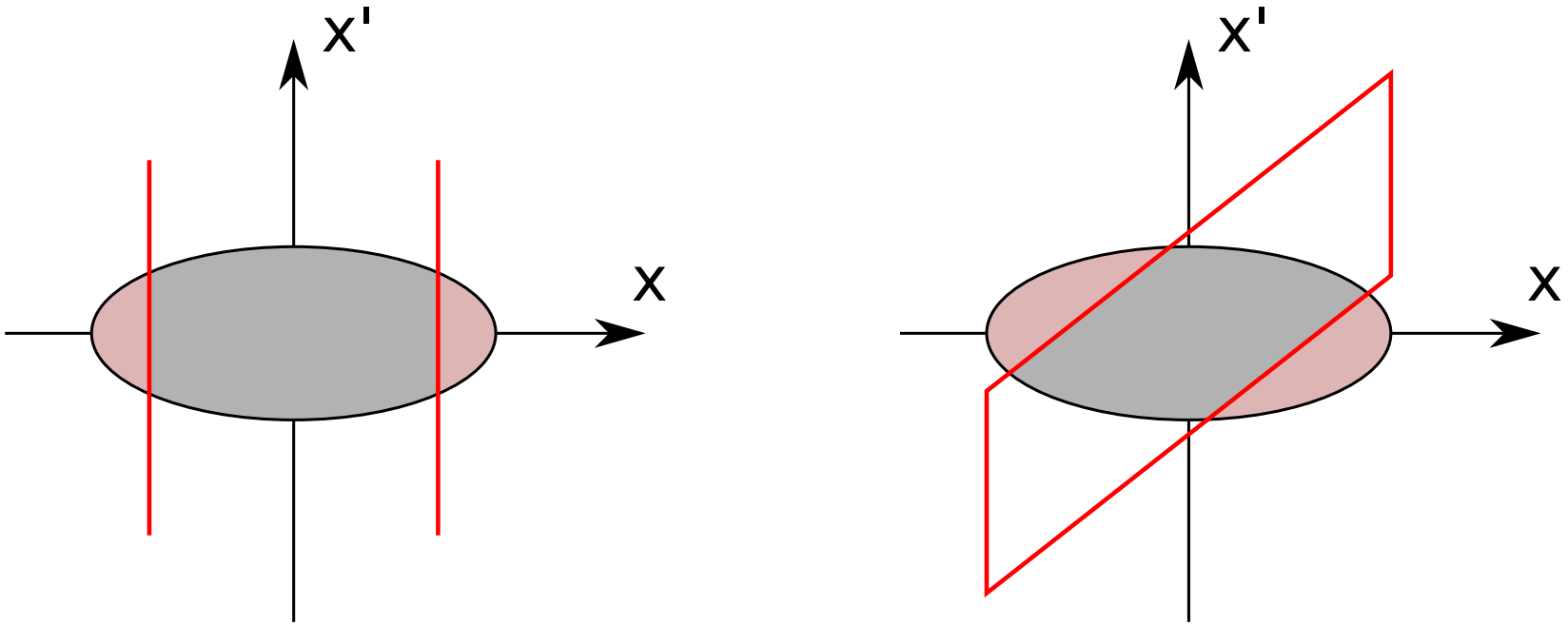

Turning the phase space pattern in both of these cases would be beneficial for improving throughput $\rightarrow$ *phase space matching*.

Emittance growth

The rms emittance can grow and shrink:

- Particle-particle scattering
- EM-field fluctuations
  - Power supply ripples
  - Plasma instabilities
- Nonlinear fields in electrostatic and magnetic optics
- Nonlinear fields from beam/plasma space charge
- Collimation
- Simulation artefact: mesh induced emittance growth

Typically accelerator systems are designed to be as linear as possible.

Beam space charge effects

Assuming constant space charge of the beam $\rho = J/v$. In cylindrical case one can calculate the E-fields from Gauss law:

$$\begin{aligned} E &= \frac{I}{2\pi\epsilon_0 v}\frac{r}{r_{\text{beam}}^2}, r < r_{\text{beam}} \\ E &= \frac{I}{2\pi\epsilon_0 v}\frac{1}{r}, r > r_{\text{beam}} \end{aligned}$$

and the potential in the beam tube:

$$\begin{aligned} \phi &= \frac{I}{2\pi\epsilon_0 v}\left[\frac{r^2}{2r_{\text{beam}}^2} + \log\left(\frac{r_{\text{beam}}}{r_{\text{tube}}}\right) - \frac{1}{2}\right], r < r_{\text{beam}} \\ \phi &= \frac{I}{2\pi\epsilon_0 v}\log\left(\frac{r}{r_{\text{tube}}}\right), r > r_{\text{beam}} \end{aligned}$$

Beam space charge effects

Potential in a 100 mm tube with a 10 mA, 10 keV proton beam

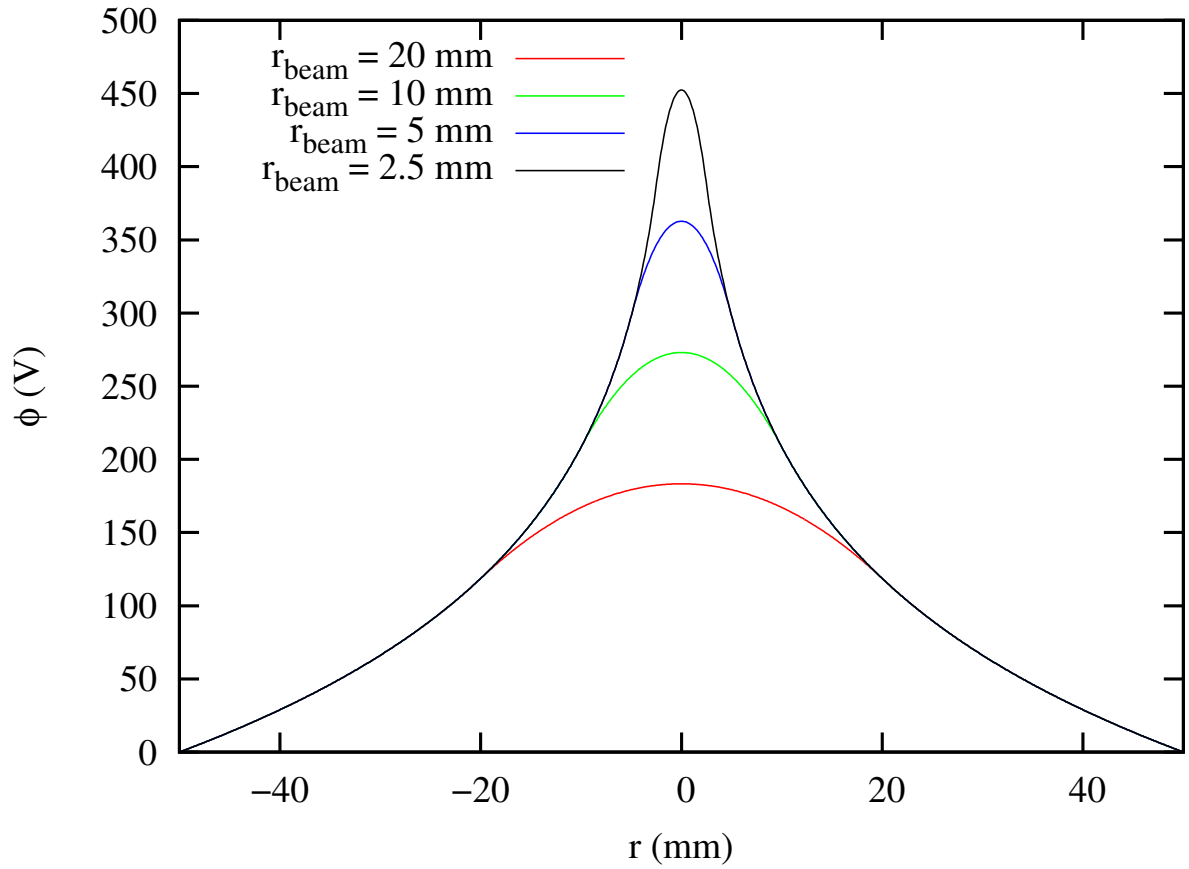

Beam space charge blow-up

Ion at the beam boundary experiences a repulsive force

$$F_r = qE_r = ma_r = \frac{qI}{2\pi\epsilon_0 r v_z}.$$

The particle acceleration is

$$a_r = \frac{d^2r}{dt^2} = \frac{d}{dt}\left(\frac{dr}{dz}\frac{dz}{dt}\right) = \cdots = v_z^2\frac{d^2r}{dz^2}.$$

Therefore

$$\begin{aligned} \frac{d^2r}{dz^2} &= \frac{1}{v_z^2}a_r = K\frac{1}{r}, \text{ where} \\ K &= \frac{qI}{2\pi\epsilon_0 m v_z^3}. \end{aligned}$$

The DE can be integrated after change of variable $\lambda = \frac{dr}{dz}$ and gives

$$\frac{dr}{dz} = \sqrt{2K\log(r/r_0)},$$

assuming $\frac{dr}{dz} = 0$ at $z = 0$.

Beam space charge blow-up

The solution is separable and can be again integrated to a final solution

$$z = \frac{r_0}{\sqrt{2K}} F\left(\frac{r}{r_0}\right), \text{ where}$$

$$F\left(\frac{r}{r_0}\right) = \int_{y=1}^{r/r_0} \frac{dy}{\sqrt{\log y}}.$$

(1) Low divergence was assumed to be able to use equation for E_r.

(2) Constant v_z was assumed (beam potential changes neglected).

Example: $r_0 = 5$ mm proton beam:

Linear effect $\Rightarrow$ No rms emittance growth with KV beam.

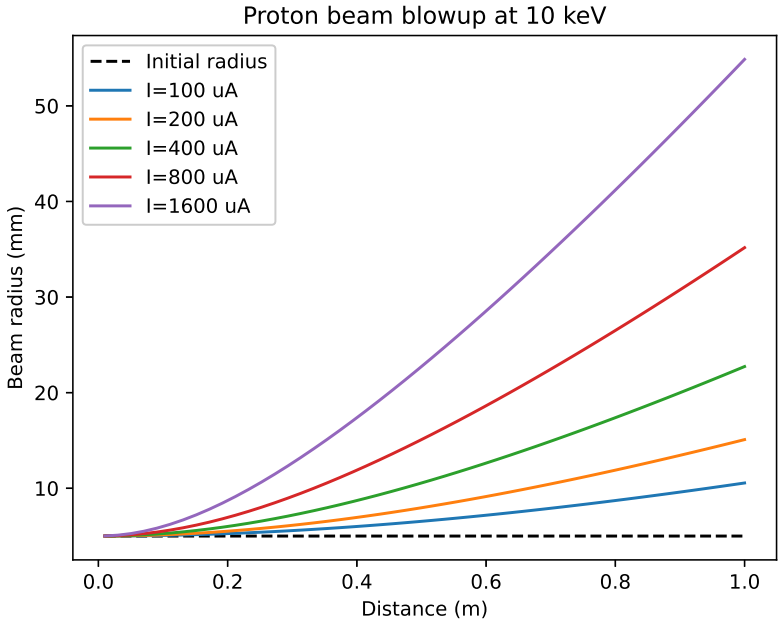

Beam space charge compensation

Transport of high-intensity, low-energy beams can be difficult due to space charge blow-up. Beam compensation helps in low E-field areas.

- Background gas ionization: e^- and X^+ created within the beam.
- Opposite sign to beam trapped in beam potential, while same sign particles accelerated out $\Rightarrow$ decreasing beam potential.
- Secondary electron emission from beam halo hitting beam tube providing compensating particles for positive beams.
- Also methods for active compensation: running electron beam in opposite direction of the main beam.
- Usually increased by feeding background gas into the beamline.

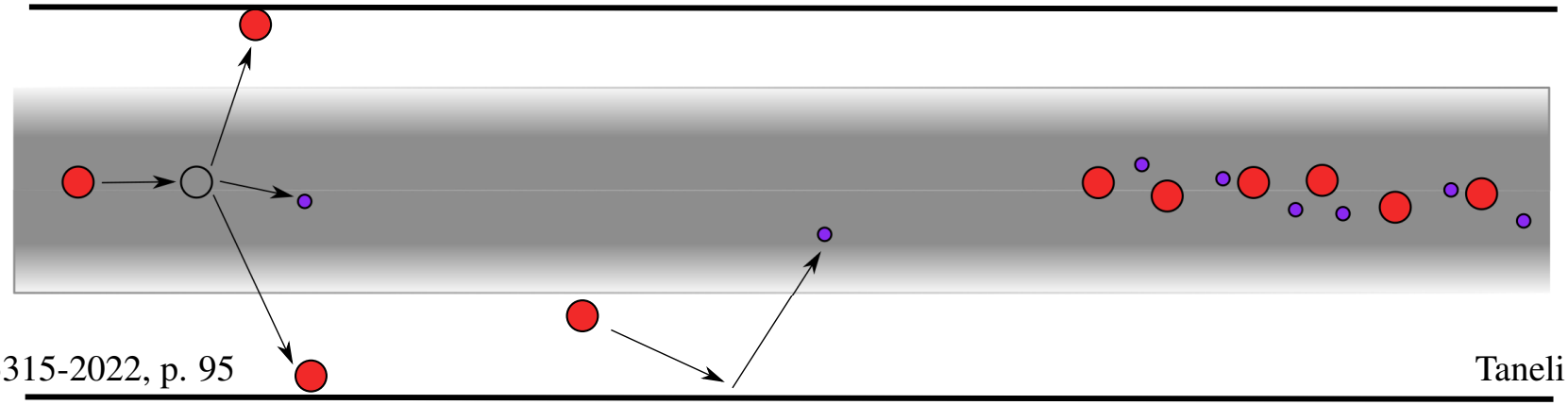

Beam space charge compension

Measurement of ion energy distribution ejected from beam

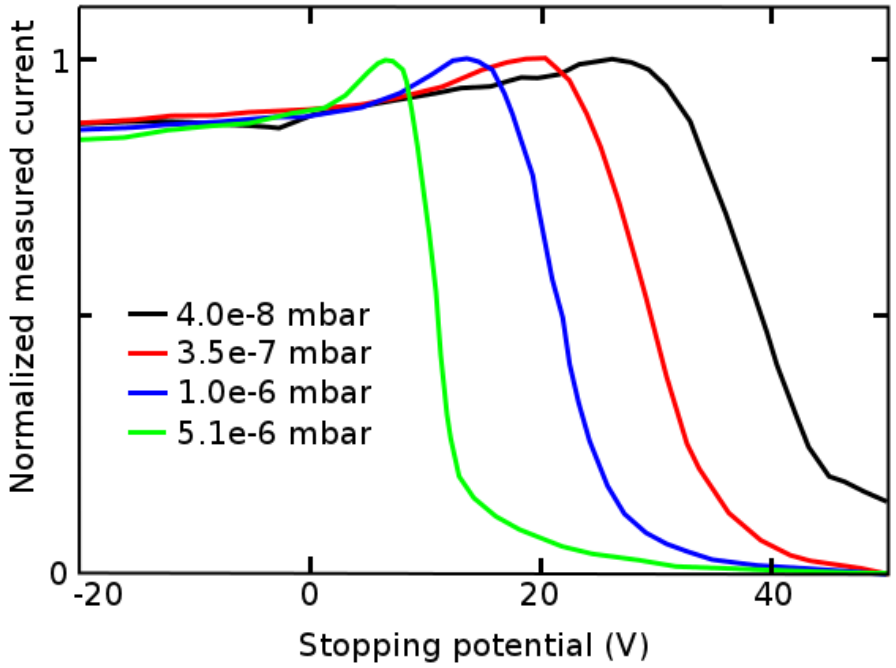

Reproduced from D. S. Todd, BIW 2008

Gives an indication of the compensation degree.

Beam space charge compension

Compensation by thermal particles trapped in the beam potential is difficult to estimate.

Creation rate

$$\frac{d\rho_c}{dt} = Jn\sigma_c$$

$$\tau = \frac{\rho_{\text{beam}}}{\left(\frac{d\rho_c}{dt}\right)} = \frac{1}{vn\sigma_c}$$

Pulsed beams may or may not be long enough for reaching equilibrium.

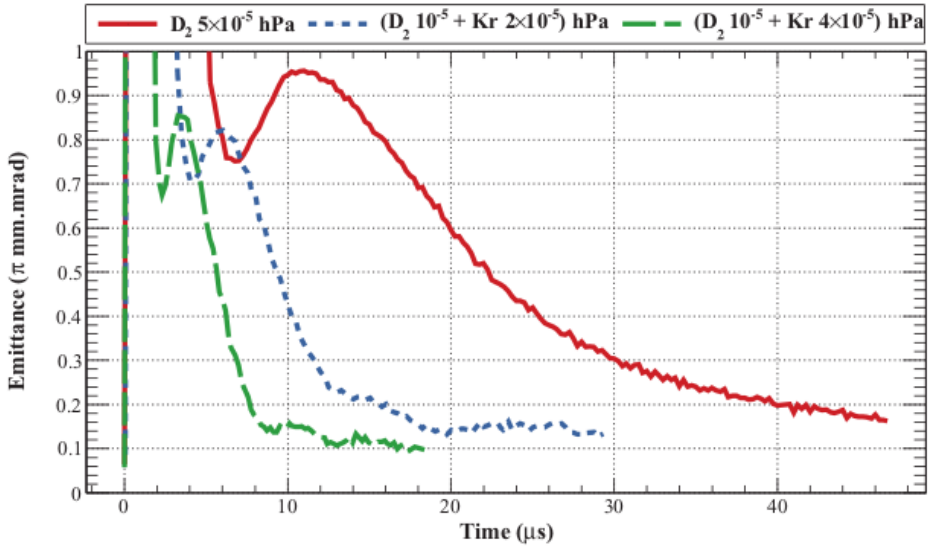

From N. Chauvin, ICIS 2011

Beam space charge compension

If creation rate is high, the SCC is finally limited by leakage of compensating particles from the potential well as SCC approaches 100 %. Electrons are fast $\Rightarrow$ X^+ SCC < 100 %
Ions are slow $\Rightarrow$ X^- overcompensation is possible.

SCC is location dependent because compensating particles move in the potential well. Leakage in the beam ends cause at least local loss of SCC. Leakage may be limited by accelerating einzel lens or by magnetic fields.

Background gas causes beam losses. Typically a 1–2 % sacrifice is sufficient for good SCC. Modelling:

- Simple model for SCC: scaling the effective beam current globally or locally with a SCC-factor.
- PIC simulation (for example WARP or SOLMAXP) with modelling of trapped particle dynamics

Diagnostics

The Faraday cup

The most simple beam *intensity* measurement device. Measures directly the flow of charges

$$I = \frac{dq}{dt} \tag{95}$$

in range from 1 pA to 1 A.

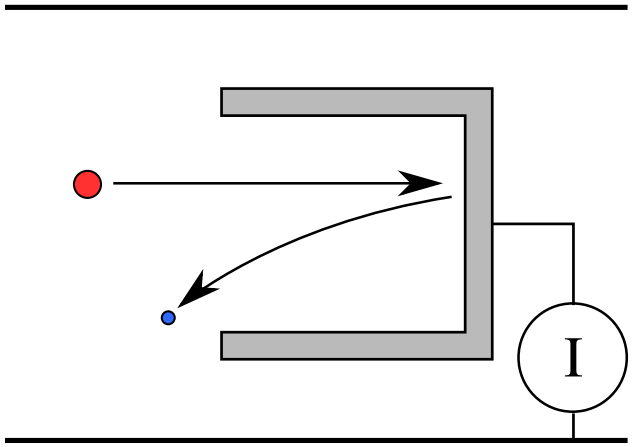

Can suffer from errors due to other charges.

An FC actuator on a beamline at JYFL.

FC secondary electron suppression

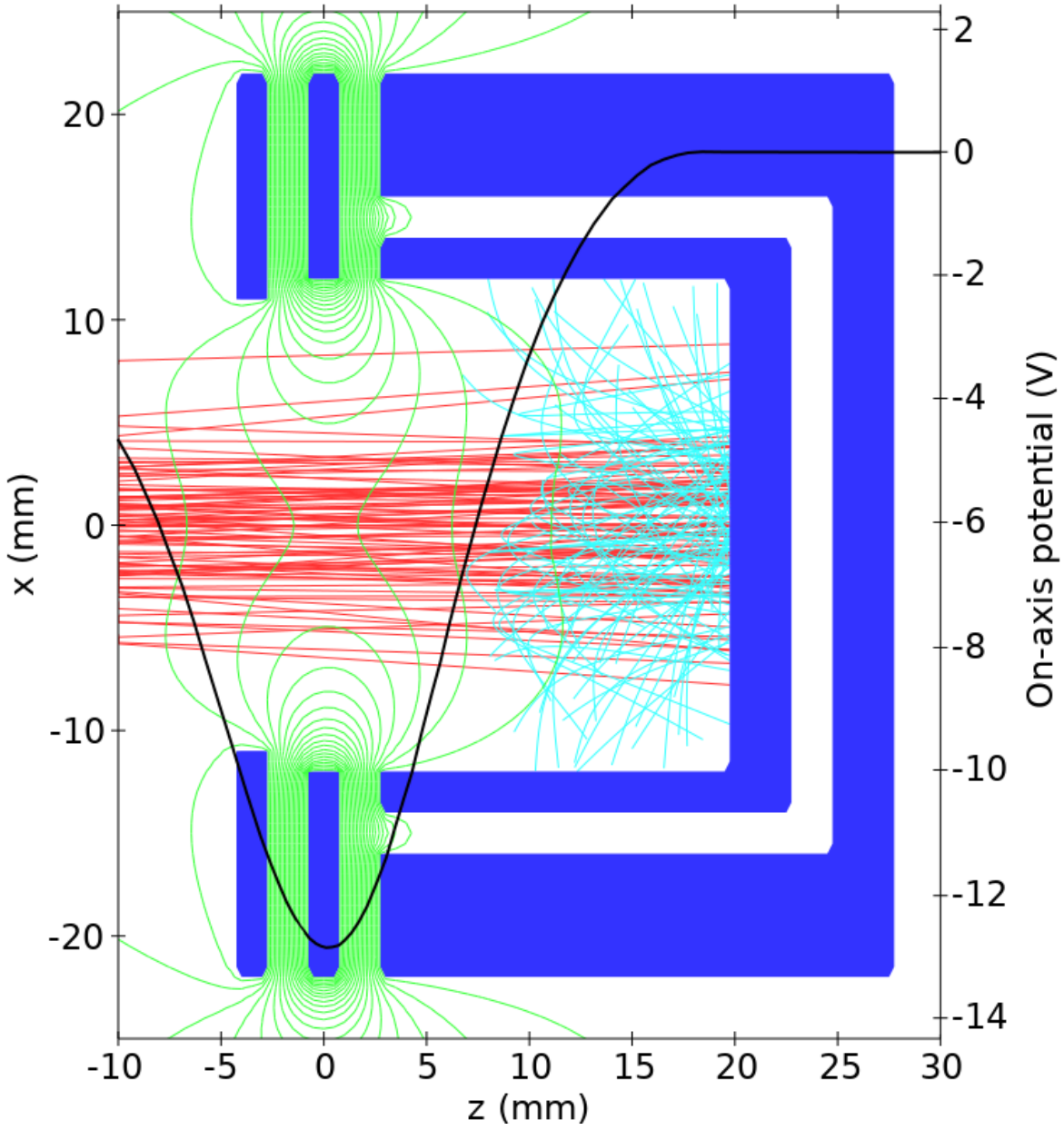

From T. Kalvas, Rev. Sci. Instrum. 93, 011501 (2022)

Intensity ranges

Examples of typical beam intensities at JYFL-ACCLAB

Location	Particle	Current	Reduced current	Particle fluence
ECR	$^{32}S^{7+}$	100 μA	14 pμA	$8.7 \cdot 10^{13}$ s^{-1}
LIISA	p	1 mA	1 pmA	$6.2 \cdot 10^{15}$ s^{-1}
MARA	$^{32}S^{7+}$	700 nA	100 pnA	$6.2 \cdot 10^{11}$ s^{-1}
RADEF	$^{126}Xe^{44+}$	7 pA	160 pfA	10^{6} s^{-1}

Beam current is flow of charges

$$I = q\Phi = Qe\Phi. \tag{96}$$

Reduced current often used for nuclear physics:

$$I^* = \frac{I}{Q} = e\Phi \tag{97}$$

Beam power

The beam power gets deposited into a Faraday cup:

$$P = E_K \Phi = qU\Phi = qU\frac{I}{q} = UI \tag{98}$$

H^- at LIISA

$$P = 10\ \text{kV} \cdot 1\ \text{mA} = 10\ \text{W}.$$

$^{32}S^{7+}$ at MARA

$$\begin{aligned} P &= 166\ \text{MeV} \cdot 700\ \text{nA}/7\ \text{e} \\ &= 166 \cdot 10^6\ \text{V} \cdot 100\ \text{nA} = 17\ \text{W} \end{aligned}$$

Protons at power cup

$$P = 90\ \text{MeV} \cdot 30\ \mu\text{A} = 2700\ \text{W}.$$

$\Rightarrow$ In most cases careful thought on cooling needed.

Collimators

Usually collimators are used to limit beam current and emittance, but can also be used to measure the *stray beam* or *beam halo*.

Due to limitations in geometry, a proper electron suppression can not be implemented and therefore the measurement is only indicative.

JYFL-ACCLAB water-cooled high-energy beam collimator with 4 states: ⌀5, ⌀10, ⌀15 mm and no collimation.

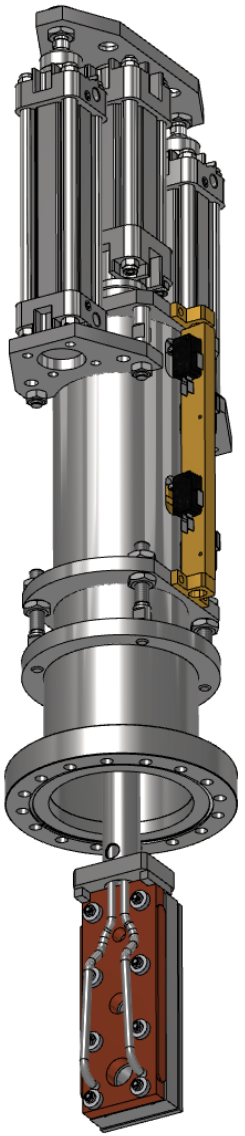

Scintillator viewers (x, y)

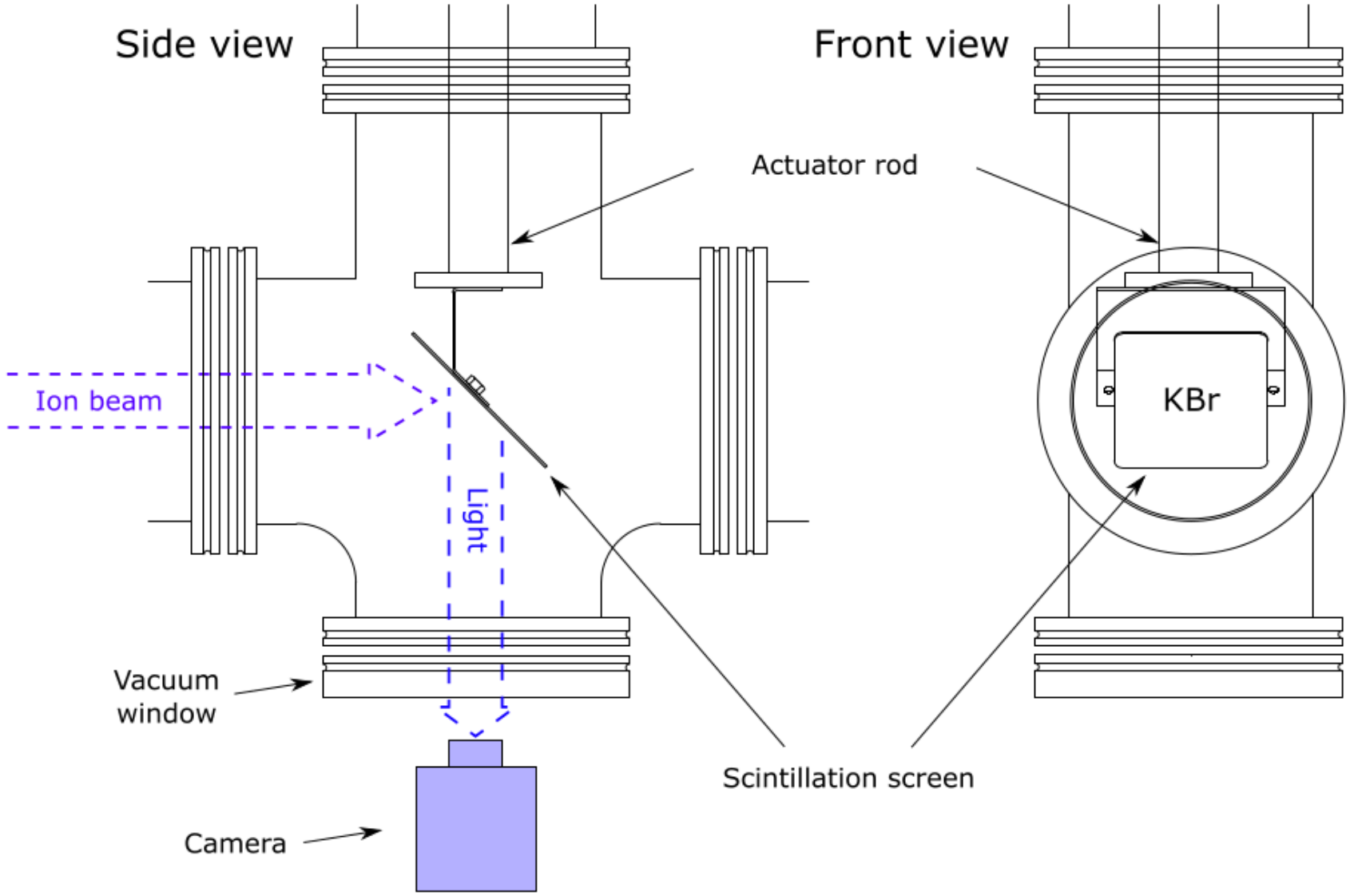

From V. Toivanen, Ph.D. Thesis, University of Jyväskylä, 2013.

Allison scanner (x, x')

The beam distribution in projected phase space (x, x') can be measured with an allison scanner scanning x with physical movement and x' with electrostatic deflector plates.

$$V_p = \frac{2dV_0}{L_{\text{eff}}} x' \tag{99}$$

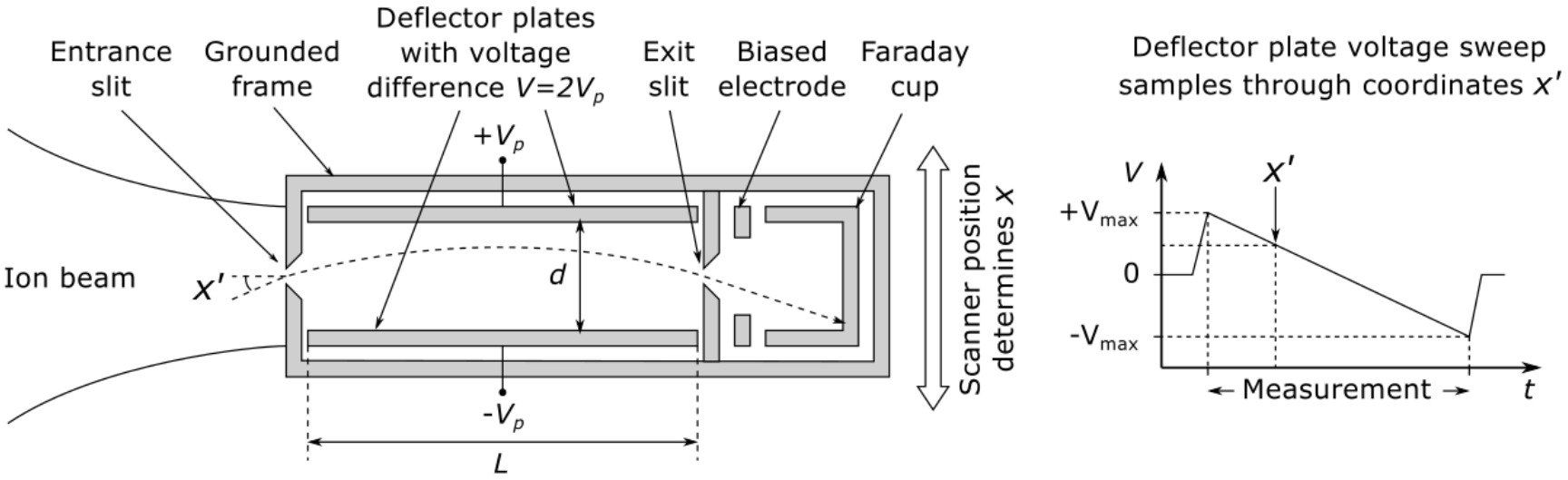

From V. Toivanen, Ph.D. Thesis, University of Jyväskylä, 2013.

Pepperpot (x, x', y, y')

The 4D phase space distribution is measured using a multi-aperture collimator.

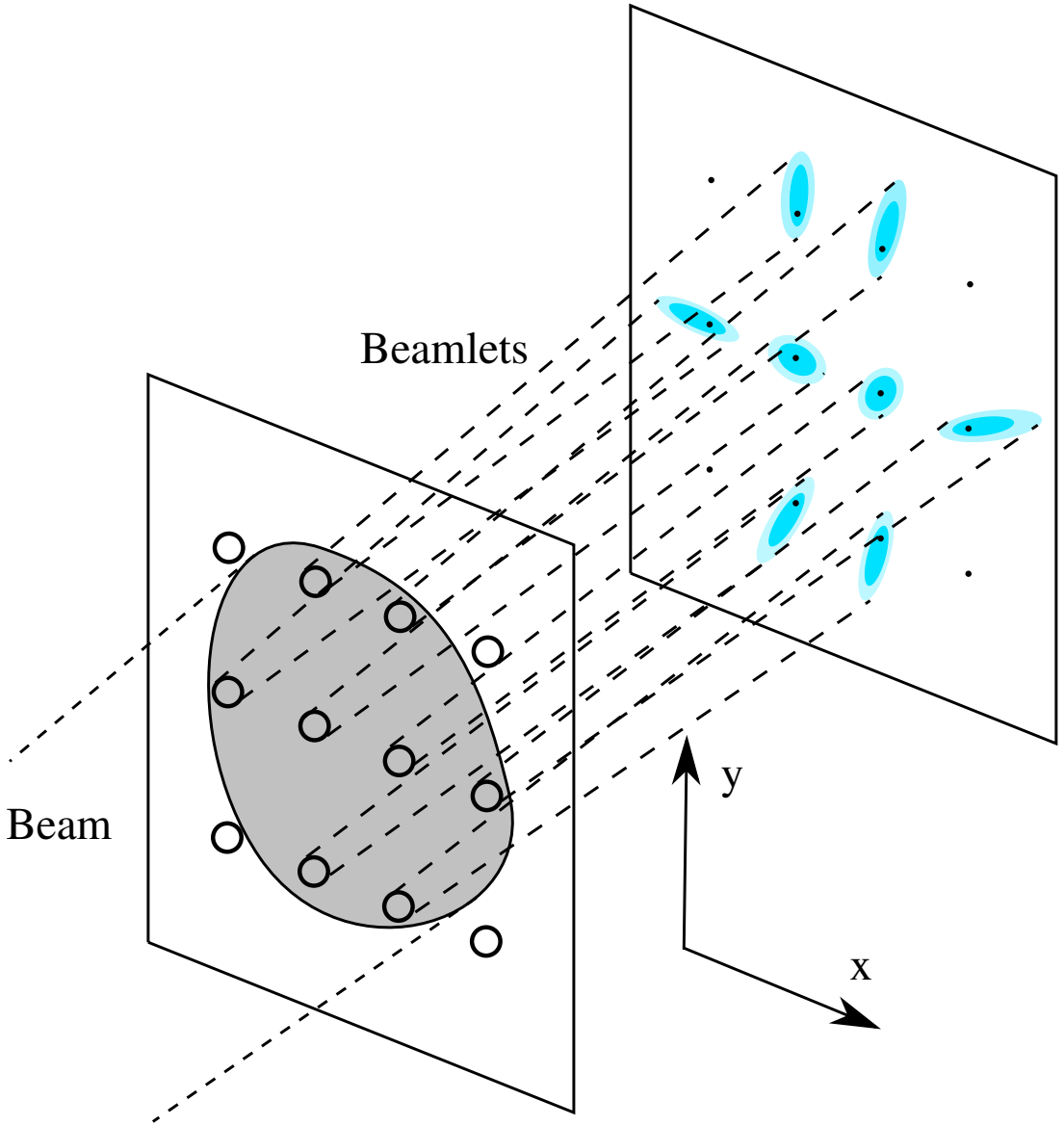

From T. Kalvas, Rev. Sci. Instrum. 93, 011501 (2022)

Many other methods

- Magnetic and capacitive pickups
- Residual gas monitors
- Scintillators
- Gas counters
- Energy measurement

Cyclotron

Classical cyclotron

A charged particle propagating in a transverse magnetic field experiences a centripetal force

$$F_r = ma_r = m\frac{v^2}{r} = qvB. \tag{100}$$

The velocity is threrefore

$$v = \frac{qBr}{m} \tag{101}$$

leading to the classical kinetic energy

$$\frac{E_K}{m} = \frac{1}{2}v^2 = \frac{1}{2}\left(\frac{qBr}{m}\right)^2. \tag{102}$$

This energy is often given as

$$\frac{E_K}{M} = K\left(\frac{Q}{M}\right)^2, \tag{103}$$

where $K = (eBr)^2/(2m_u)$.

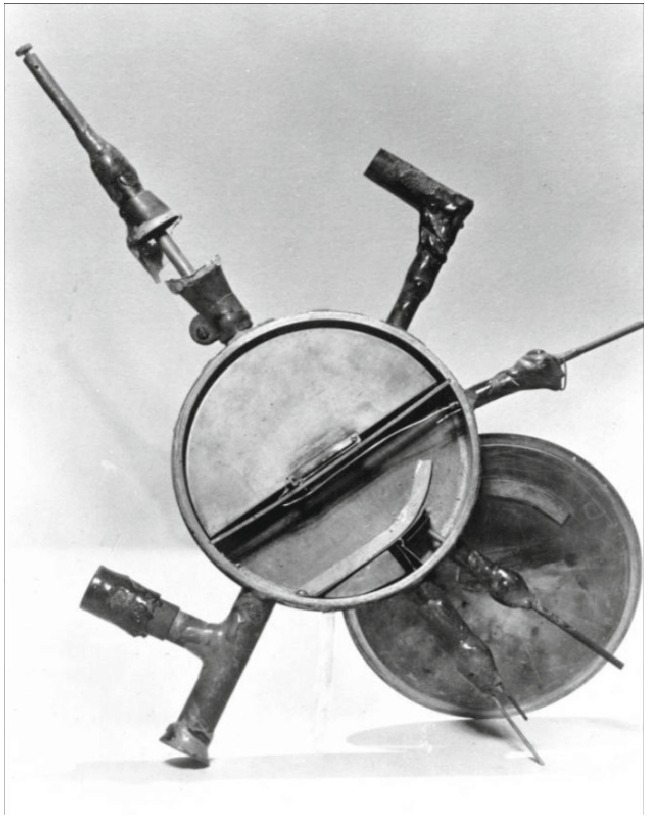

The first cyclotron by Ernest O. Lawrence 1929–1930.

Classical cyclotron

The orbit/cyclotron frequency

$$f_c = \frac{1}{T} = \frac{v}{2\pi r} = \frac{qB}{2\pi m} \tag{104}$$

is not dependent on radius r, which allows the use of a fixed acceleration frequency (RF) at the cyclotron frequency:

$$f_{\mathrm{RF}} = f_c \tag{105}$$

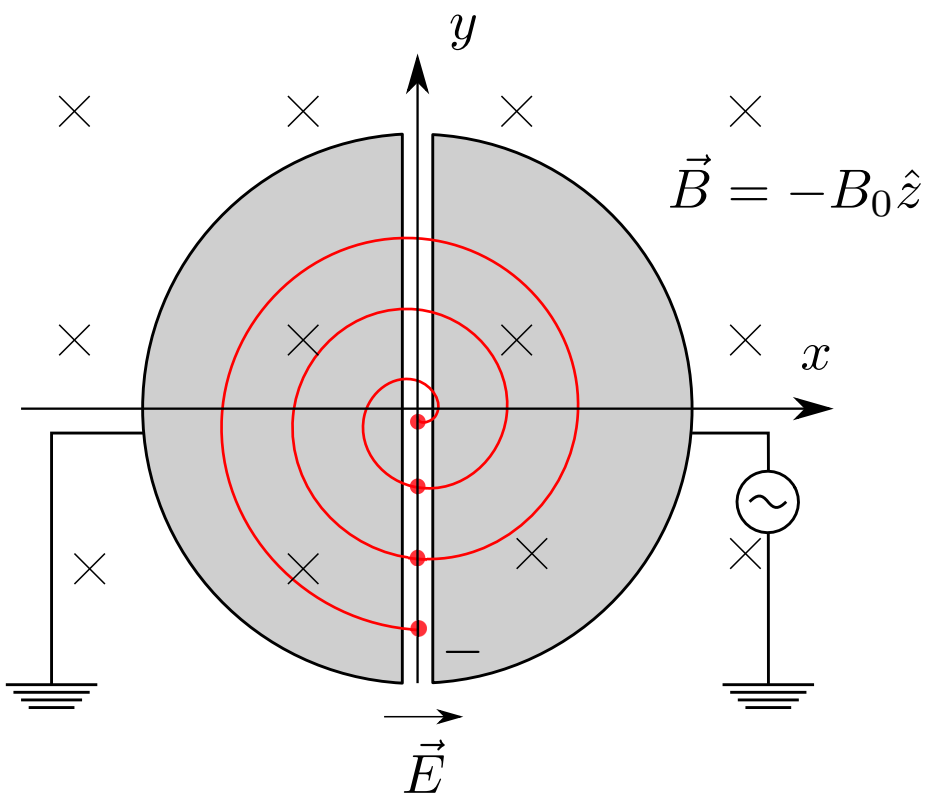

Focusing

The particles tend to spread due to finite emittance and space charge. Focusing is needed to transport any particles through hundreds of turns.

Radial ("horizontal") focusing

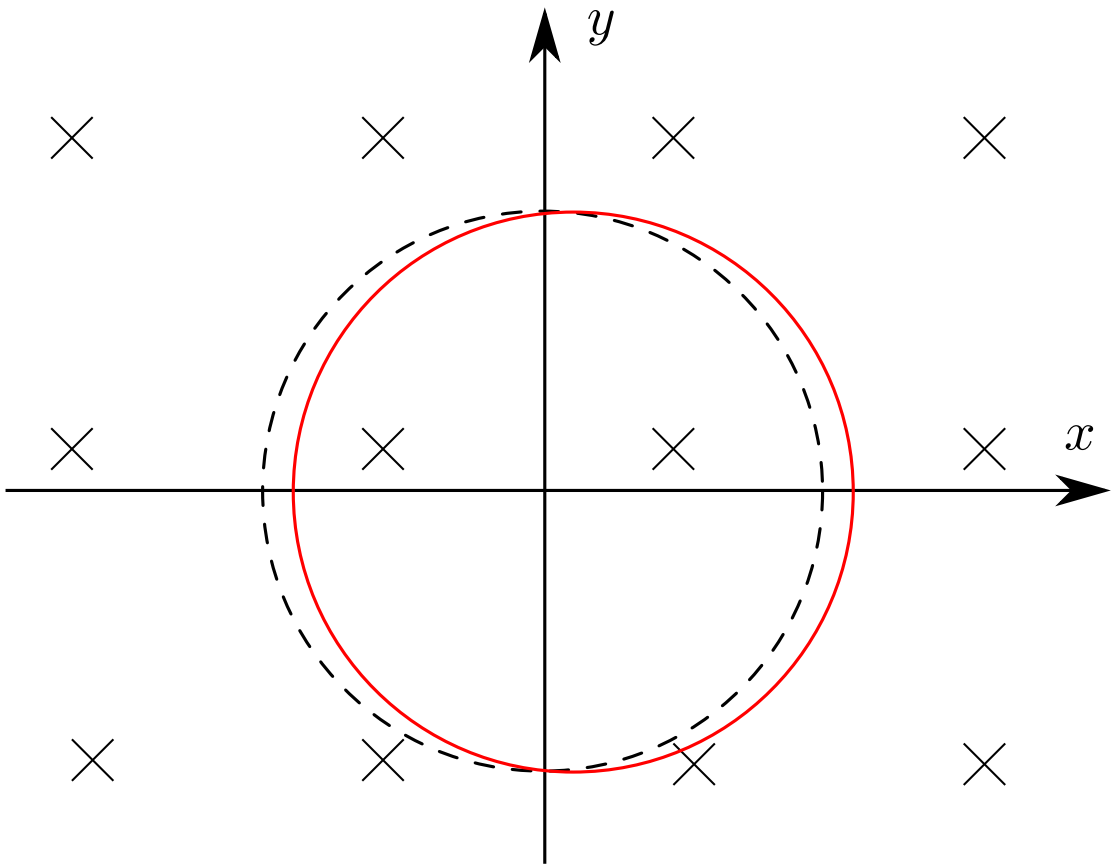

Weak focusing

Axial ("vertical") focusing

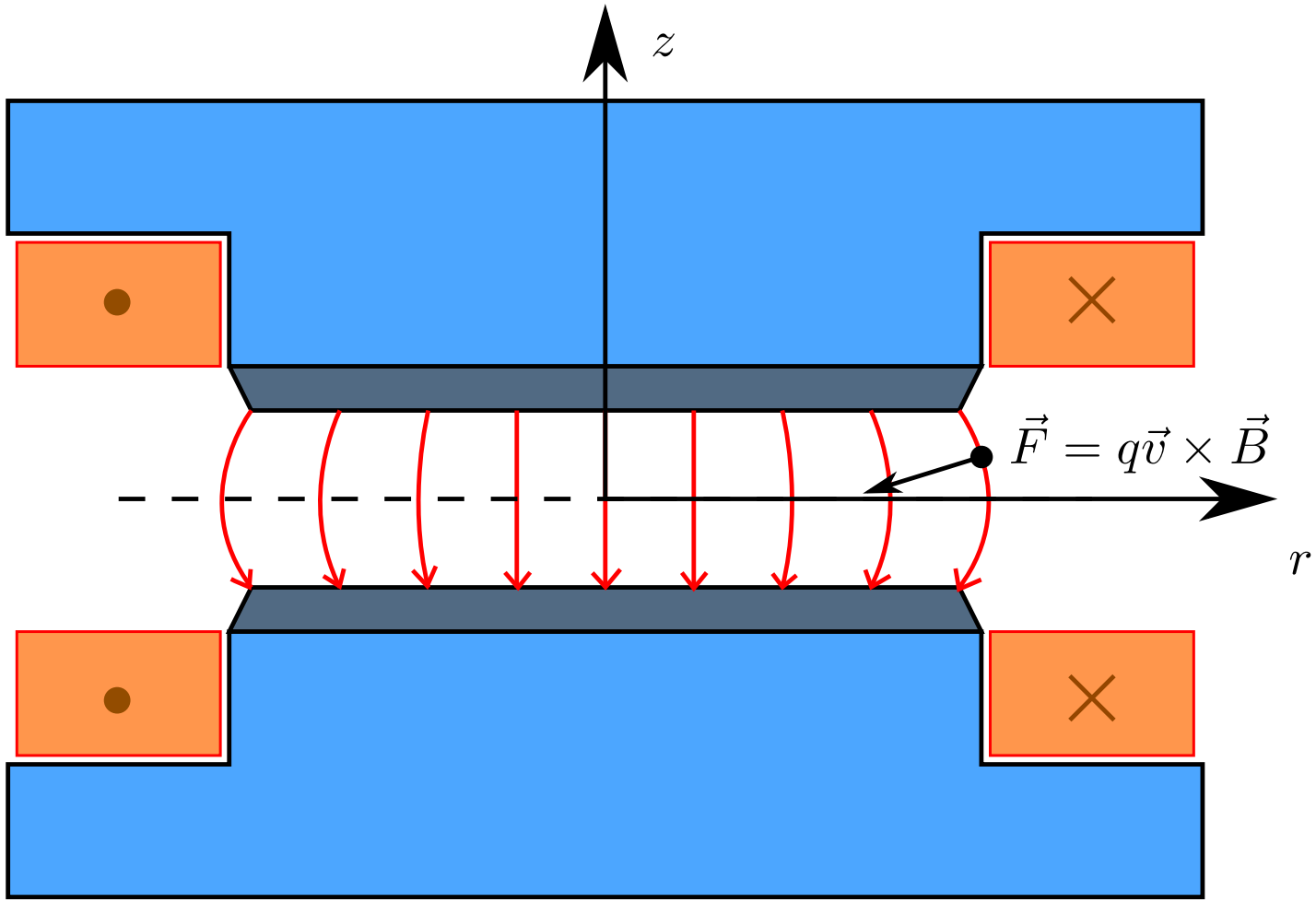

Longitudinal focusing

Nonexistent in cyclotrons, best if acceleration per turn maximized. Particles maintain their initial phase.

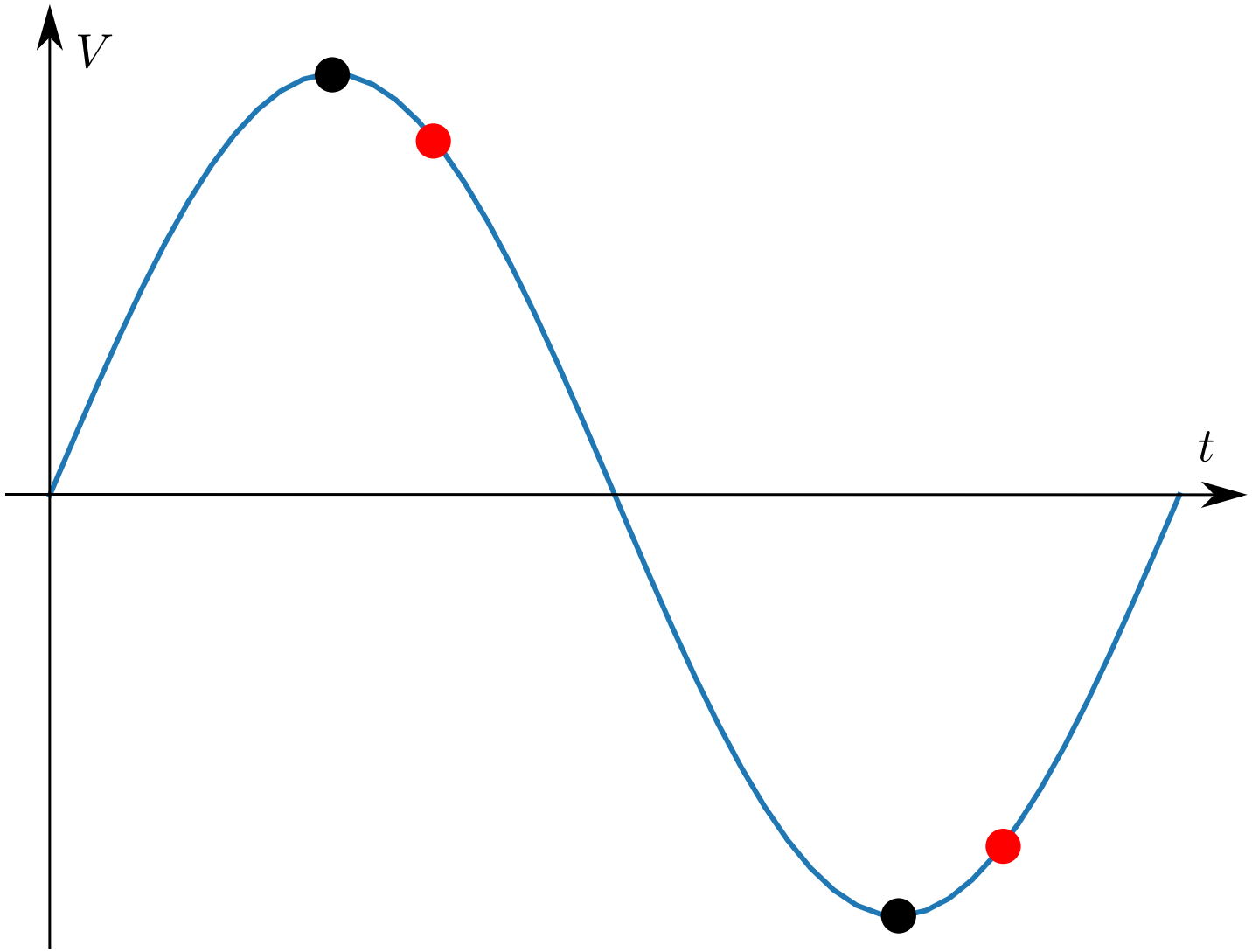

Classical cyclotron energy limit

As particle velocity approaches speed of light the cyclotron frequency decreases due to the change of relativistic mass

$$f_c = \frac{qB}{2\pi\gamma m_0}. \tag{106}$$

The phase error of the particle accumulated in N turns

$$\Delta\phi = 2\pi N \frac{T_c - T_{RF}}{T_{RF}} = 2\pi N \left(\frac{f_{RF}}{f_c} - 1 \right). \tag{107}$$

With $v/c = 10$ %, the relativistic $\gamma = 1/\sqrt{1-(v/c)^2} \approx 1.005$ leading to a critical phase error of

$$\Delta\phi = 2\pi 50 \left(\frac{1}{\gamma} - 1 \right) \approx \frac{\pi}{2} \tag{108}$$

in 50 turns using constant f.

Relativistic isochronous cyclotron

The isochronous keeps the cyclotron frequency constant by adjusting the magnetic field according the particle velocity

$$B = \frac{\gamma m_0 v}{qr} = \frac{m_0}{qr\sqrt{\frac{1}{v^2} - \frac{1}{c^2}}}. \tag{109}$$

By using particle velocity

$$v = \frac{2\pi r}{T} = 2\pi r f \tag{110}$$

one gets

$$B = \frac{m_0}{q\sqrt{\left(\frac{1}{2\pi f}\right)^2 - \left(\frac{r}{c}\right)^2}} \tag{111}$$

showing that the magnetic field should increase with increasing radius
$\Rightarrow$ breaks weak focusing.

Isochronous AVF cyclotron JYFL-K130

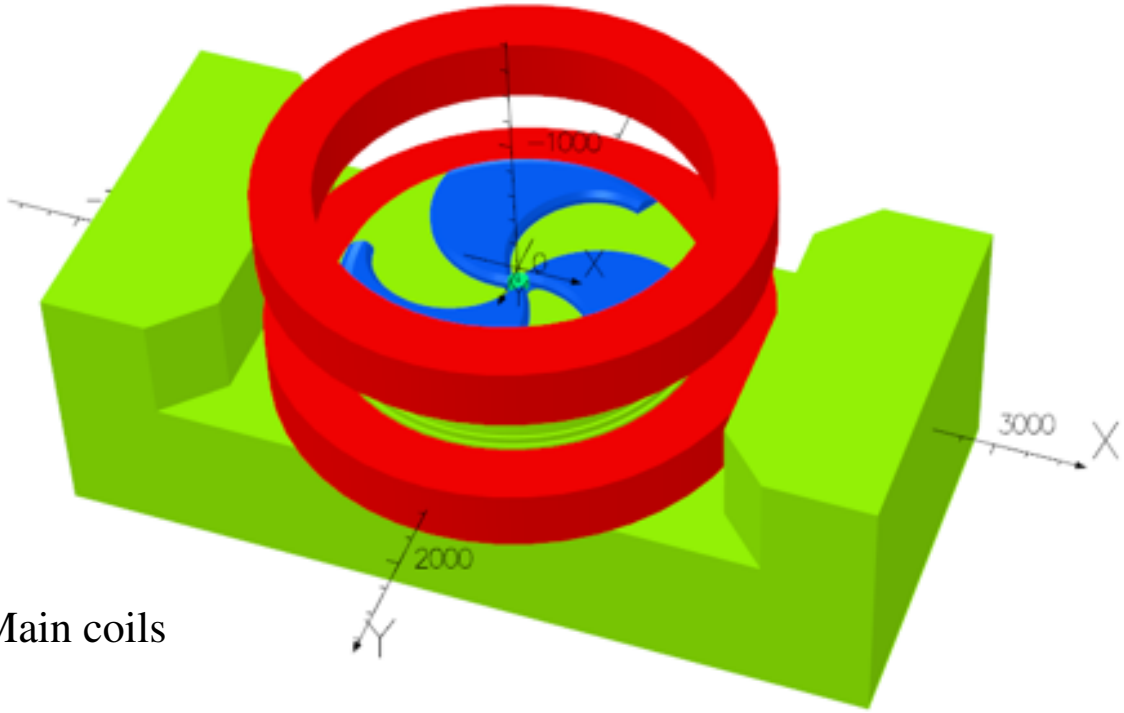

Main coils

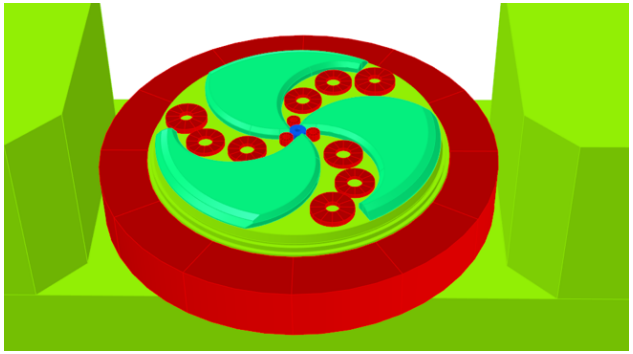

Harmonic coils

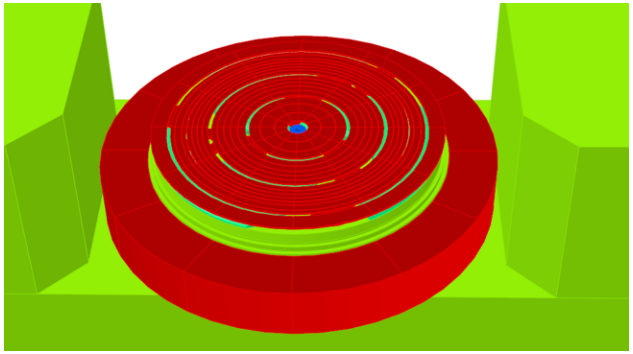

Trim coils

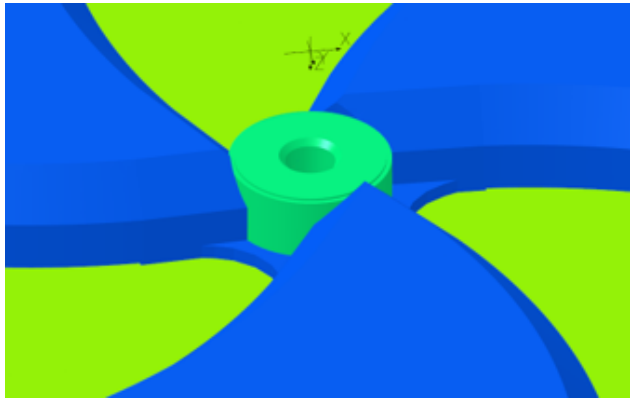

Center plug

AVF focusing

Same principle as with dipole edge focusing.

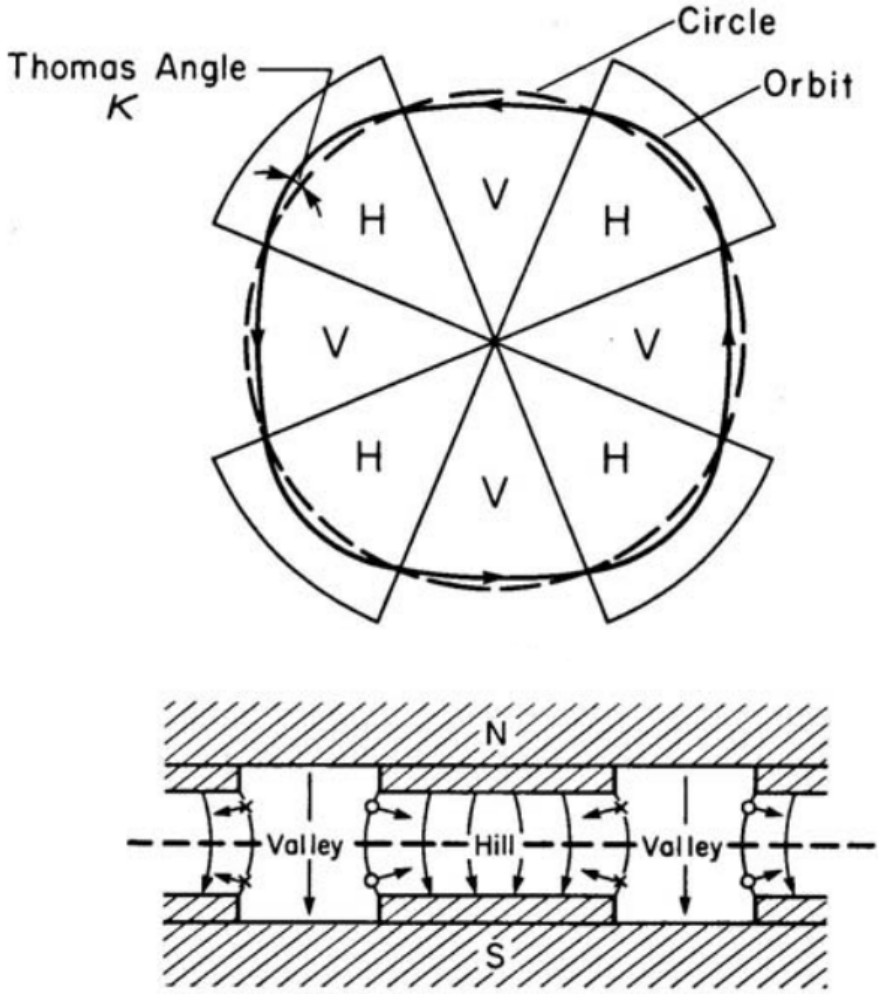

M. K. Craddock, Cyclotrons and Fixed-Field Alternating-Gradient Accelerators

Spiralled AVF focusing

Stronger focusing with spiralled sectors

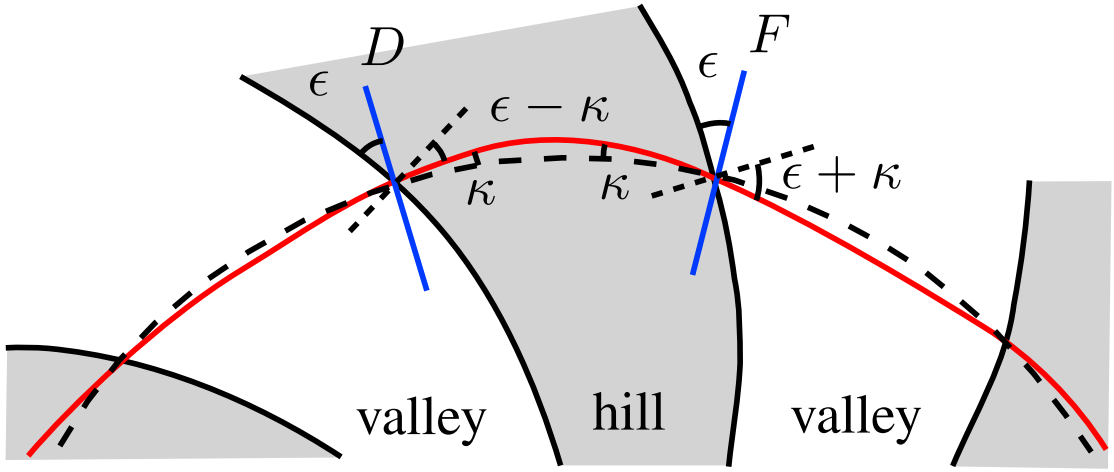

Leads to F-D-F-D-. . . structure if $\epsilon > \kappa$, which is focusing overall (same as quad doublet, triplet).

Trim coils for isochronism

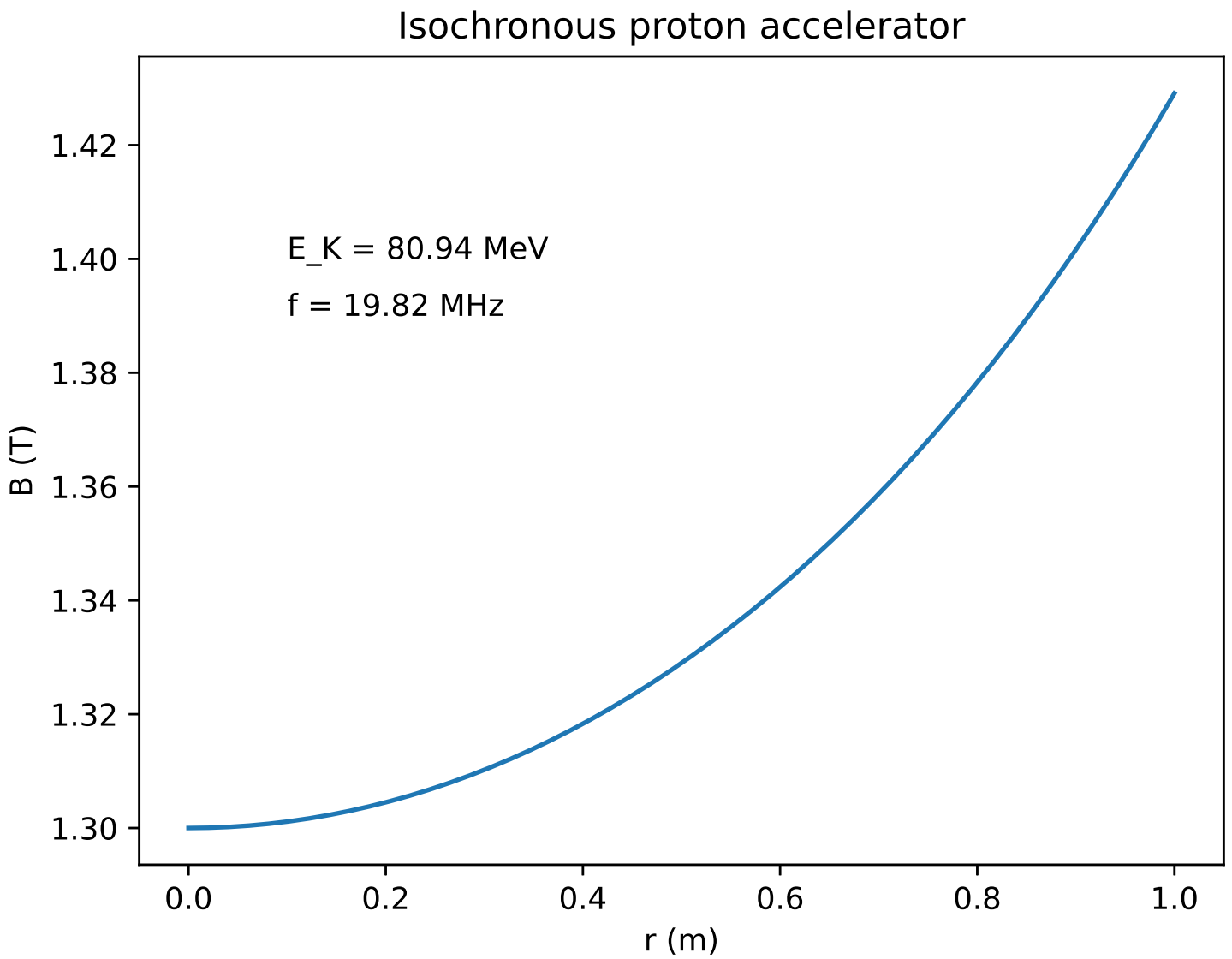

Trim coils for isochronism

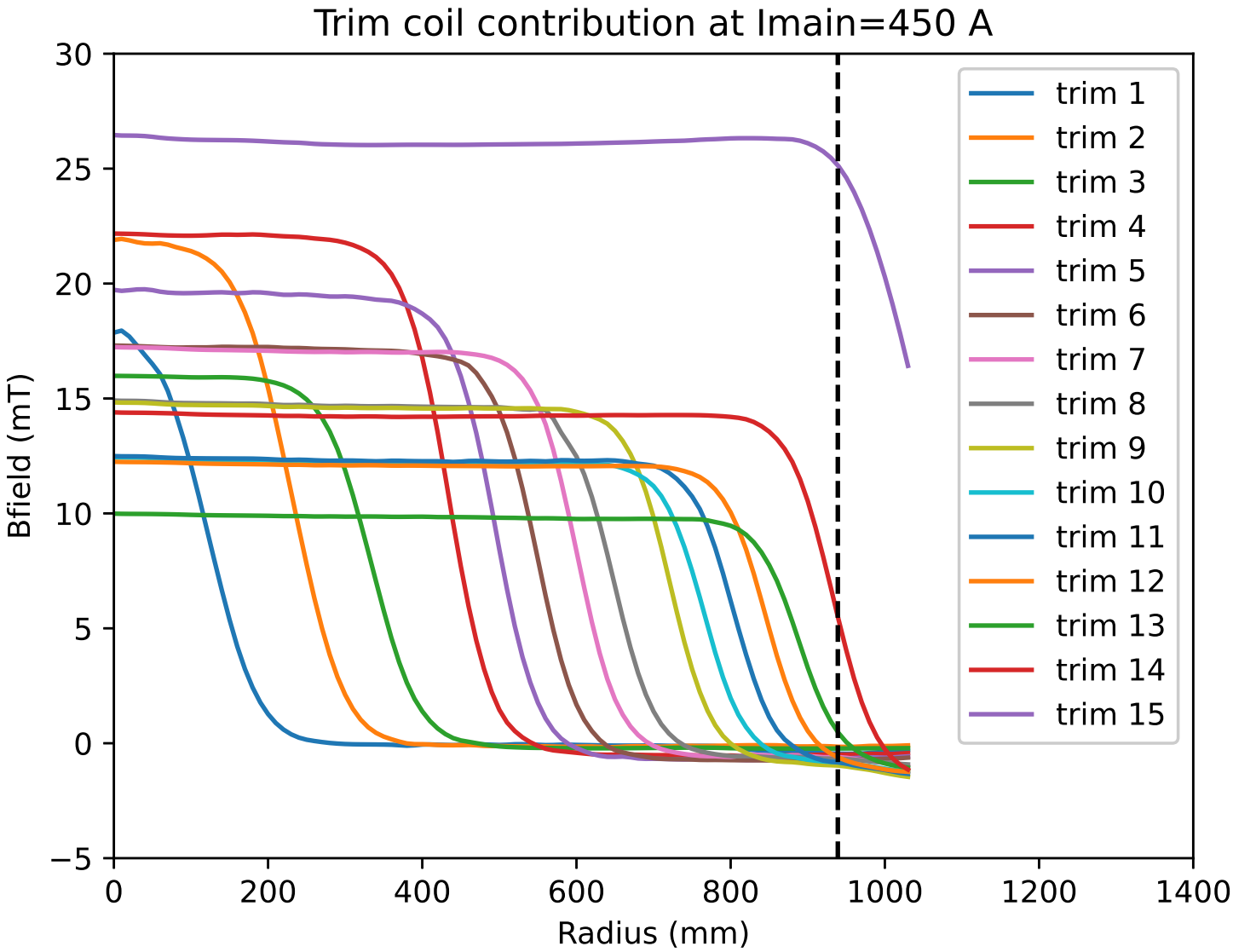

Trim coils for isochronism

```
Give Q, A, E/A or Imain : 8 19.988051 20.7624

WARNING ! - I HAVE TO EXTRAPOLATE
--------------------------------------------------------------------------------
      Control settings for K130
--------------------------------------------------------------------------------
 Mass (amu) and charge (e)               19.99     8
 Energy (MeV/u)                          20.77
 Main coil (A)                           975.0
 Harmonic number                             1
 Frequency (MHz)                          10.5791
 Dee voltage (kV)                         31.6
--------------------------------------------------------------------------------
       Trim coils                        (A)
--------------------------------------------------------------------------------
     1                  8.1
     2                 12.2
     3                 -0.5
     4                  8.1
     5                 -9.2
     6                 10.2
     7                 -2.3
     8                 -3.7
     9                  8.3
    10                 -9.9
    11                 33.6
    12                 19.1
    13                -25.4
    14                -74.4
    15                  0.0

--------------------------------------------------------------------------------
       Injection
--------------------------------------------------------------------------------
 Injection voltage (kV)                     10.04
 Spiral voltage (kV) corrected           +-  1.67
```

Acceleration

Harmonic acceleration

From unrelativistic energy, eq. (102) and frequency, eq. (104) one gets

$$\frac{E_K}{m} = \frac{1}{2}(2\pi f_c)^2. \tag{112}$$

To have a wide energy range for a machine, one needs a wide frequency range.

Problematic especially at the low end of the energy range as wavelength

$$\lambda = \frac{c}{f} \tag{113}$$

becomes long and RF resonators (usually $\lambda/2$ or $\lambda/4$ long) become large.

RF range can be extended with harmonic modes for acceleration:

$$f_{RF} = h f_c \tag{114}$$

RF resonator with moving shunt

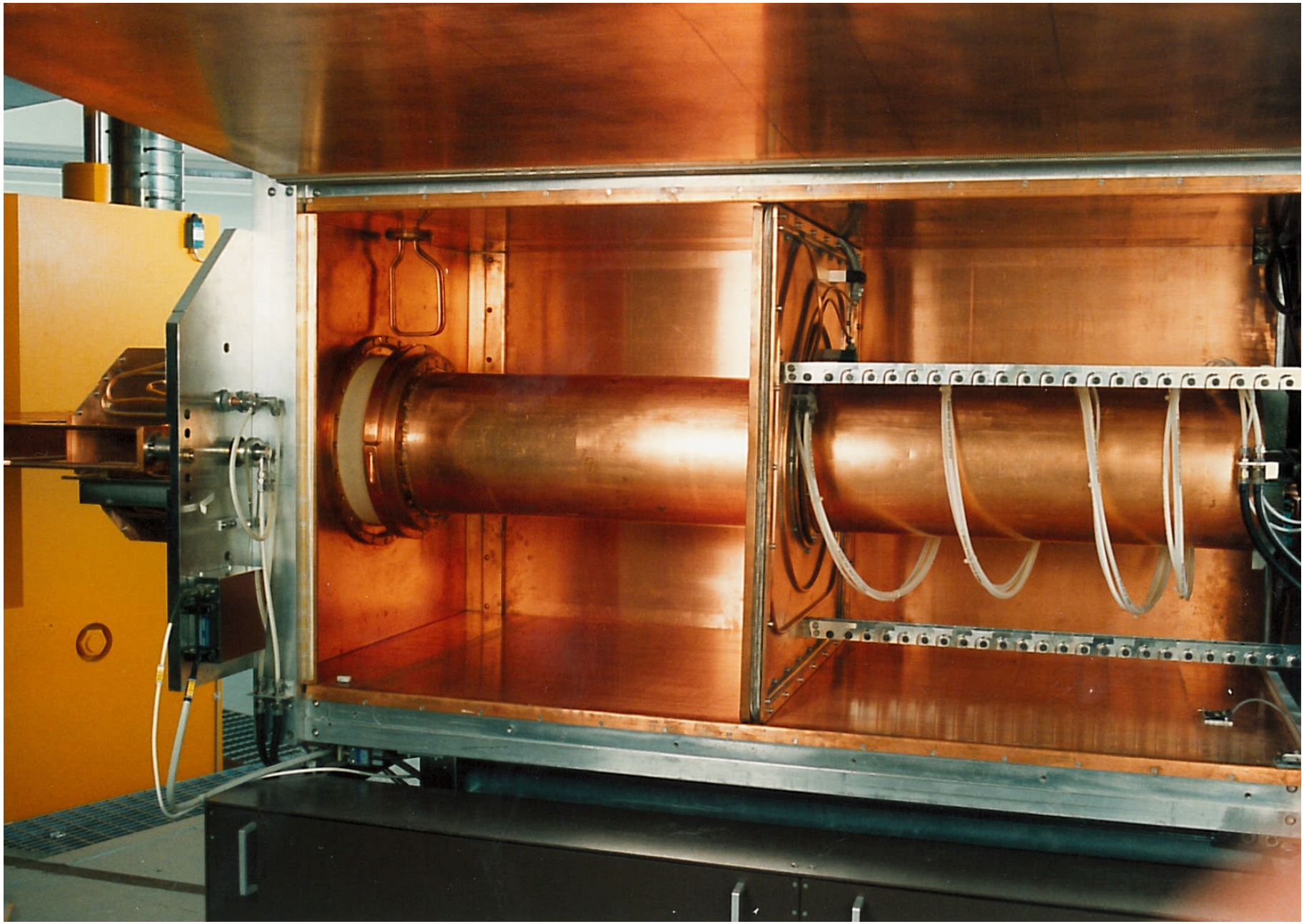

Harmonic acceleration

K130 RF: 10–21 MHz enables $f_c = 5$–10.5 MHz with $h = 2$ and $f_c = 3.3$–7 MHz with $h = 3$.

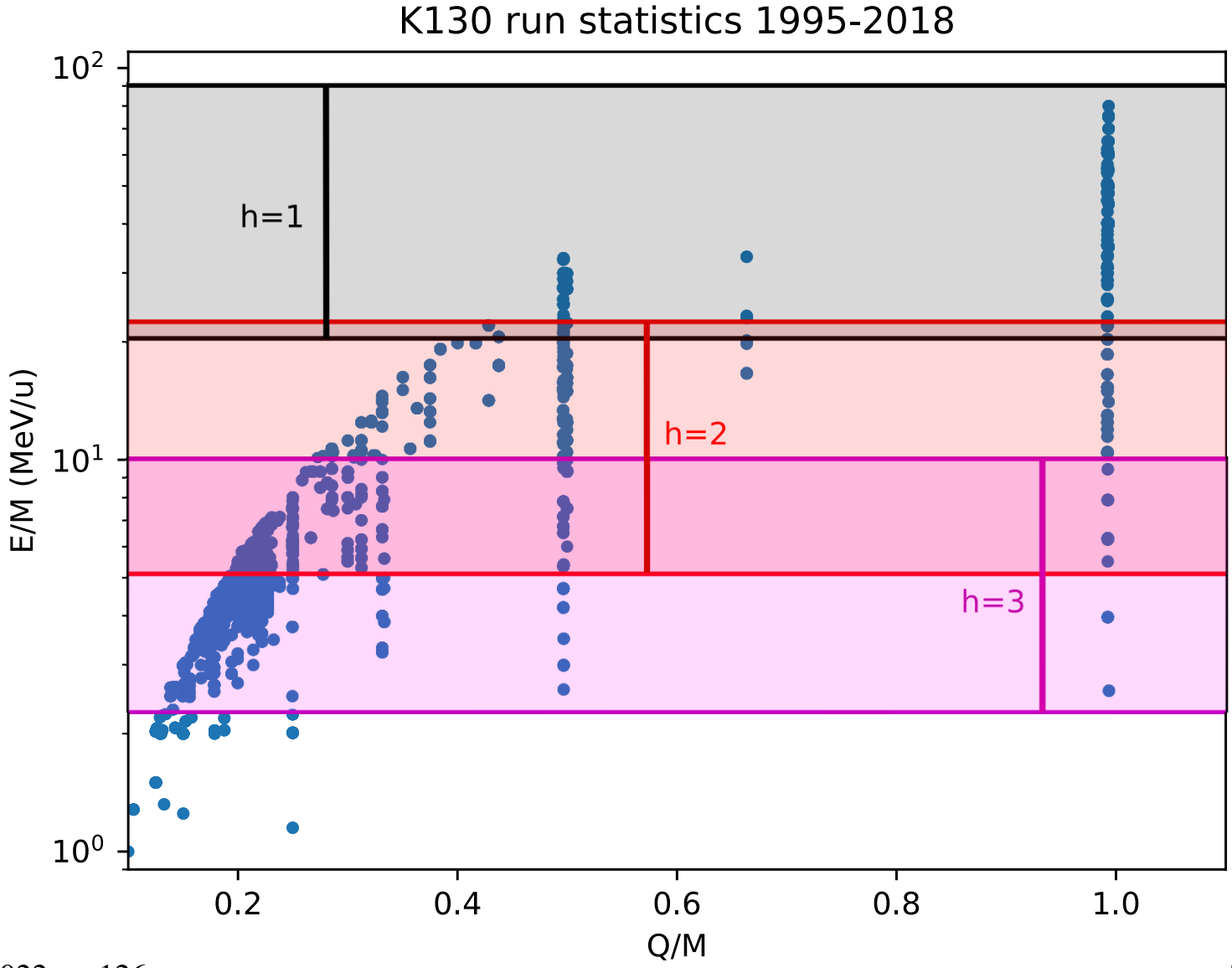

Cyclotron with two (four) dees

Having two ($\sim 90^\circ$) dees has the advantage of enabling the use of all harmonics $h = 1, 2, 3, \ldots$

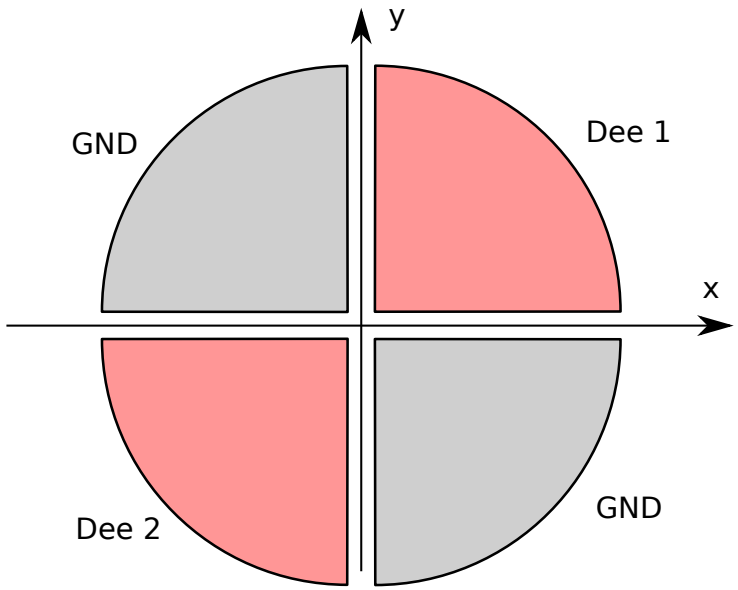

With h=1: Dee1 and Dee2 have 180° phase difference.

With h=2: Dee1 and Dee2 have same phase.

With h=3: Dee1 and Dee2 have 180° phase difference.

Cyclotron with two (four) dees

Dee phasing for K130 with 78° dees

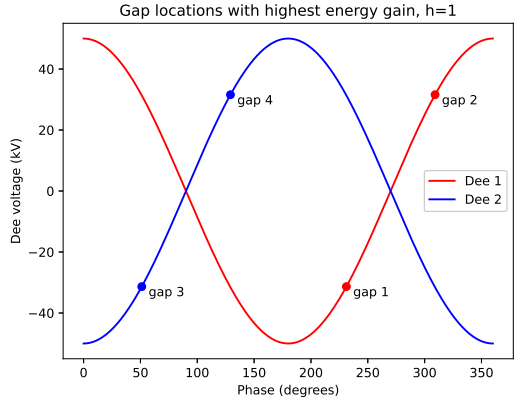

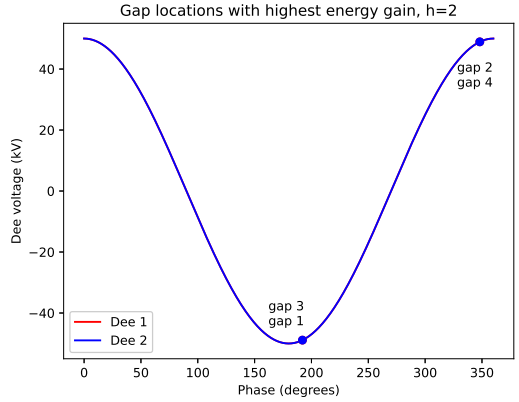

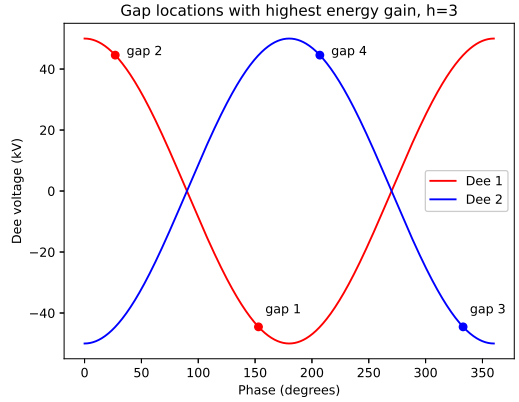

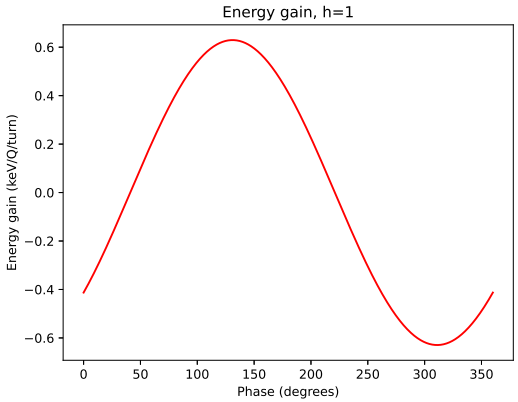

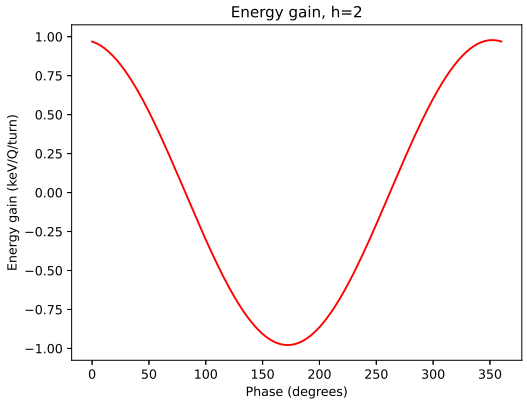

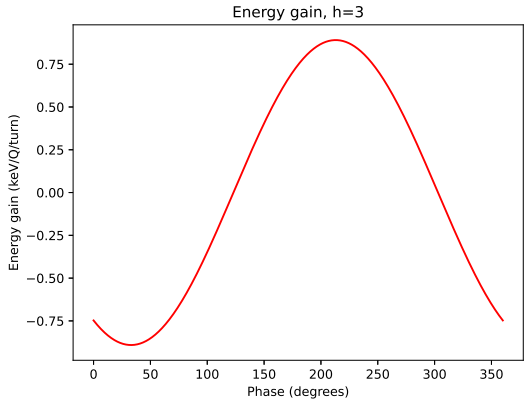

Injection to cyclotron

Low energy beam injection to cyclotron is typically done axially (z) through the iron yoke. Turning the beam to acceleration plane (xy) is done using

- Inflector (K130 and other "modern" machines) or
- $45°$ reflector / electrostatic mirror

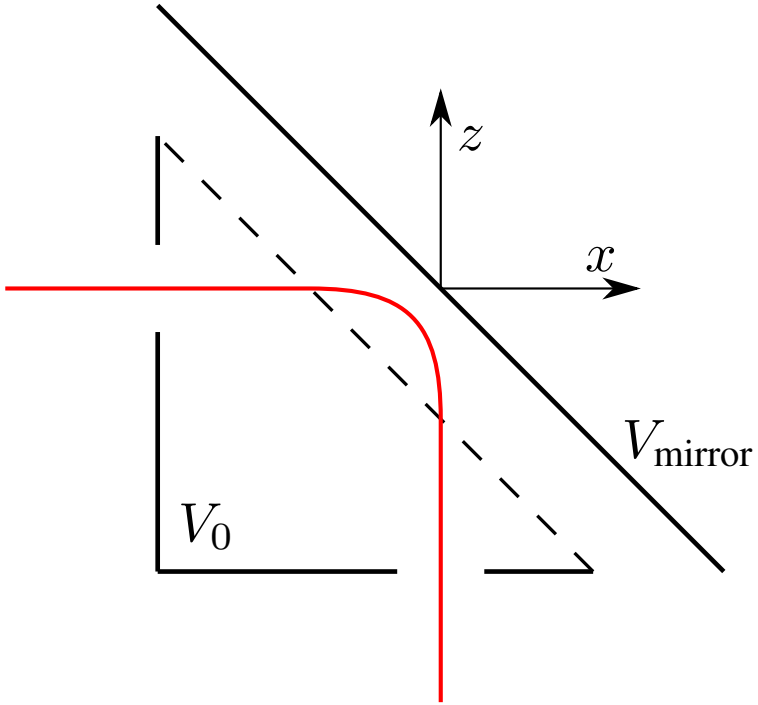

Inflectors

Definition of local coordinates:

- Coordinate axis $\hat{v}$ is parallel to velocity vector.
- Coordinate axis $\hat{h}$ is perpendicular to v and in plane with xy.
- Coordinate axis $\hat{u} = \hat{h} \times \hat{v}$.

Inflector design points:

1. E_h is perpendicular to the velocity in the xy plane (direction of magnetic force).
2. E_u is constant (Belmont-Pabot case) or $E_u^2 + E_h^2$ is constant.
3. E_v is zero.

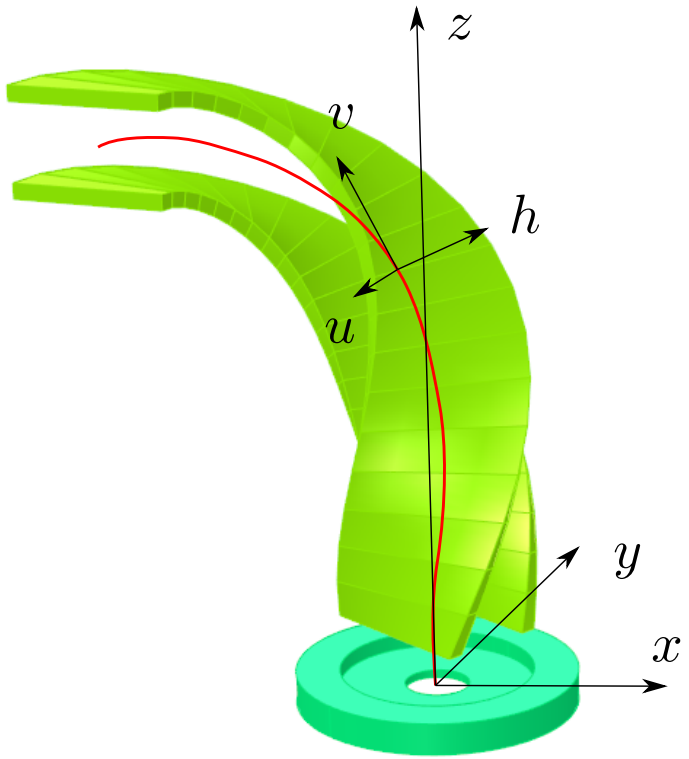

Belmont-Pabot inflector

Central ray trajectory for the Belmont-Pabot case is analytic if B_z constant:

$$x = \frac{A}{2}\left[\frac{2}{1-4K^2} + \frac{\cos(2K-1)b}{2K-1} - \frac{\cos(2K+1)b}{2K+1}\right] \tag{115}$$

$$y = \frac{A}{2}\left[\frac{\sin(2K+1)b}{2K+1} - \frac{\sin(2K-1)b}{2K-1}\right] \tag{116}$$

$$z = -A\sin b, \tag{117}$$

where $0 \leq b \leq \frac{\pi}{2}$ and

$$b = \frac{v_0 t}{A} \tag{118}$$

$$A = \frac{m v_0^2}{q E_u} \tag{119}$$

$$K = \frac{A}{2\rho} + \frac{k}{2}. \tag{120}$$

Belmont-Pabot inflector

The k adjusts the slant of the inflector as

$$\vec{E} = E\big(\sin\theta\hat{h} + \cos\theta\hat{u}\big) \tag{121}$$

$$\tan\theta = k\sin b \tag{122}$$

$$E = E_u\sqrt{1 + (k\sin b)^2} \tag{123}$$

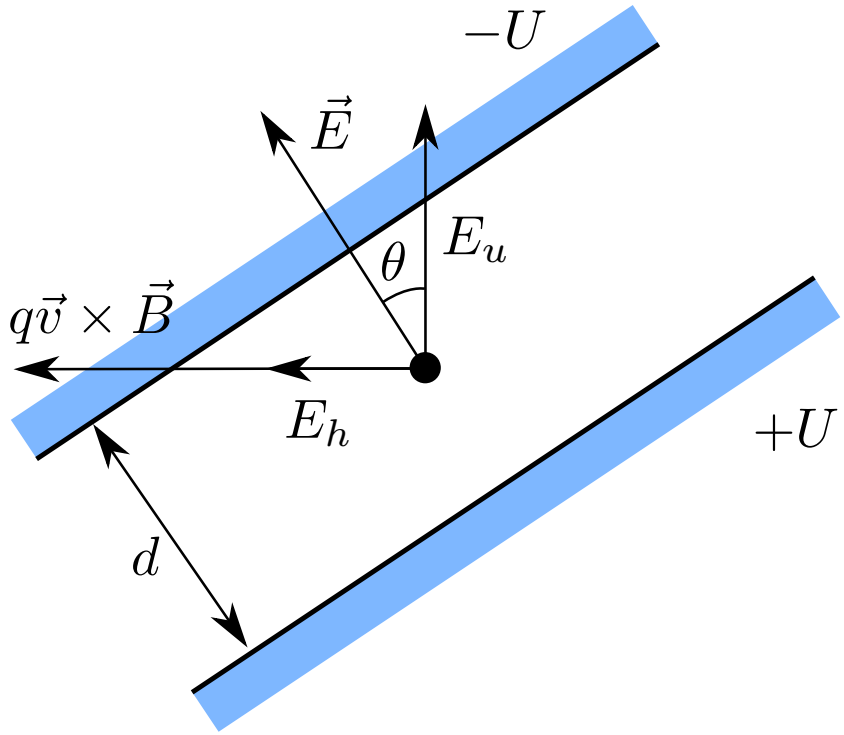

Electrode distance decreases along inflector if $k \neq 0$.

Belmont-Pabot inflector

A/ρ and k selected to find suitable inflector geometry

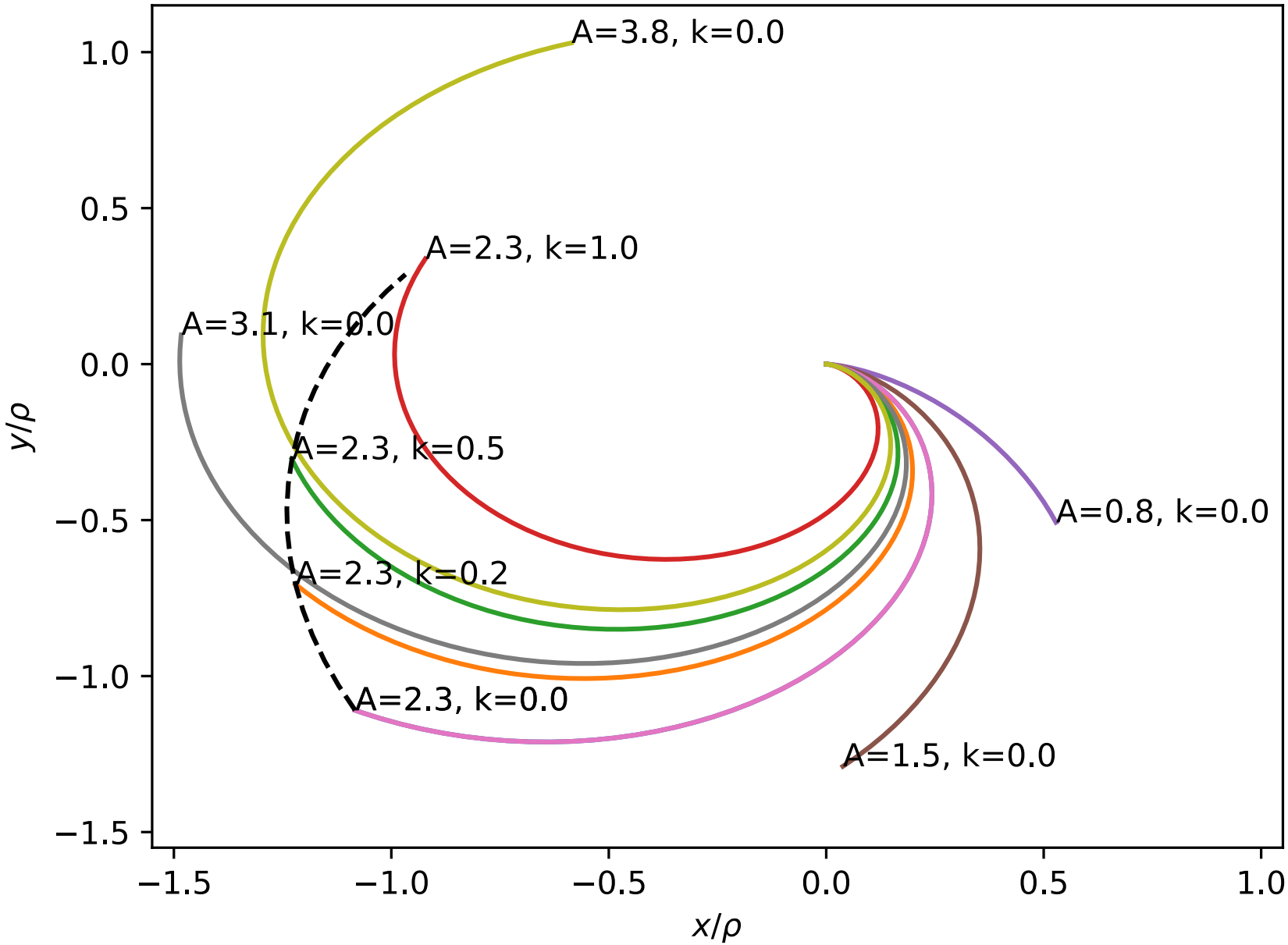

Central region

K130 has three inflectors for the three harmonics. Inflector parameters chosen to optimize accelerated beam centering. Central region case separates inflector from dees.

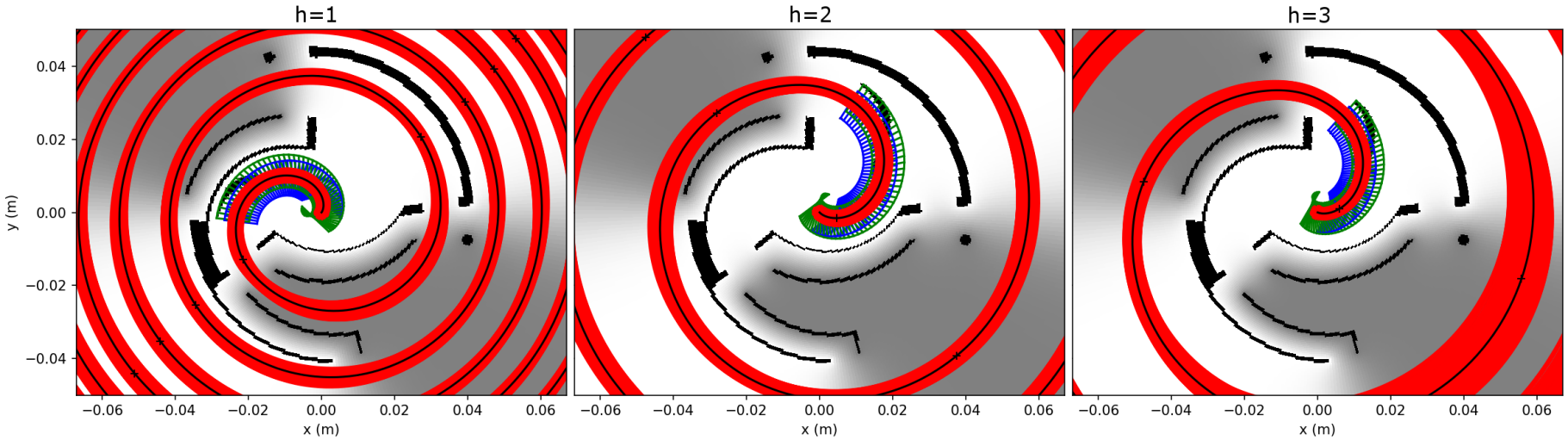

These figures from a new high energy central region designed for K130.

Phase acceptance

Beam acceptance is not $360^\circ \Rightarrow$ Bunching the DC beam improves throughput.

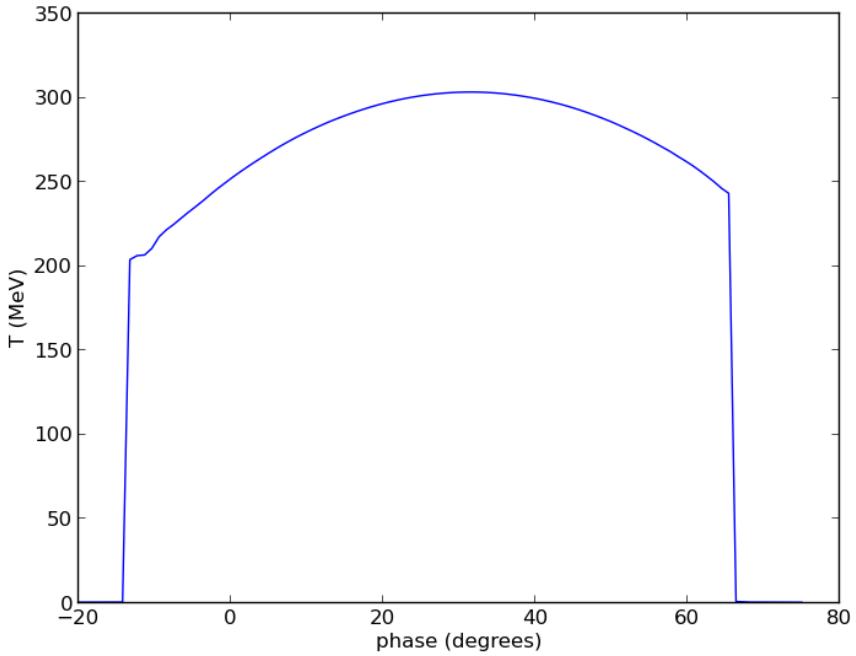

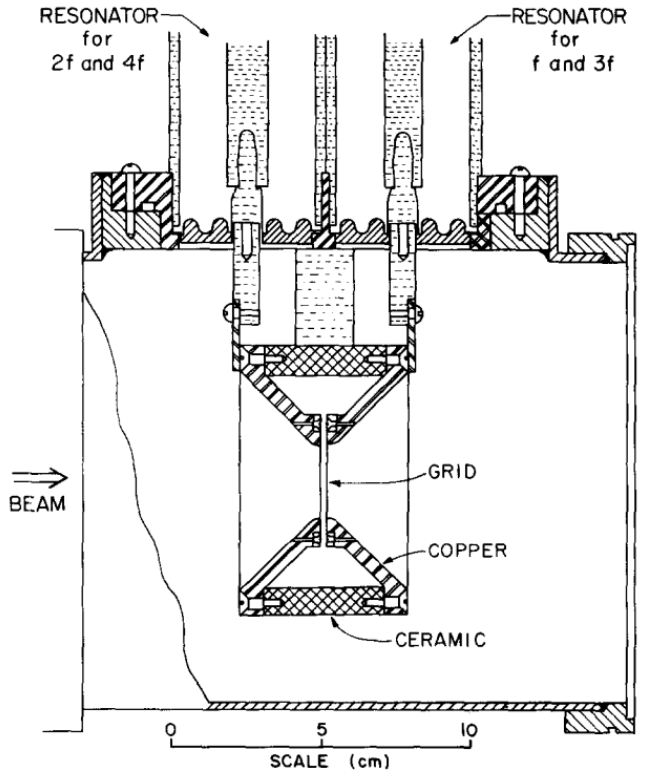

When $\tau_{RF} \ll T$

$$\Delta E \approx \frac{2t}{T} E_0, \tag{124}$$

where T is the flight time to point of focus.

See F. J. Lynch, et al., Nucl. Instrum. Meth. 159, 245 (1979).

Bunched beam

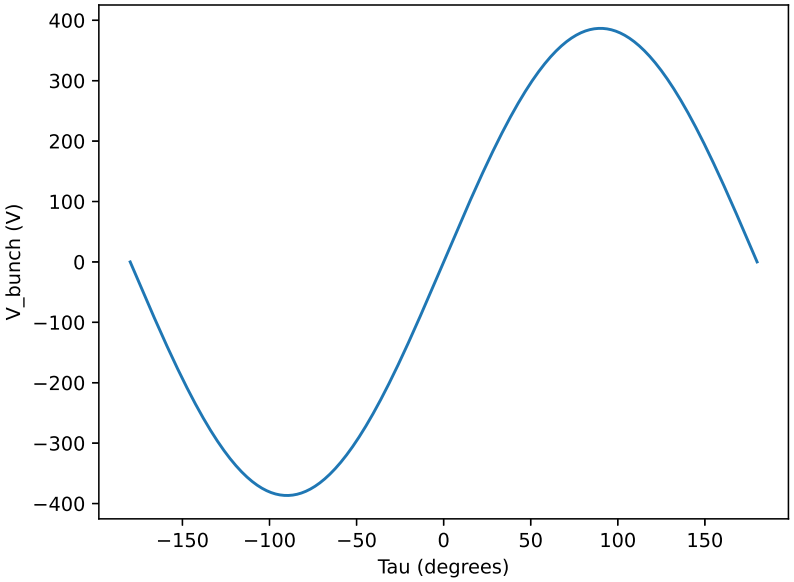

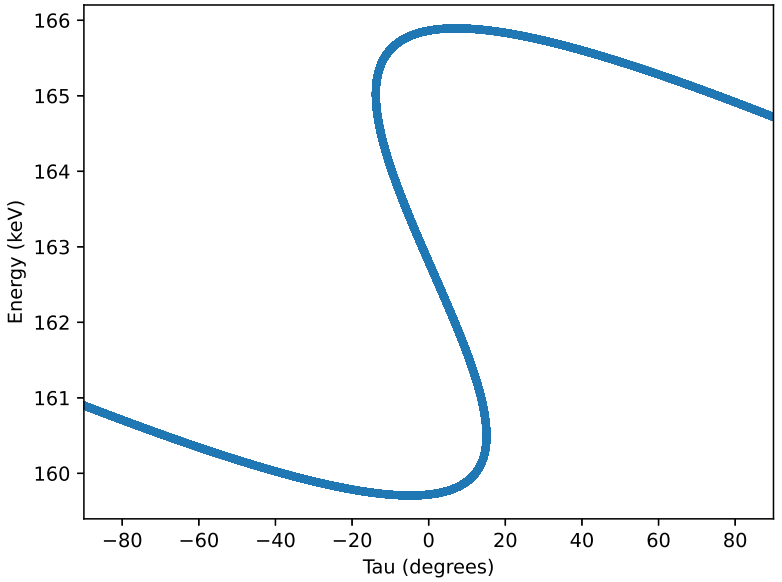

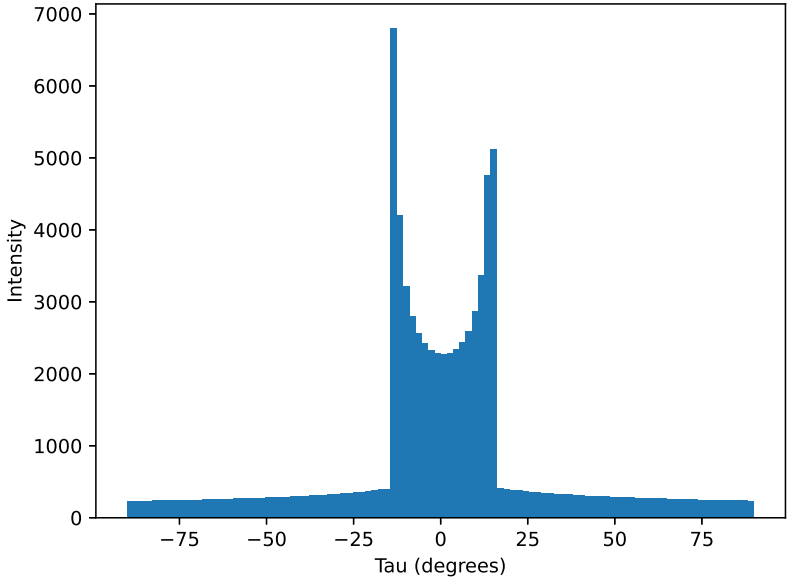

Inflector changer

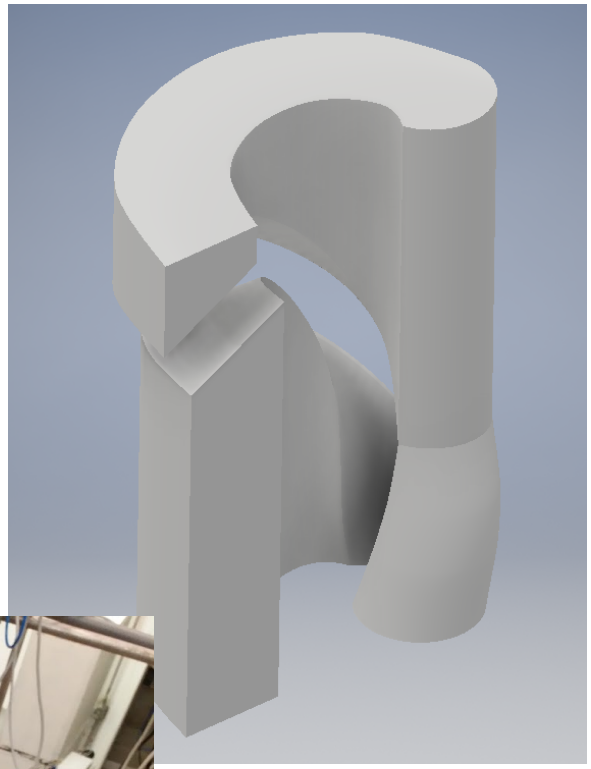

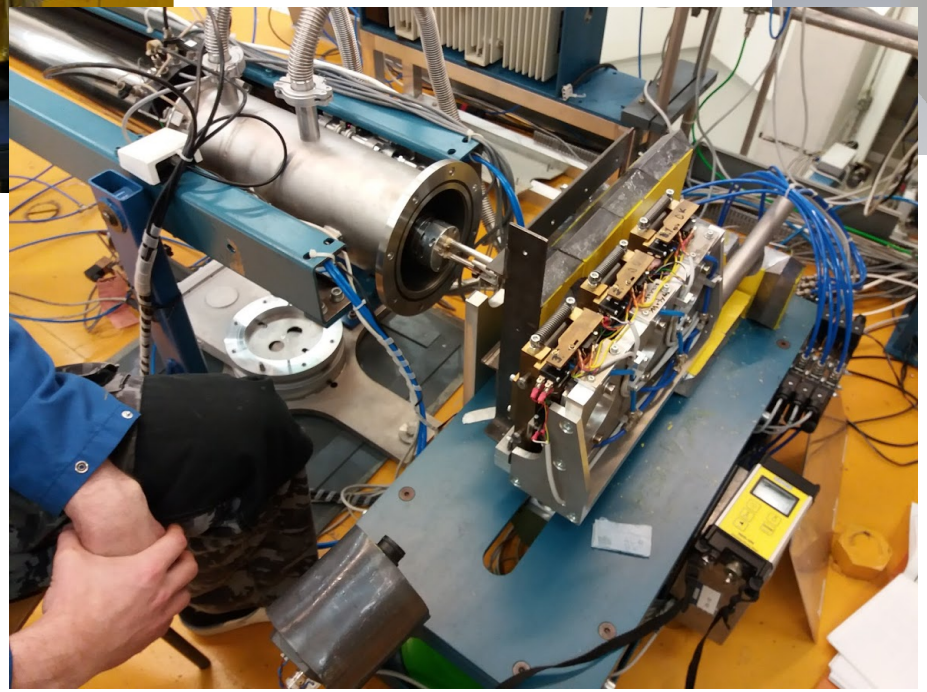

Extraction

The first turns are well separated, but not at the extraction radius.

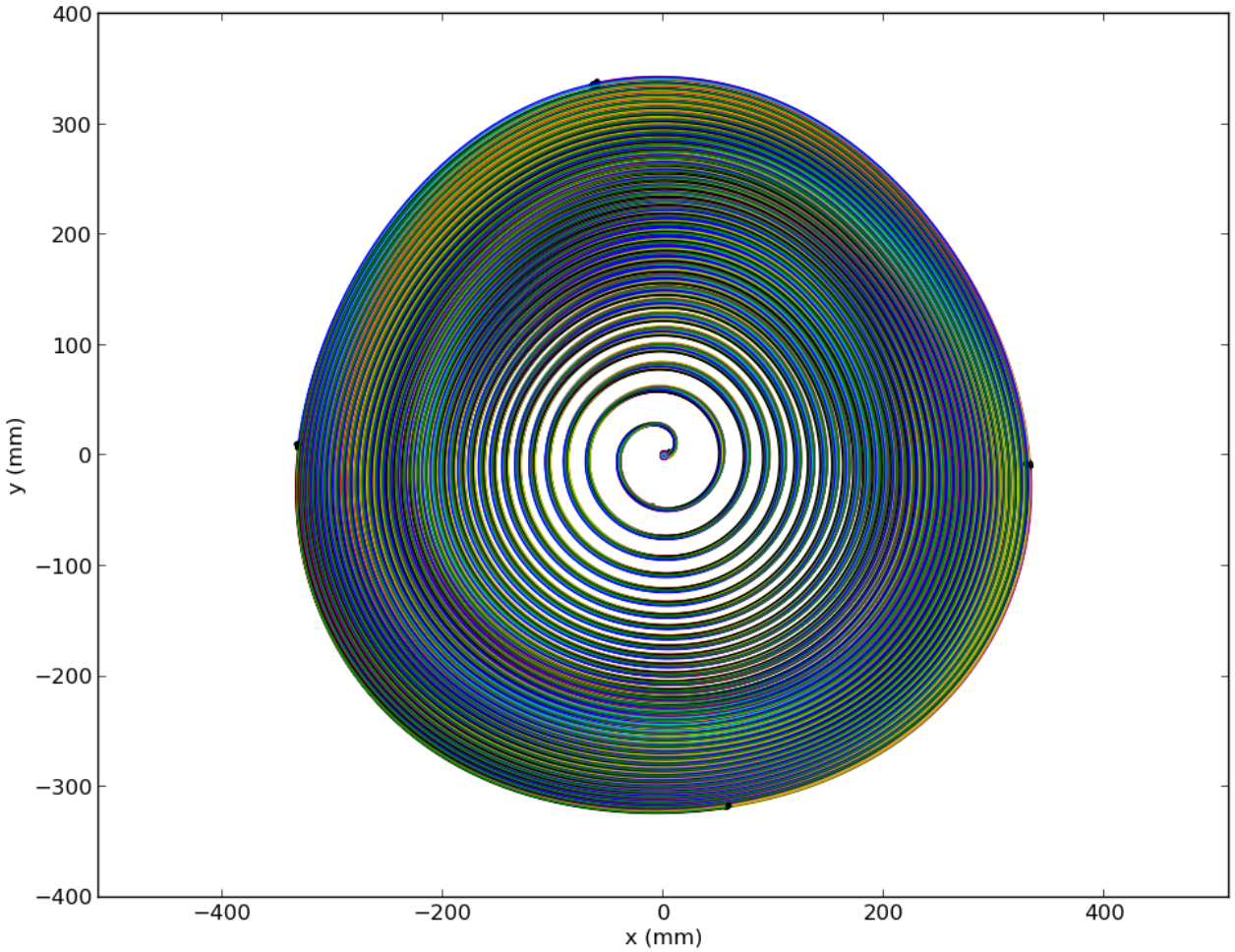

How to extract beam in a controlled manner?

H^- extraction

The easy case: H^- is accelerated, stripped with a thin carbon foil at final radius to produce protons (H^+).

Particle radius of curvature $r = \frac{mv}{qB}$ changes from negative to positive and allows easy extraction.

Poor energy resolution. Low losses.

Carbon foils most commonly used for stripping.

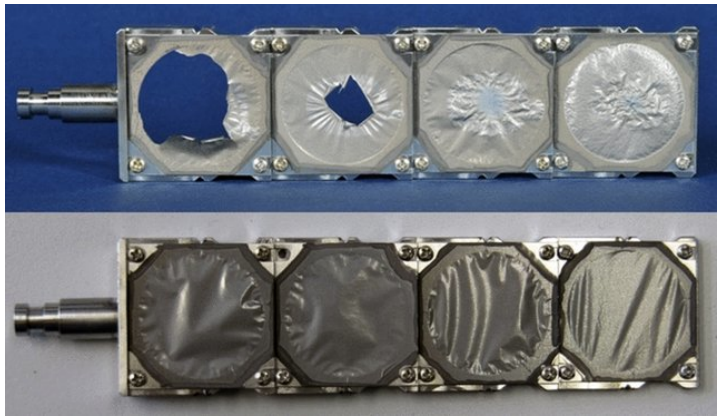

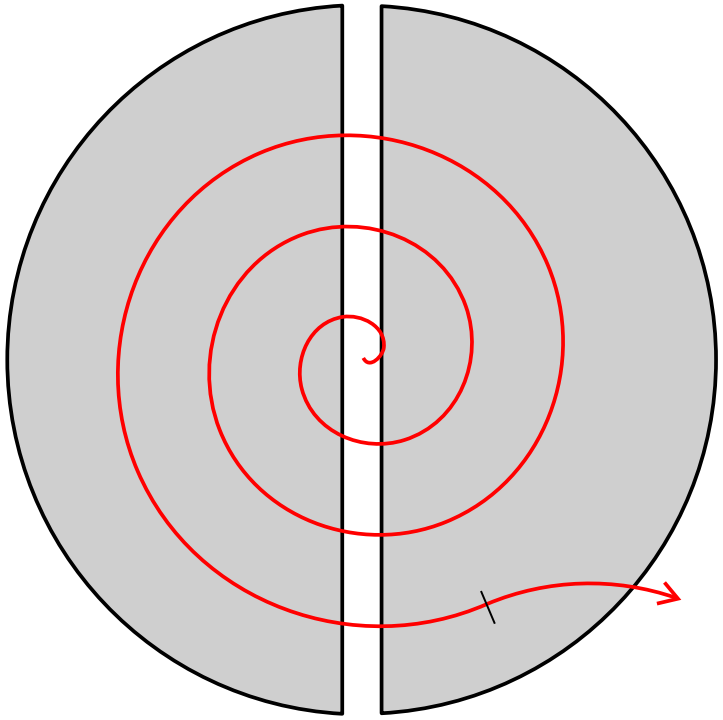

Electrostatic deflector

An electrostatic deflector plate is used to increase orbit separation at extraction.

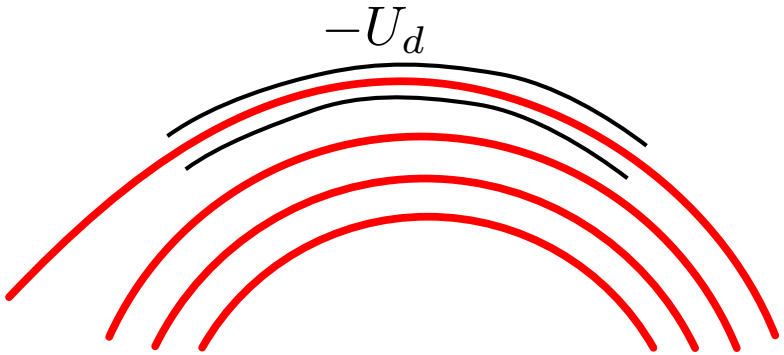

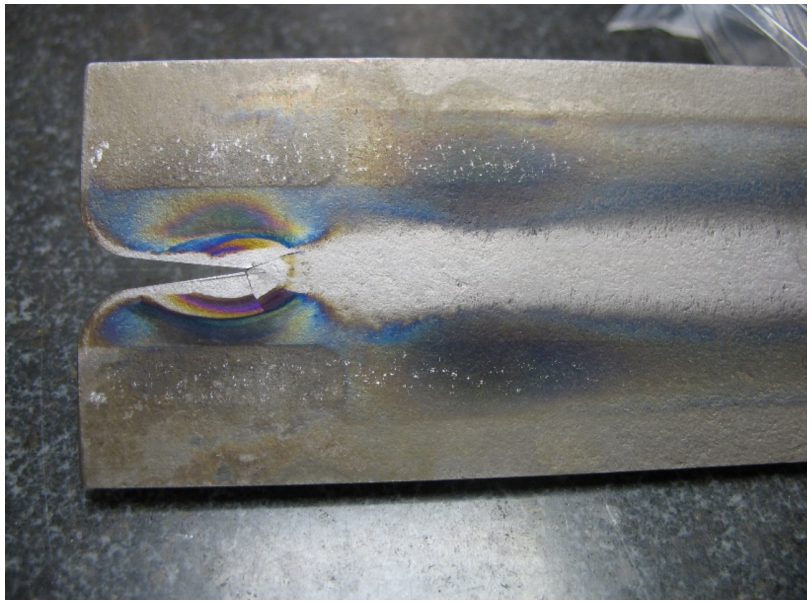

A thin sheet of 0.25–1 mm (septum) separates electric field from other orbits.

Experiences a high power load from stray beam.

After the deflector the beam is further separated by EMC, passive channels, etc.

Precessional extraction

Before deflector an initial separation is needed. This is produced with a perturbance from harmonic coils and a $\nu_r = 1$ resonance in the radial focusing.

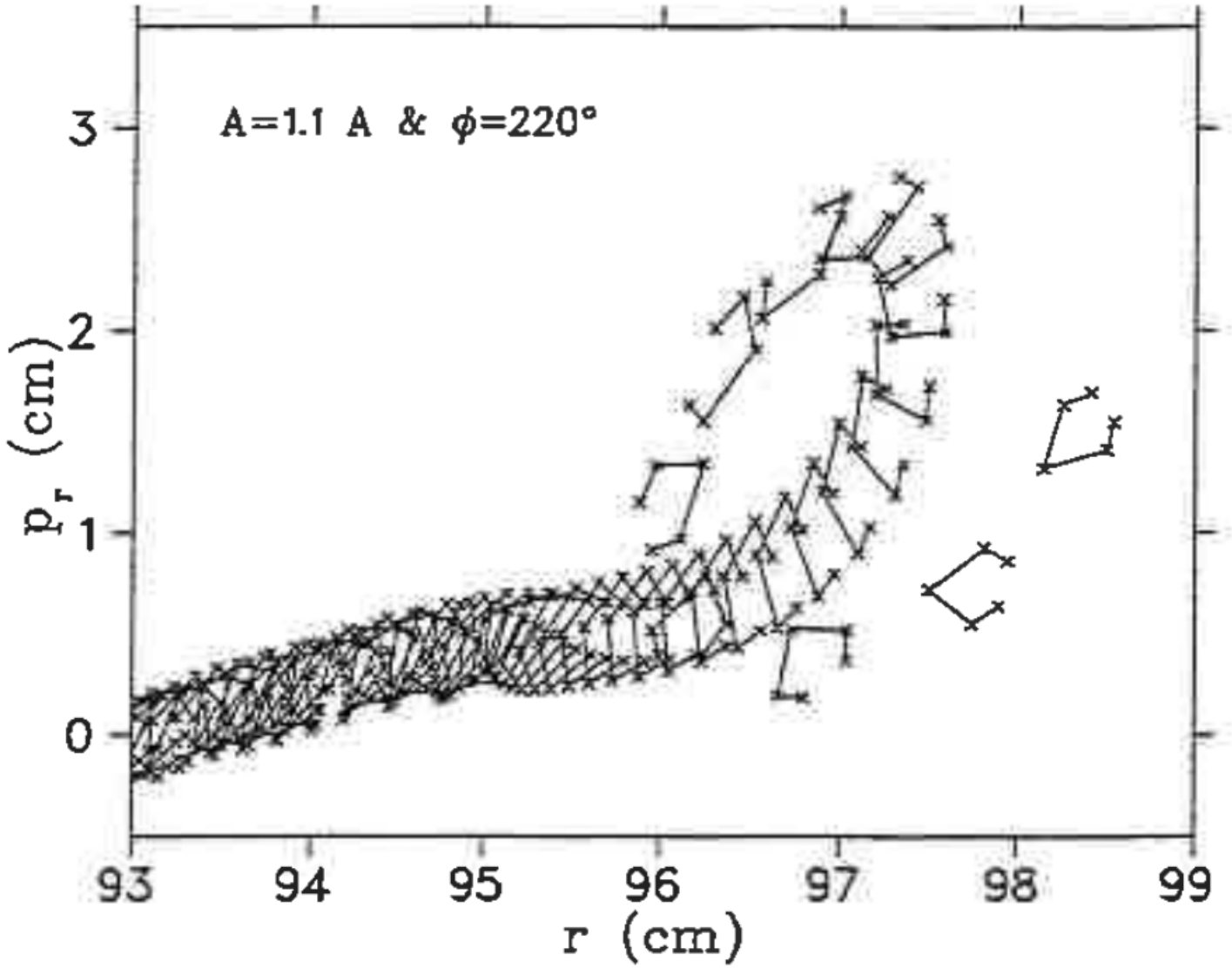

Diagnostics within the cyclotron

- Inflector as FC
- Main probe
- Deflector probe

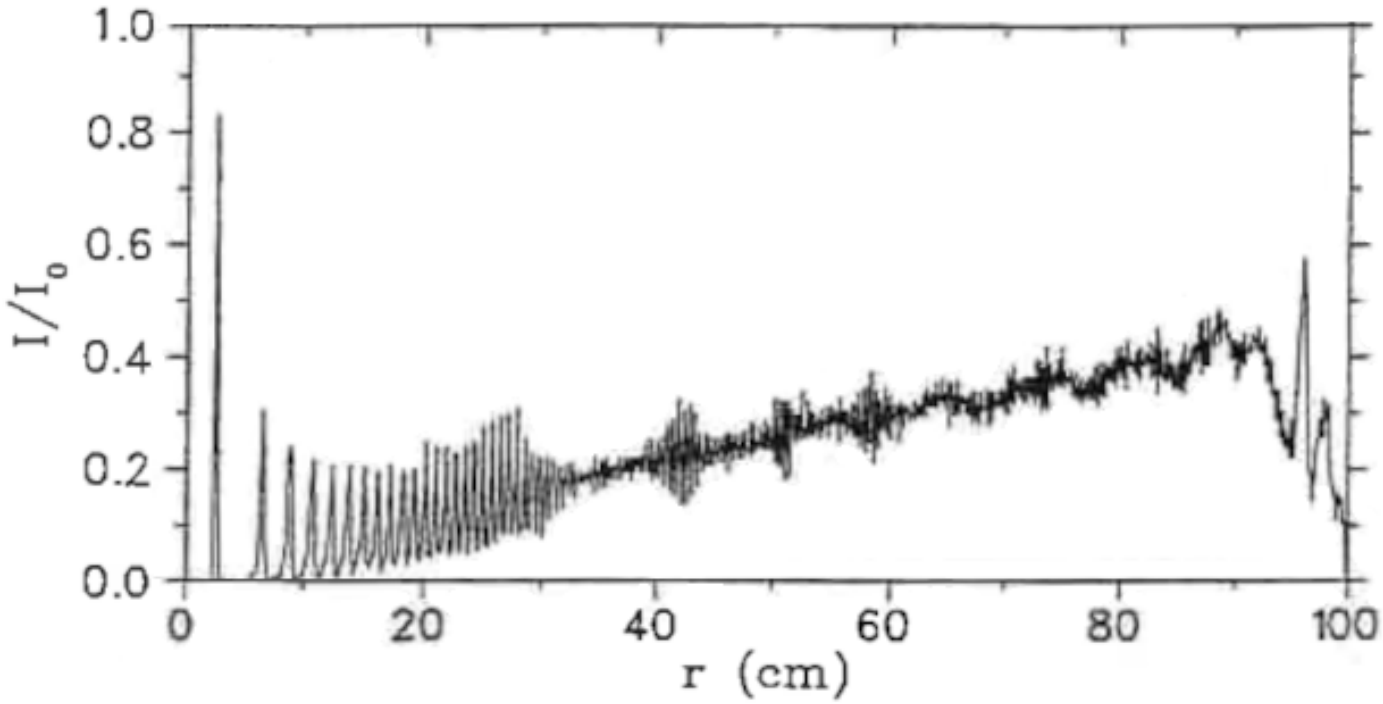

Vacuum physics and technology

Ideal gas

The ideal gas law relates the particle density, temperature and pressure:

$$p = nkT. \tag{125}$$

Pressure units:
1 atm = $1.01325 \cdot 10^5$ Pa or N/m^2
1 bar = 10^5 Pa
1 mbar = 1 hPa = 100 Pa
1 atm = 760 torr or mmHg

Force:

$$F = PA \tag{126}$$

Pressure difference typically 1 bar: $\varnothing$10 cm pipe $\Rightarrow$ F = 785 N

Ideal gas

The particle speeds in thermodynamic equilibrium (usually) are given by MB:

$$f(v) = \left(\frac{m}{2\pi kT}\right)^{3/2} 4\pi v^2 \exp\left(-\frac{mv^2}{2kT}\right) \tag{127}$$

with most probably speed

$$v_p = \sqrt{\frac{2kT}{m}}, \tag{128}$$

mean speed

$$\langle v \rangle = \sqrt{\frac{8kT}{\pi m}} \tag{129}$$

and rms-speed

$$v_{rms} = \sqrt{\langle v^2 \rangle} = \sqrt{\frac{3kT}{m}}. \tag{130}$$

Ideal gas

The distribution of the velocity vector is a product of three independent normal (Gaussian) distributions

$$f_v(v_x, v_y, v_z) = \left(\frac{m}{2\pi kT}\right)^{3/2} \exp\left(-\frac{m(v_x^2 + v_y^2 + v_z^2)}{2kT}\right) \tag{131}$$

with variance $\frac{kT}{m}$.

The mean speeds at NTP (293 K) gas are:
N_2 ($M = 28$): $\langle v \rangle = 470$ m/s
He ($M = 4$): $\langle v \rangle = 1245$ m/s
H ($M = 2$): $\langle v \rangle = 1761$ m/s

Mean free path

The number of collision a molecule experiences per unit time is

$$N \approx \pi D^2 \langle v \rangle n, \tag{132}$$

where D is the molecule diameter. This leads to a mean free path of molecules

$$\lambda = \frac{\langle v \rangle}{N} = \frac{1}{\sqrt{2}\pi D^2 n}. \tag{133}$$

With nitrogen molecule radius of 0.3 nm, $\lambda \approx 80$ nm and scales linearly with pressure or particle density, i.e.

$$\lambda n \propto \lambda P = \text{const.} \tag{134}$$

Gas glow regimes

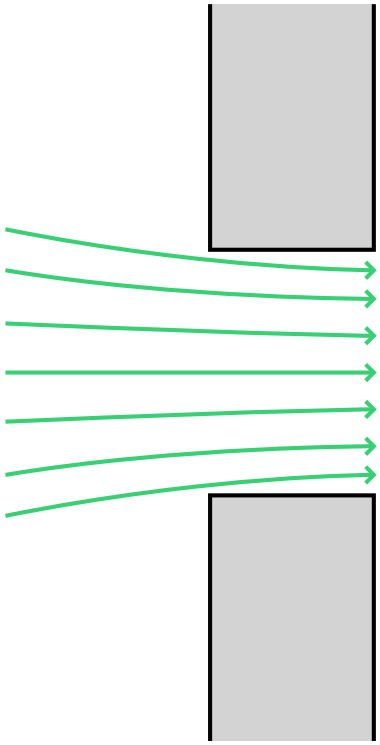

Viscous

$\lambda \ll L$

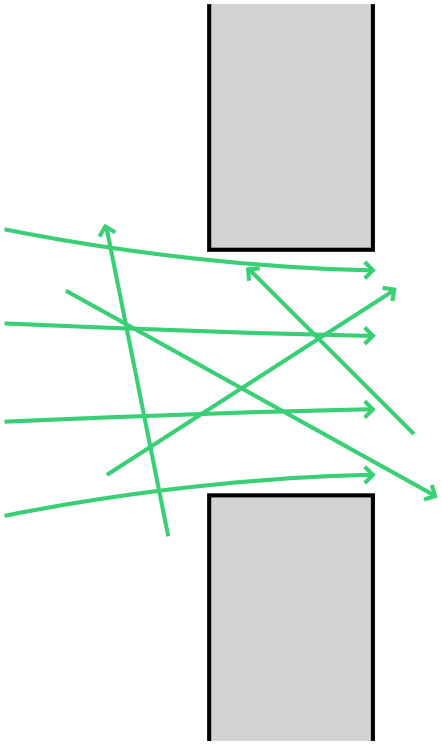

Intermediate

$\lambda \sim L$

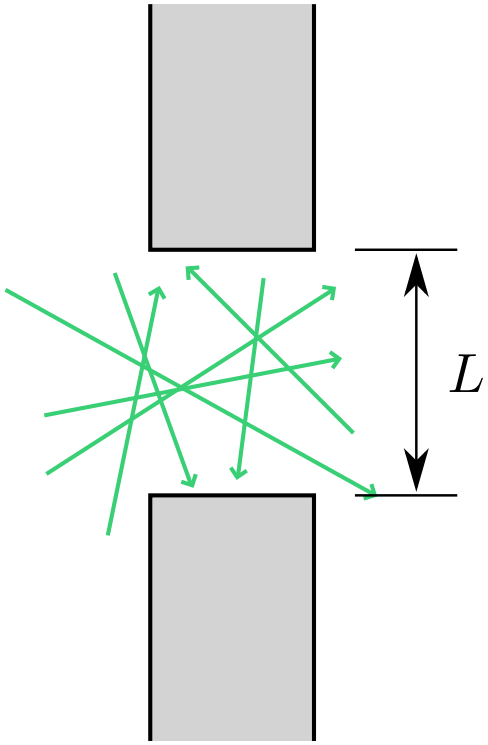

Molecular

$\lambda \gg L$

Numbers and terminology

Vacuum region	P (mbar)	λ (m)
Rough Vacuum	$1 - 10^3$	100 μm – 100 nm
Intermediate Vacuum	$10^{-3} - 1$	100 mm – 100 μ
High Vacuum	$10^{-6} - 10^{-3}$	100 m – 100 mm
Good High Vacuum	$10^{-9} - 10^{-6}$	100 km – 100 m
Ultra High Vacuum	$< 10^{-9}$	$>$ 100 Mm

Residual gas

Pumping from atmospheric pressure towards better vacuum:

- Initially air
- Rough vacuum: thin air
- Intermediate vacuum: solids/liquids start boiling from surfaces (outgassing)
- High vacuum: mainly gases from surfaces, 90 % water
  Gradually decreases, CO, CO_2 increase
- UHV: mainly hydrogen (difficult to pump)

Generally not air at high vacuum, unless leaks in system. Contaminants, oils, moisture, etc. easily dominate.

Pumping speed and throughput

Typically the pumping speed is defined as

$$S = \frac{dV}{dt} \tag{135}$$

and gas throughput as

$$Q = SP = \frac{dV}{dt}P. \tag{136}$$

A flow channel has a conductance C, which defines the throughput as

$$Q = C(P_1 - P_2), \tag{137}$$

which is analogous to Ohms law (C is the reciprocal of resistance $1/R$).
Conductances in series:

$$C_{\text{series}} = C_1 + C_2 + \cdots . \tag{138}$$

Conductances in parallel:

$$\frac{1}{C_{\text{parallel}}} = \frac{1}{C_1} + \frac{1}{C_2} + \cdots . \tag{139}$$

Conductivity of a long pipe

In laminar flow regime:

$$C_{\text{lam}} = \frac{\pi D^4}{128 \eta L} \langle P \rangle \tag{140}$$

In molecular flow regime:

$$C_{\text{mol}} = \frac{\langle v \rangle \pi D^3}{12 L} \tag{141}$$

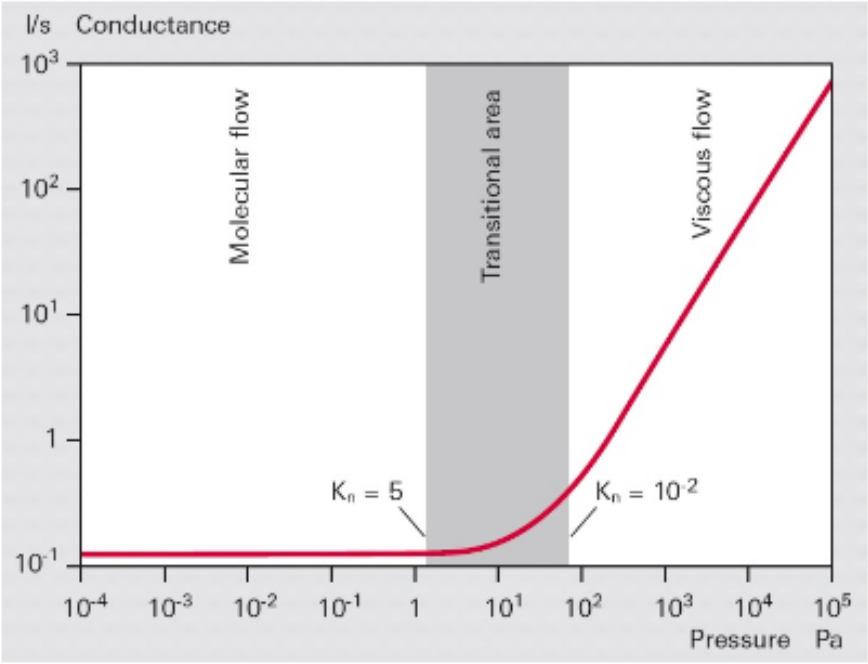

From Pfeiffer, Introduction to Vacuum Technology

Theoretical vacuum system

Vacuum system with volume V is pumped with pumping speed S, while outgassing q from the vacuum chamber surface area A introduces gas into the volume.

The ultimate vacuum arises from equilibrium of gas flows

$$qA = PS, \qquad (142)$$

thus the ultimate vacuum is

$$P = \frac{qA}{S}. \qquad (143)$$

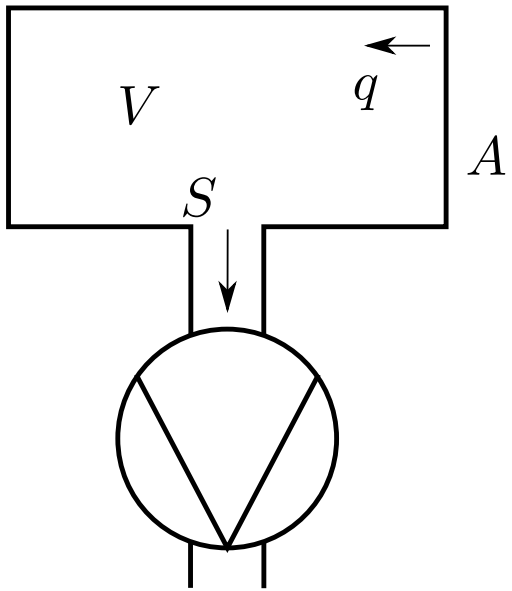

The dynamic pressure arises from DE

$$V\frac{dP}{dt} = qA - SP \qquad (144)$$

with a solution

$$P(t) = K\exp\left(-\frac{S}{V}t\right) + \frac{qA}{S}. \qquad (145)$$

Pumps

- Rotary vane pumps
- Rotary piston pumps
- Roots pumps
- Scroll pumps
- Membrane pumps
- Turbo molecular pumps
- Diffusion pumps
- Getter pumps
- Ion pumps
- Cryogenic pumps

Rotary vane and piston pumps

- Rough pumping: 10^{-3} – 1000 mbar
- 10 – 200 m^3/h
- Oil sealed
- Backing for diffusion and turbo pumps

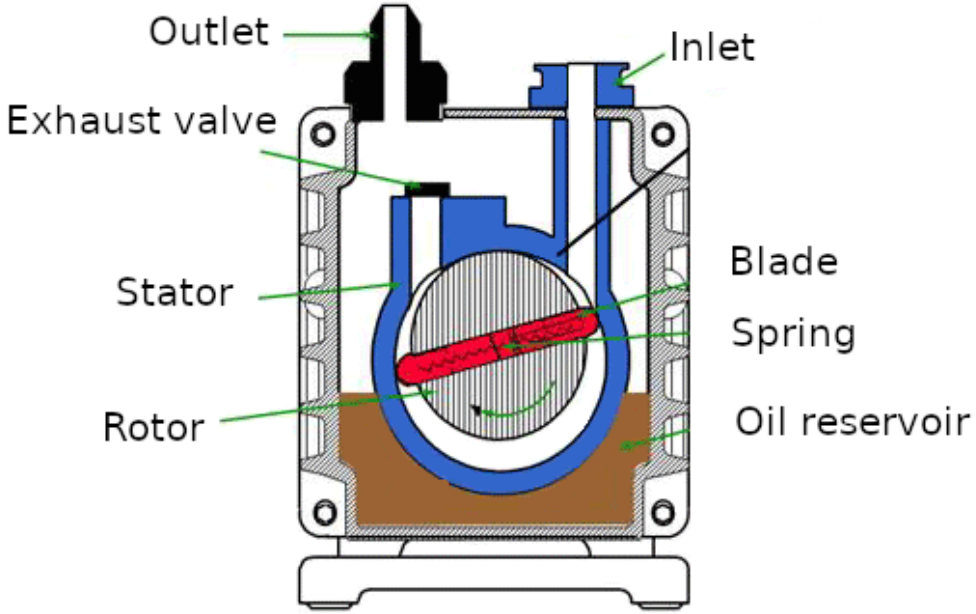

Roots pumps

- Rough pumping: 10^{-4} – 1000 mbar
- $N \times 100$ m^3/h
- Contact free (no oil in vacuum)
- Typically used as a booster with other mechanical pumps

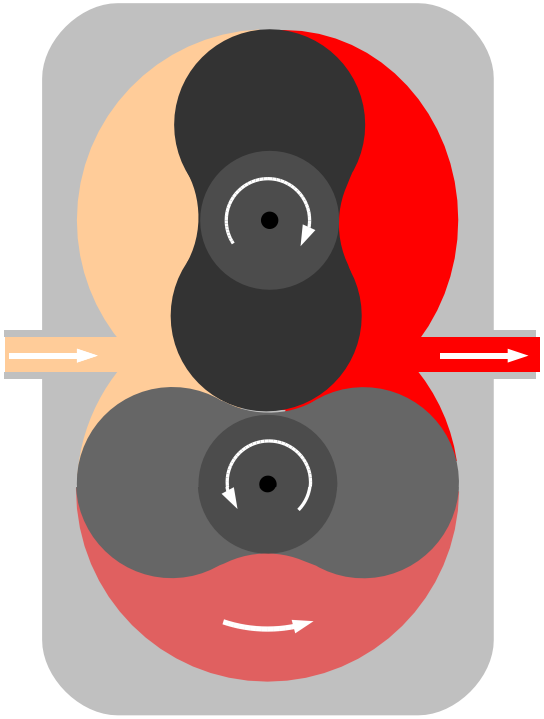

Scroll pumps

- Rough pumping: 10^{-2} – 1000 mbar
- $N \times 10$ m^3/h
- Dry pump (no oil in vacuum)
- Typically used for roughing and as a backing pump for turbos

Membrane pumps

- Rough pumping: 10^{-1} – 1000 mbar
- < 1 m^3/h (you don't want to do roughing)
- Dry pump (no oil in vacuum)
- Typically used as backing pump for turbos

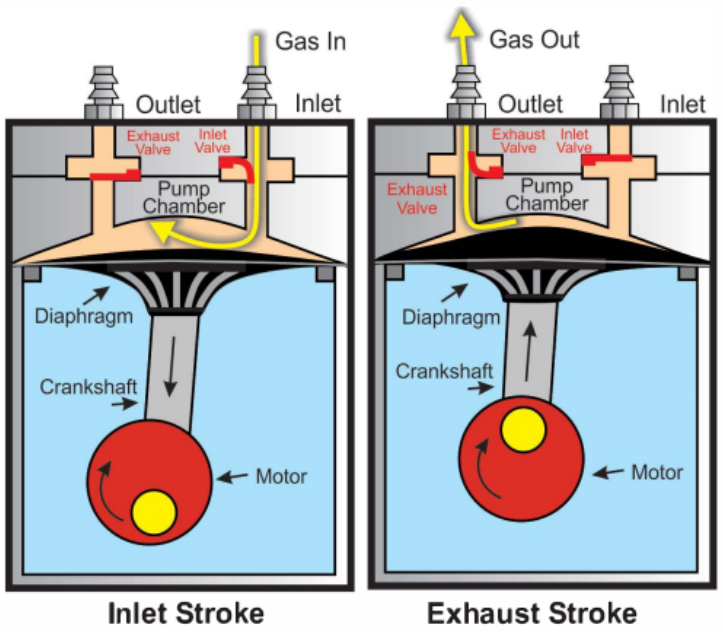

Turbomolecular pumps

- High speed turbine, vane speed higher than molecular speed
- Produces momentum transfer and thus pumping in several stages
- Lubricated, maglev or hybrid bearings
- From 10^{-1} to 10^{-10} mbar
- Turbo pumps need backing
- Are highly sensitive to impurities and high pressure

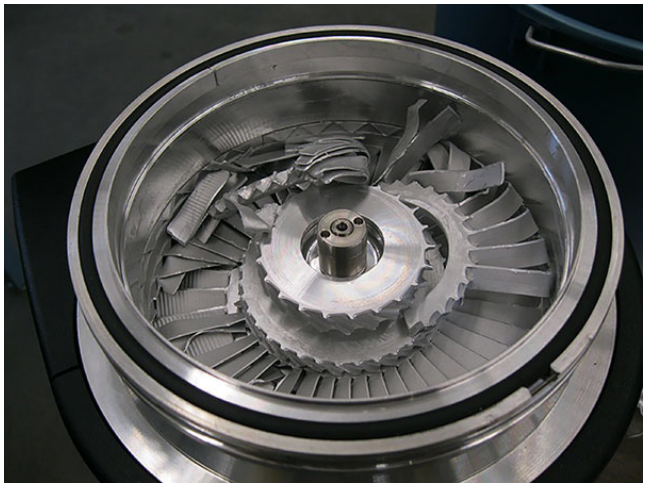

Cryogenic pumps

- Traps gases on a cryogenic (~ 8 K) surface
- Usually two-stage with 80 K baffles for water
- Second stage for the rest
- Down to 10^{-9} mbar
- Charcoal granules for adsorbing helium and hydrogen, which are not frozen at these temperatures
- Needs regeneration when “full”

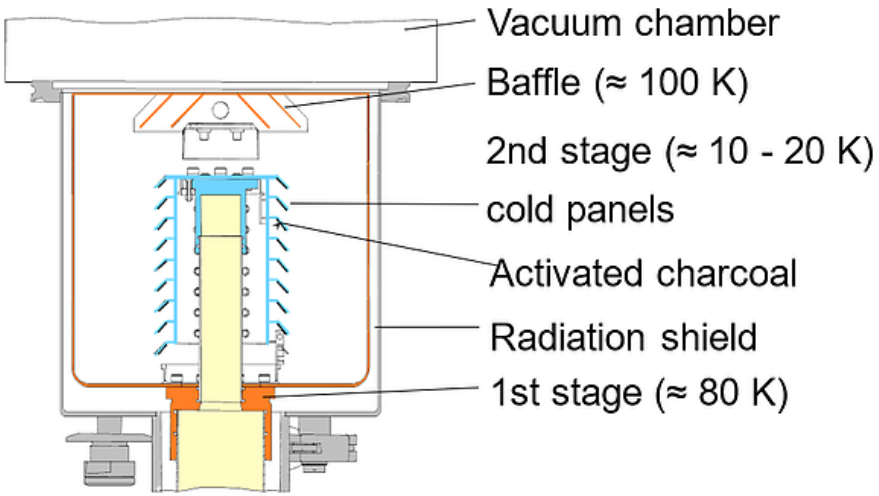

Pirani gauge

- Thermal conductivity gauge
- Measures temperature of a heated filament in vacuum
- Works from 10^{-3} to 1000 mbar
- Somewhat accurate from $5 \cdot 10^{-3}$ to 1 mbar

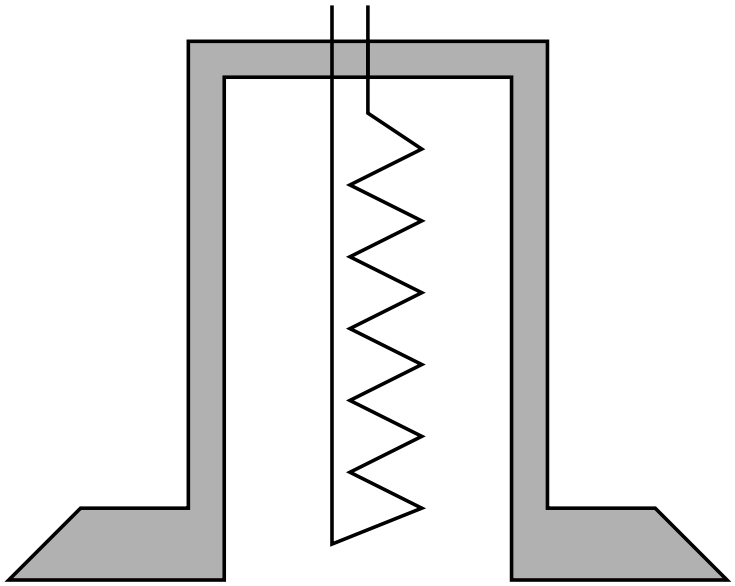

Penning gauge

- High voltage accelerates electrons in a magnetic field
- Ionizes residual gas, producing a current
- Current is proportional to vacuum
- Somewhat dependent on gas species
- Somewhat accurate from 10^{-8} to 10^{-3} mbar
- Destructive currents at high pressure

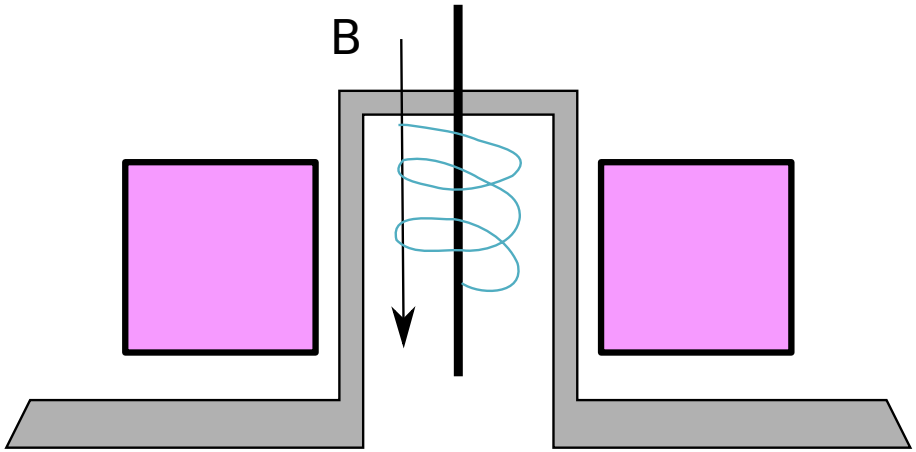

Capacitive gauge

- Measures the force of the pressure on a membrane
- Membrane moves as a function of the force, changing the capacitance on a measurement circuit.
- Accurate readings from 1 to 2000 mbar.

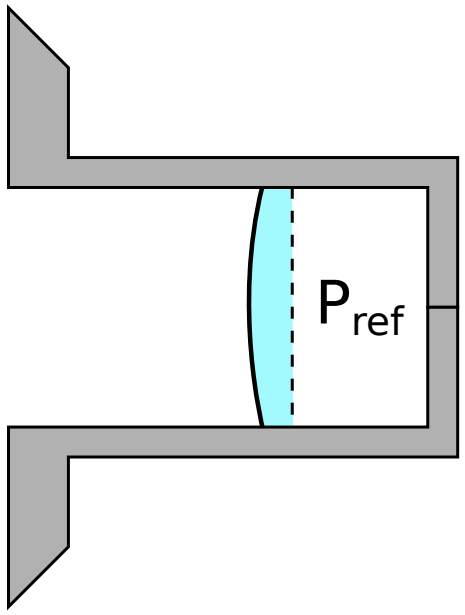

ISO-K flanges

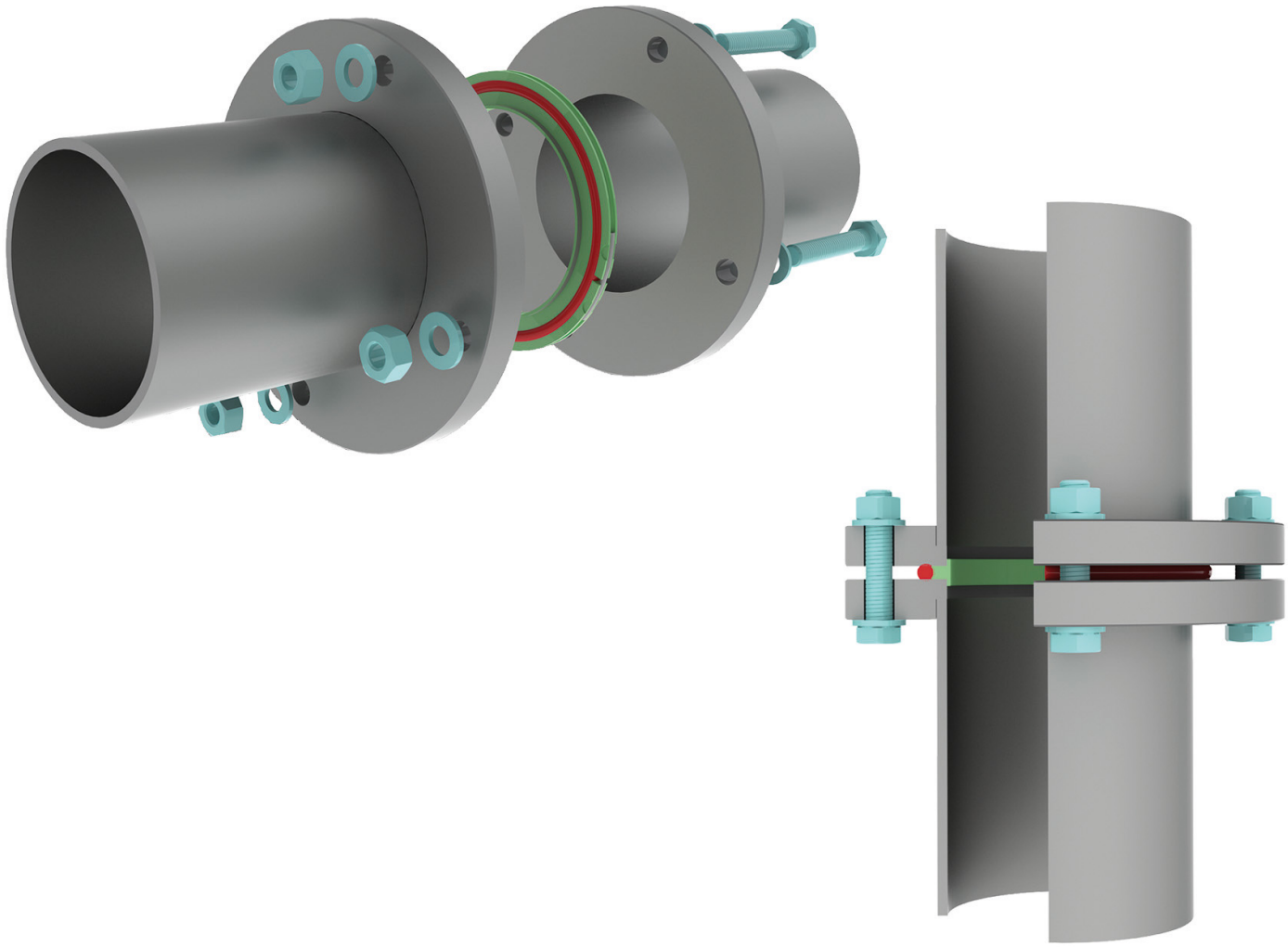

Sizes from $\varnothing 63$ to $\varnothing 500$ mm, image from Pfeiffer

ISO-F flanges

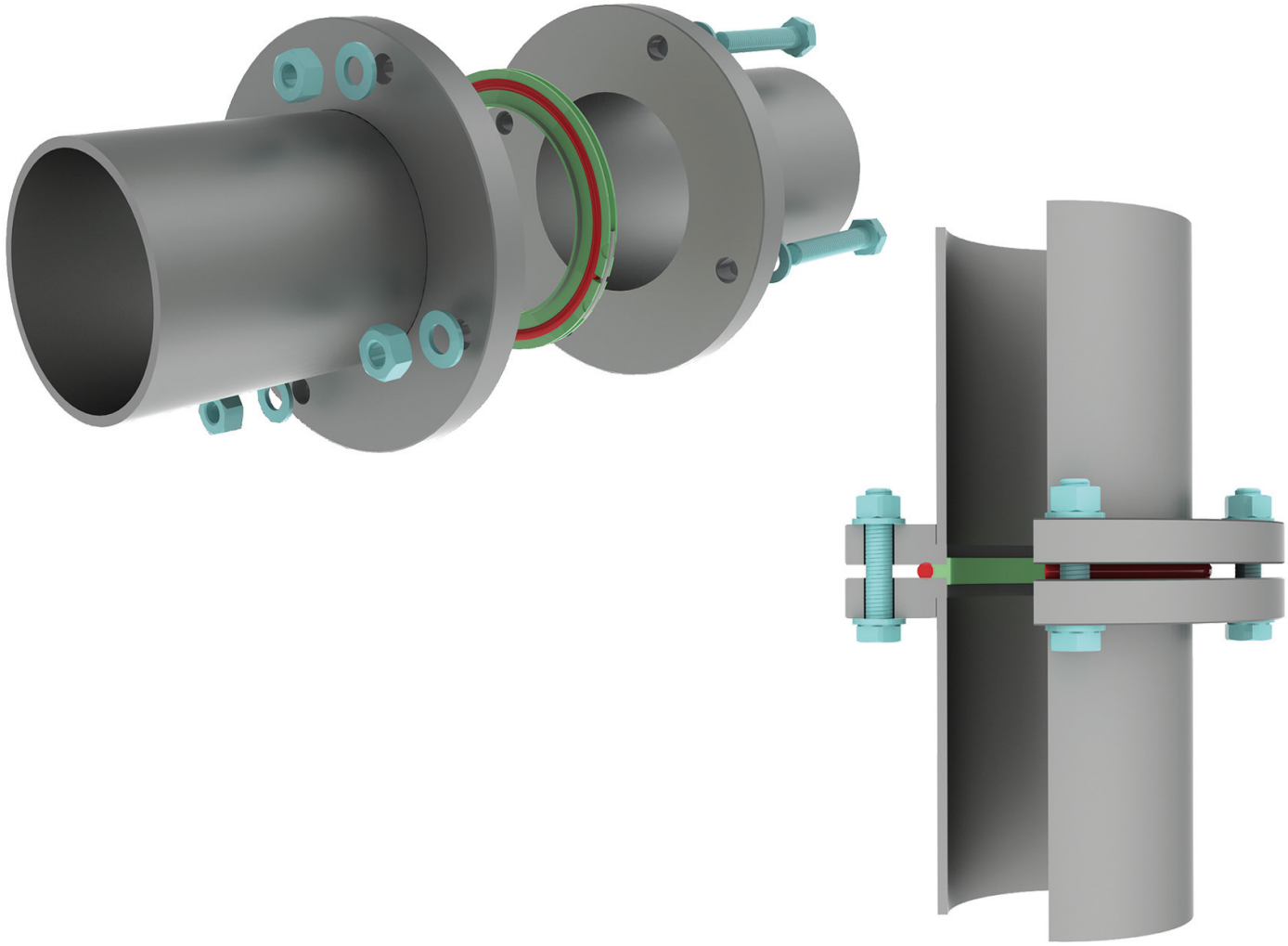

Sizes from $\varnothing 63$ to $\varnothing 500$ mm, image from Pfeiffer

ISO-KF flanges

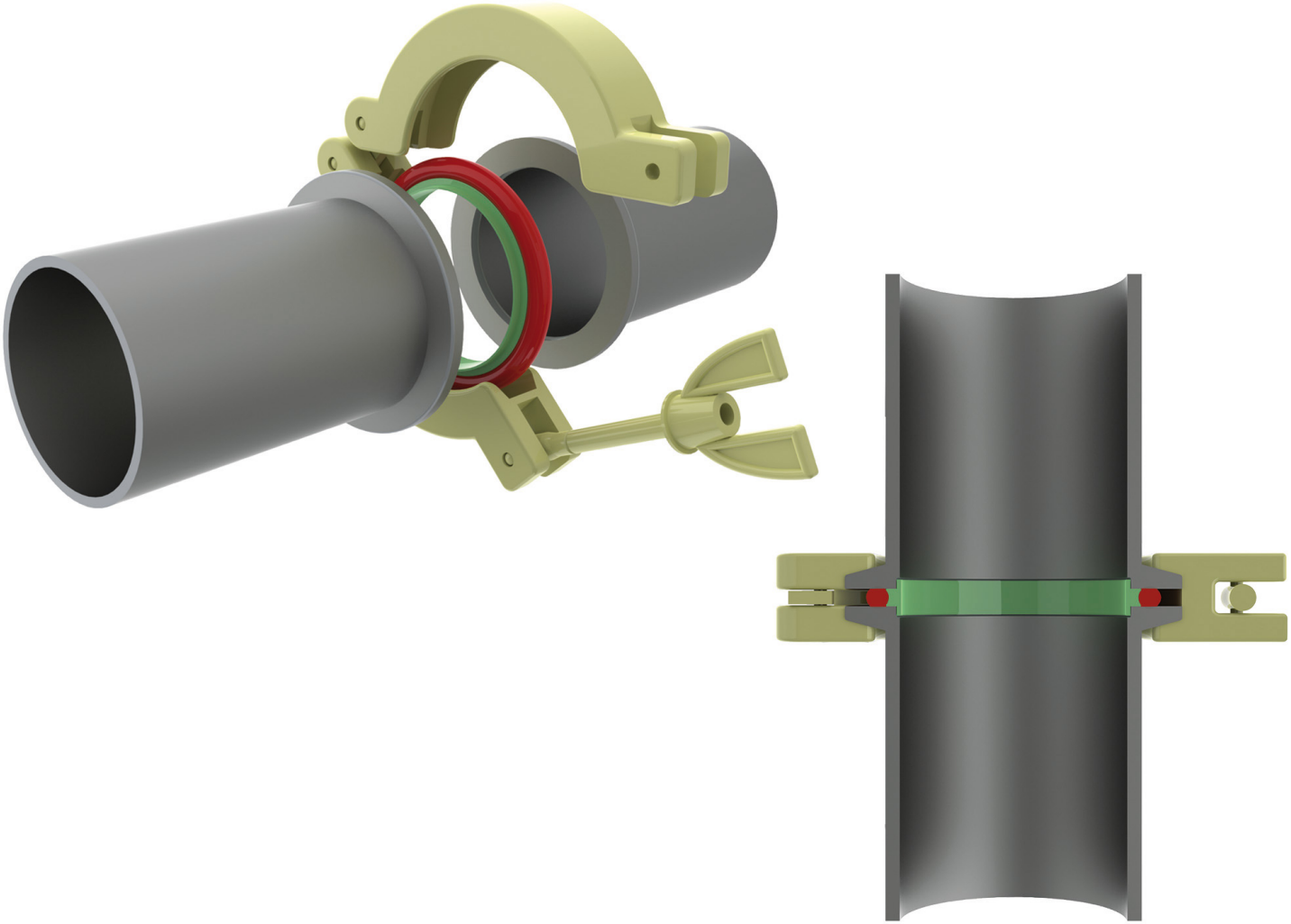

Sizes from $\varnothing 16$ to $\varnothing 50$ mm, image from Pfeiffer

CF flanges (UHV)

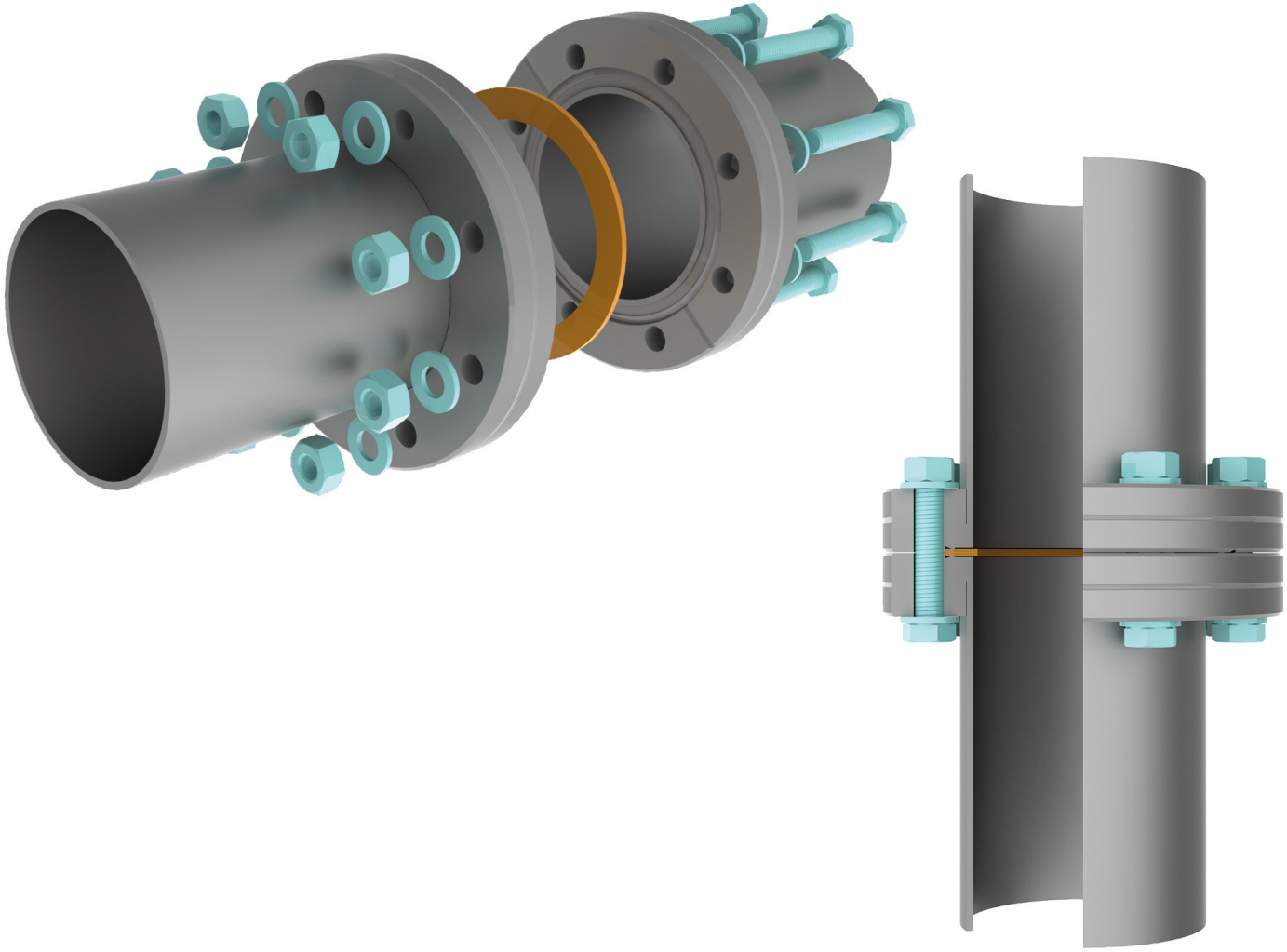

Sizes from $\varnothing 16$ to $\varnothing 250$ mm, image from Pfeiffer

Gate valves

- For separating vacuum regions / pumps
- Large opening in beam pipes (usually $\varnothing 100$ mm).
- Allows maintenance, etc.
- O-ring seals become dirty near ion sources
- Opens instantaneously (1–5 sec), causing possibly destructive pressure changes
- Will not survive running beam on the gate

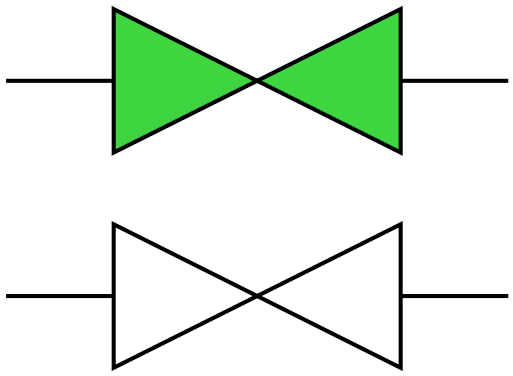

Other valves

Angle valves

- For separating vacuum regions in smaller sizes ($< \varnothing 50$ mm).
- Used mainly for prevacuum / roughing
- Not for running beam through

Leak valves

- For leaking small amounts of gas into vacuum
- Not to be used for shutting off — overtightening may be destructive
- Leak valves leak!

Minimal vacuum system